Student participation supported by
Arctic Natural Sciences Program
National Science Foundation

42nd International

PROGRAM & ABSTRACTS

7-9 March 2012, Winter Park, Colorado

Arctic Workshop 2012

Hosted by
Institute of Arctic and Alpine Research
University of Colorado at Boulder

Compiled in 2012 by:

Institute of Arctic and Alpine Research (INSTAAR)

This report may be cited as:

42nd International Arctic Workshop, Program and Abstracts 2012. Institute of Arctic and Alpine Research (INSTAAR), University of Colorado at Boulder, 115 pp.

This report is distributed by:

Institute of Arctic and Alpine Research
University of Colorado at Boulder
1560 30th Street
Campus Box 450
Boulder, CO 80309-0450
http://instaar.colorado.edu

Cover photo:

James Balog (Photographer, Extreme Ice Survey, and INSTAAR affiliate) sits with his daughter Simone and Adam LeWinter (EIS, now CRREL) besides the terminus of the Columbia Glacier in Alaska's Chugach Range.

The Extreme Ice Survey, together with glaciologists Tad Pfeffer (INSTAAR) and Shad O'Neel (USGS), and grad student Ethan Welty (INSTAAR), is using time lapse cameras to document, in unprecedented detail, the glacier's dynamic retreat.

Credit: Ethan Welty (weltyphotography.com). August 2009.

PROGRAM AND ABSTRACTS

42nd ANNUAL INTERNATIONAL ARCTIC WORKSHOP

March 7 - 9, 2012

Winter Park, Colorado

INSTAAR - Institute of Arctic and Alpine Research

University of Colorado at Boulder

Organizing Committee:

Tad Pfeffer
Wendy Roth
David Lubinski
Anne Jennings

Introduction

Overview and history

The 42nd Annual International Arctic Workshop will be held March 7 - 9, 2012, at the Winter Park Mountain Lodge in Winter Park, Colorado. The meeting is hosted by the Institute of Arctic and Alpine Research (INSTAAR), University of Colorado at Boulder. This workshop has grown out of a series of informal annual meetings started by John T. Andrews and sponsored by INSTAAR and other academic institutions worldwide. In keeping with this tradition, there are no formalized topics and the workshop has been organized around themes developed from the abstracts submitted.

Web site

http://www.colorado.edu/INSTAAR/AW/

Registration

Please check in or register on (1) Tuesday evening at the Icebreaker between 5 - 8pm, or (2) Wednesday morning between 8:00 – 8:45 am. At registration you will receive the Program and Abstracts, as well as other workshop information.

Posters

At registration you will receive information on where to set up your poster. Please put it up as early as possible, and leave it up as late as possible during the workshop.

Presentation Files (i.e., PowerPoint)

Please load your presentation onto our computer during the Icebreaker on Tuesday 5-8 pm or the Check-In/Registration on Wednesday 8:00–8:45 am. Time during breaks is limited.

NSF Support

The Arctic Natural Sciences Program at the National Science Foundation's Office of Polar Programs (NSF-OPP-ARC-ANS) supports student participation in the Workshop through a 3-year grant to INSTAAR.

Arctic Workshop 2012
Program Summary

TUESDAY 6 MARCH 2012		
5:00 - 8:00 pm	**Evening Reception, Check in & Registration** (Hors d'oeuvres, lemonade, and water will be served; drink tickets for wine or beer; load presentations onto computer; put up posters)	Shadow Mountain

WEDNESDAY 7 MARCH		
7:00 – 8:30 am	Continental Breakfast	Shadow Mountain
8:00 – 8:45	**Check-in & Registration** (load presentations onto computer)	"
9:00	**Workshop Welcome & Introduction**	"
9:20	**North Atlantic Paleoenvironments**	"
10:20	Morning Break	"
10:50	**Change, Adaptation, & Colonization**	"
12:00	LUNCH provided	"
1:00 pm	**Glaciology**	"
2:20	Afternoon Break	"
2:30	**POSTERS I (odd numbered posters)**	Grand Lake
5:00	End of Day	
5:30 – 8:00	Student Pizza and Beer Party (students only)	Shadow Mountain

THURSDAY 8 MARCH		
7:15 – 8:45 am	Continental Breakfast	Shadow Mountain
9:00	**Announcements**	"
9:10	**Glacial History I**	"
10:10	Morning Break	"
10:30	**Glacial History II**	"
11:30	Special Talk: Ryan Vachon	"
12:00	LUNCH provided	"
1:30pm	**Geomorphology & Osteohistology**	"
2:50	Afternoon Break	"
3:00	**POSTERS II (even numbered posters)**	Grand Lake
5:00	End of Main Sessions	"
6:00	**Workshop Dinner Provided** (Hors d'oeuvres, meal, lemonade, drink tickets for beer or wine)	Shadow Mountain
6:00	**Dinner Keynote: Julie Brigham-Grette "(Arctic) Confessions of a Woman Who Can't Say No"**	"
9:00	End of Day	

Program Summary

FRIDAY 9 MARCH 2012		
7:30 – 8:45 am	Continental Breakfast	Shadow Mountain
9:00	**Announcements**	“
9:10	**Lacustrine I**	“
10:10	Morning Break	“
10:40	**Lacustrine II & More**	“
11:40	**Discuss Future of Workshop & Workshop Wrap Up**	“
12:00	LUNCH provided	“
1:30	**End of Meeting.** *Thanks for coming!*	“

Notes

Program Details

PM - TUESDAY 6 MARCH 2012

5:00 to 8:00pm **Evening Reception, Check in, & Registration** (Shadow Mountain)
Hors d'oeuvres, lemonade, and water will be served; drink tickets for wine or beer; load presentations onto computer; put up posters in Grand Lake Room.

AM – WEDNESDAY 7 MARCH 2012

07:00 to 8:30 **Continental Breakfast** (Shadow Mountain)

08:00 **Check-in & Registration** (Shadow Mountain)
(Load presentations onto our computer)

09:00 **Workshop Welcome & Introduction** (Shadow Mountain)
Tad Pfeffer (INSTAAR, Arctic Workshop Director)

North Atlantic Paleoenvironments

09:20 **PALEOMAGNETIC SYNCHRONIZATION AND LAND – SEA PALEOCLIMATIC CORRELATIONS FROM ICELAND**
Geirsdottir, Aslaug; Miller, Gifford H.; Olafsdottir, Saedis; Larsen, Darren [pg. 38]

09:40 **A HIGH RESOLUTION STUDY OF HISTORICAL CLIMATE CHANGES AND HUMAN IMPACTS ON THE NORTH ATLANTIC - NORTH SEA BOUNDARY: THE SHETLAND ISLANDS CLIMATE AND SETTLEMENT PROJECT**
Bigelow, Gerald F.; Jones, Michael E.; Retelle, Michael J.; Johnson, Beverly J.; Ambrose Jr., William G. [pg. 15]

10:00 **SIGNAL OF PERSISTENT MULTIDECADAL VARIABILITY IN WINTERTIME SEA-ICE RECORDS: LINKAGES TO THE ATLANTIC MULTIDECADAL OSCILLATION**
Miles, Martin; et, al. [pg. 60]

10:20 Morning Break

AM – WEDNESDAY 7 MARCH 2012

Change, Adaptation, & Colonization

10:50 **UNPRECEDENTED RECENT SUMMER WARMTH IN ARCTIC CANADA**
Miller, Gifford; Refsnider, Kurt; Lehman, Scott; Southon, John [pg. 62]

11:10 **CLIMATE ADAPTATION IN LANDSCAPES AND SEASCAPES OF NORTHERN NORWAY: CHALLENGES AND OPPORTUNITIES**
Ogilvie, Astrid E; Amundsen, Helene; Hovelsrud, Grete K [pg. 62]

11:30 **BLACK SPRUCE COLONIZATION OF FOREST-TUNDRA SNOW PATCHES OF EASTERN CANADA**
Truchon-Savard, Alexandre; Payette, Serge [pg. 81]

12:00 **LUNCH provided** (Shadow Mountain)

PM – WEDNESDAY 7 MARCH 2012

Glaciology

1:00 **COUPLED ICE SHEET/CLIMATE SIMULATIONS OF GREENLAND EVOLUTION IN HIGH-CO_2 CONDITIONS: SENSITIVITY TO MODELLED POLAR AMPLIFICATION**
Fyke, Jeremy G.; Weaver, Andrew J.; Eby, Michael [pg. 36]

1:20 **STRAIN RATE ESTIMATES ON MOUNT HUNTER, ALASKA: WHAT CAUSES CREVASSING AT AN ICE DIVIDE?**
Campbell, Seth W; Kreutz, Karl J; Arcone, Steven A; Osterberg, Erich C [pg. 24]

1:40 **FRESHWATER RUNOFF AND MASS TRANSFER FROM THE GREENLAND ICE SHEET AT KANGERLUSSUAQ, WEST GREENLAND**
Mikkelsen, Andreas B; Hasholt, Bent; Overeem, Irina; Hudson, Ben; Nielsen, Morten H [pg. 57]

2:00 **LAND ICE AND SEA LEVEL: UPDATE**
Pfeffer, W. Tad [pg. 65]

2:20 Afternoon Break

PM – WEDNESDAY 7 MARCH 2012

POSTERS I (odd numbered posters, Grand Lake) Wed. 2:30 to 5:00 pm

1 **FJORD-FLOOR SEDIMENTOLOGY AND GEOCHEMISTRY AT THE KRONEBREEN GLACIER, SVALBARD, NORWAY: APPLYING PALEOCLIMATIC TECHNIQUES IN A GLACIMARINE SETTING**
McGregor, Daren A; Brigham-Grette, Julie; Powell, Ross [pg. 56]

3 **USING CLAY MINERALOGY TO ANALYZE SEDIMENT SOURCES, KRONEBREEN AND KONGSVEGEN GLACIERS, SVALBARD, NORWAY**
Ceperley, Elizabeth G; Brigham-Grette, Julie; Powell, Ross; Swanson, Susan [pg. 28]

5 **INFLUENCE OF MARINE AND CLIMATIC DYNAMICS ON SHORT TERM CALVING PROCESSES AT THE KRONEBREEN-KONGSVEGEN GLACIER SYSTEM, SVALBARD**
Siegel, Rebecca; Brigham-Grette, Julie; Powell, Ross; Roof, Steve [pg. 79]

7 **TREE-RING DATING AND GLACIAL STRATIGRAPHY OF THE MID HOLOCENE HISTORY OF WACHUSETT INLET, GLACIER BAY NATIONAL PARK AND PRESERVE, SE ALASKA** [pg. 4]
Appleton, Sarah N; Wiles, Greg C; Lawson, Daniel E; Wilch, Joe T; Wiesenberg, Nick

9 **A COMPARISON OF TWO LAKE SEDIMENT RECORDS ON ADAK ISLAND, ALASKA AND THE POTENTIAL FOR A RECONSTRUCTING PRECIPITATION TO 2 KA**
Krawiec, Anne C.; Kaufman, Darrell S.; Vaillencourt, David A. [pg. 45]

11 **DEVELOPING K-5 AND PUBLIC OUTREACH PRODUCTS FOR ALASKAN GLACIOLOGY AND SEA LEVEL USING THE IPAD APP PLATFORM**
Kreutz, Noah; Plourde, Joshua; Campbell, Seth; Kreutz, Karl; Wanamaker, Alan (K Kreutz is presenter) [pg. 48]

13 **HYDRO-CLIMATE AND SEDIMENT VARIATIONS AT ALLISON LAKE, SOUTH-CENTRAL ALASKA.**
Arnold, Megan S; Kaufman, Darrell [pg. 6]

15 **TWO-STEP DEGLACIATION OF THE UMANAK TROUGH, WEST GREENLAND**
Jennings, Anne E; Sheldon, Christina; Andrews, John T; Hogan, Kelly; Dowdeswell, Julian A; Ó Cofaigh, Colm; Kilfeather, Aoibheann [pg. 41]

17 **PROPAGATING ATMOSPHERIC PATTERNS ASSOCIATED WITH SEA ICE MOTION THROUGH THE FRAM STRAIT**
Liptak, Jessica; Strong, Courtenay [pg. 50]

19 **THE ECOLOGY OF DECAYING ICE-WEDGES: NOVEL HABITATS IN A POLAR DESERT**
Becker, Michael S; Pollard, Wayne H [pg. 13]

21 **TRACING GROWING DEGREE-DAYS AND CO_2 CONCENTRATION USING** *BETULA GLANDULOSA* **LEAF CUTICLE CHARACTERISTICS**
Holmquist, James R; Wagner-Cremer, Friederike [pg. 40]

23 **CLIMATE INDUCED CHANGES OF THE TREE-LINE ECOTONE IN THE POLAR URALS AND IMPACTS ON LAND-SURFACE PROPERTIES**
Mazepa, Valeriy; Ivanov, Valeriy; Shiyatov, Stepan (Ivanov is presenter) [pg. 52]

PM – WEDNESDAY 7 MARCH 2012

5:00 End of Day

5:30 to 8:00pm **Student Pizza and Beer Party** (Shadow Mountain) (students only)

AM – THURSDAY 8 MARCH 2012

07:15 to 08:45 **Continental Breakfast** (Shadow Mountain)

9:00 **Announcements & Review** (Shadow Mountain)

Glacial History I

09:10 **WHEN GLACIERS LEFT, AND WHEN THEY CAME BACK: NEW ^{10}BE AGES ON DEGLACIATION AND NEOGLACIATION IN THE BROOKS RANGE, ARCTIC ALASKA**
Badding, Michael E; Briner, Jason P; Kaufman, Darrell S [pg. 9]

09:30 **ON THE SPATIAL DISTRIBUTION OF GLACIAL EROSION RATES IN THE ST. ELIAS MOUNTAINS, ALASKA**
Barker, Adam D; Hallet, Bernard; Headley, Rachel M [pg. 12]

09:50 **THE IMPACT OF GLACIAL EROSION ON NORTHERN SHIELDS**
Ebert, Karin; Hall, Adrian M; Kleman, Johan [pg. 34]

10:10 Morning Break

Glacial History II

10:30 **LATE WEICHSELIAN ICE SHEET CONFIGURATION IN NORTHWEST SPITSBERGEN, FROM 10BE DATING AND LITHOLOGICAL STUDIES OF ERRATIC BOULDERS AND BEDROCK**
Gjermundsen, Endre F; Briner, Jason P; Salvigsen, Otto; Akçar, Naki; Kubik, Peter W; Gantert, Niklas; Hormes, Anne [pg. 39]

10:50 **AN ALASKAN CORDILLERAN ICE SHEET REFUGIUM IN SITKA SOUND DURING THE LAST GLACIAL MAXIMUM**
Powell, Ross D.; Dzuryak, John-Franklin [pg. 67]

11:10 **THE YOUNGER DRYAS COLD INTERVAL WAS NOT THAT COLD: INSIGHTS FROM BAFFIN ISLAND, ARCTIC CANADA**
Young, Nicolas E; Briner, Jason P [pg. 93]

AM – THURSDAY 8 MARCH 2012

11:30 *Special Talk*
WORKSHOPS POSITIONING YOUTH AS FILM PRODUCERS OF CRITICAL GLOBAL SYSTEMS: AUTHENTIC ARCTIC CONTENT FROM NORTHWEST GREENLAND
Vachon, Ryan [pg. 97]

Vachon founded Earth Initiatives, a non-profit organization, to promote the communication of crucial science issues to public audiences. One of his projects is teaching filmmaking to young students. His talk focuses on his recent workshops with middle and high school students in Northwest Greenland. The students were tasked with helping "us" (educators, scientists, parents, politicians and businesses) effectively convey key science concepts and issues to the public. The students started with existing video footage about the scientific research taking place in the Thule, Greenland region. They then modified, added or omitted content to tell engaging stories. They worked with each other and instructors to direct filming, define messages, refine storylines, establish voice, and edit content. They had a lot of fun... and also happened to learn some fundamentals of arctic science as well as strengthen their knowledge of Science, Technology, Engineering and Math (STEM).

12:00 **LUNCH provided** (Shadow Mountain)

PM – THURSDAY 8 MARCH 2012

Geomorphology & Osteohistology

1:30 **IDENTIFICATION OF PERMAFROST SLOPE DISTURBANCES USING MULTI-TEMPORAL IMAGERY AND CHANGE DETECTION TECHNIQUES, CAPE BOUNTY, MELVILLE ISLAND, NUNAVUT**
Rudy, Ashley; Lamoureux, Scott F; Treitz, Paul [pg. 76]

1:50 **ROUGHNESS OF GLACIALLY ABRADED BOULDERS MEASURED WITH USE OF HANDYSURF E35-B ELECTRONIC PROFILOMETER AND ITS POTENTIAL FOR RELATIVE DATING: A CASE OF FLÁAJÖKULL MORAINES (SE ICELAND)**
Dąbski, Maciej [pg. 30]

2:10 **GEOMORPHOLOGICAL MAPPING OF QUATERNARY LANDFORMS AND SEDIMENTS FOR GEOHAZARD ASSESSMENT IN SELECTED CULTURAL HERITAGE SITES ON SVALBARD**
Sessford, Evangeline G; Hormes, Anne; Etzelmüller, Bernd [pg. 77]

2:30 **COMPARATIVE OSTEOHISTOLOGY OF *PYGOSCELIS* PENGUINS: IMPLICATIONS FOR BEHAVIORAL AND ENVIRONMENTAL INFLUENCES ON BONE GROWTH**
Wilson, Laura E [pg. 89]

2:50 Afternoon Break

PM - THURSDAY 8 MARCH 2012

POSTERS II (even numbered posters, Grand Lake) Thurs. 3:00 – 5:00 pm

2 **SUBMARINE LANDFORMS IN A SURGE-TYPE TIDEWATER GLACIER REGIME, ENGELSKBUKTA, SVALBARD**
Roth, George E; Noormets, Riko; Powell, Ross D; Brigham-Grette, Julie [pg. 73]

4 **CHARACTERIZING FJORD OCEANOGRAPHY NEAR THE TIDEWATER GLACIER FACES IN KONGSFJORDEN, SVALBARD**
Rajagopalan, Daksha M; Brigham-Grette, Julie; Powell, Ross D; Timmermans, Mary-Louise [pg. 70]

6 **MONITORING FJORD FLOOR SEDIMENTOLOGY AND GEOCHEMISTRY IN AN ICE-PROXIMAL REGION: A CASE STUDY FROM THE KRONEBREEN-KONGSVEGEN CONFLUENT TIDEWATER GLACIAL SYSTEM**
Valletta, Rachel D.; Brigham-Grette, Julie; Powell, Ross; Scholz, Christopher A. [pg. 87]

8 **HOLOCENE CLIMATIC VARIABILITY AND EXTENT OF THE SHERIDAN GLACIER INFERRED FROM THE SEDIMENT OF CABIN LAKE, ALASKA**
Zander, Paul D; Kaufman, Darrell S; Anderson, R Scott [pg. 94]

10 **HYDROGEN ISOTOPES OF N-ALKANOIC ACIDS FROM LAKE SEDIMENTS REFLECT CHANGES IN ANNUAL PRECIPITATION OVER THE 20TH CENTURY, ADAK ISLAND, ALASKA.**
Vaillencourt, David A; Kaufman, Darrell S; D'Andrea, William J; Anderson, Scott [pg. 83]

12 **PHYTOLITHS FROM SANAK ISLAND, WESTERN GULF OF ALASKA**
Wilbur, Cricket C; Jordan, James J; Pearsall, Deborah M [pg. 89]

14 **HOLOCENE DYNAMICS OF RIPARIAN ECOSYSTEMS ALONG A SUBARCTIC RIVER (BONIFACE RIVER, QUÉBEC)**
St-Amour, Francis; Payette, Serge [pg. 80]

16 **VOLCANIC, ANTHROPOGENIC, AND CLIMATIC INFLUENCES ON HOLOCENE ECOSYSTEM DYNAMICS USING MULTIPLE PROXY ANALYSES OF A LAKE SEDIMENT CORE FROM VESTRA GÍSLHOLTSVATN, SOUTHWESTERN ICELAND**
Christensen, Celene L; Miller, Gifford H; Geirsdóttir, Áslaug [pg. 29]

18 **MARINE EVIDENCE FOR A GLACIAL ICE STREAM IN AMUNDSEN GULF, CANADIAN ARCTIC ARCHIPELAGO.**
MacLean, Brian; Blasco, Steve; Bennett, Robbie; Lakeman, Tom; Hughes-Clarke, John; Kuus, Pim; Patton, Eric [pg. 51]

20 **FORAGING ECOLOGY AND SUMMER FEEDING GROUNDS OF BOWHEAD WHALES (BALAENA MYSTICETUS) IN THE EASTERN CANADIAN ARCTIC**
Pomerleau, Corinne; Ferguson, Steven H; Lesage, Veronique; Winkler, Gesche [pg. 65]

22 **ASSESSING TREND AND VARIATION OF ARCTIC ICE EXTENT DURING 1979-2010 FROM AN ICE EDGE LATITUDE PERSPECTIVE**
Xia, Wentao; Xie, Hongjie; Ackley, Stephen Fred [pg. 92]

24 **NORTH ATLANTIC SUBPOLAR GYRE DYNAMICS IN THE ABSENCE OF MAJOR FRESHWATER FORCING**
Quillmann, Ursula; Jennings, Anne E; Marchitto Jr., Thomas M; Andrews, John T; Haflidason, Haflidi; Hall, Ian R [pg. 68]

PM – THURSDAY 8 MARCH 2012

WORKSHOP BANQUET AND KEYNOTE (Shadow Mountain)

6:00 **WORKSHOP BANQUET PROVIDED**
(Hors d'oeuvres, meal, lemonade, water, drink tickets for beer or wine)

6:00 **DINNER KEYNOTE**

Julie Brigham-Grette
Professor of Geosciences
University Massachusetts Amherst

"(Arctic) Confessions of a Woman Who Can't Say No"

Brigham-Grette will draw on decades of experience doing field work in Russia and other areas of the Arctic. Her informative (and perhaps amusing) talk centers on international collaboration, persistence and serendipity.

Dr. Julie Brigham-Grette has been teaching at the University of Massachusetts Amherst for 25 years. She has been conducting research in the Arctic for over 30 years including eight field seasons in remote parts of northeast Russia, participating in both the science program as well as dealing with complex logistics.

Brigham-Grette's research interests and experience span the broad spectrum from the regional stratigraphy of glacial and interglacial marine and glacimarine sequences in coastal environments, to continental shelf stratigraphy and paleoceanography, especially in the Bering Strait region. She has lead many research projects including being US Chief scientist of the Lake El'gygytgyn Drilling Program in Arctic Russia. That project helped improve understanding of terrestrial Arctic change since the middle Pliocene. She is a member of the university's Climate System Research Center.

Brigham-Grette has long emphasized teaching, advising, and mentoring of both graduate and undergraduate students (many of them women). And not just students from her university. She also mentors undergraduate students from four colleges near UMassAmherst. Brigham-Grette recently helped undergraduates from six colleges gain research experience by studying tidewater glaciomarine processes in Svalbard, Norway.

9:00 pm End of the Day

AM – FRIDAY 9 MARCH 2012

07:30 to 08:45 **Continental Breakfast** (Shadow Mountain)

9:00 **Announcements & Review** (Shadow Mountain)

Lacustrine I

09:10 **A LACUSTRINE RECORD OF MIDDLE- TO LATE-HOLOCENE GLACIATION FROM KURUPA LAKE, NORTH-CENTRAL BROOKS RANGE, ARCTIC ALASKA**
Boldt, Brandon ; Kaufman, Darrell S; Briner, Jason P [pg. 17]

09:30 **USING REWORKED BIVALVES AND PROGLACIAL-THRESHOLD LAKES TO CONSTRAIN GREENLAND ICE MARGIN CHANGE DURING THE HOLOCENE: NEW RESULTS FROM UPERNAVIK ISSTRØM**
Briner, Jason P; Håkansson, Lena; Bennike, Ole; Kaufman, Darrell [pg. 23]

09:50 **SEDIMENTARY AND GEOCHEMICAL EVIDENCE OF RECENT MARINE TRANSGRESSION IN THE SEDIMENTS OF A HYPERSALINE COASTAL BASIN, SHELLABEAR LAKE, MELVILLE ISLAND, NORTHWEST TERRITORIES**
Kathan, Kasey; Lamoureux, Scott; Dugan, Hilary [pg. 43]

10:10 Morning Break

Lacustrine II & More

10:40 **WESTERN ARCTIC VULNERABILITY TO CLIMATE VARIABILITY OVER THE PAST 3.6 MYR: A NEW VIEW FROM SEDIMENTS DRILLED AT LAKE EL'GYGYTGYN, WESTERN BERINGIA**
Brigham-Grette, Julie; Melles, Martin; Minyuk, Pavel; Lake Elgygytgyn Science Team [pg. 22]

11:00 **NON-LINEAR HOLOCENE CLIMATE EVOLUTION IN THE NORTH ATLANTIC: A HIGH-RESOLUTION, MULTI-PROXY RECORD OF GLACIER ACTIVITY AND ENVIRONMENTAL CHANGE FROM HVÍTÁRVATN, CENTRAL ICELAND**
Larsen, Darren J; Miller, Gifford H; Geirsdóttir, Áslaug; Ólafsdóttir, Sædís [pg. 49]

11:20 **CHANGES IN SEDIMENT PROVENANCE AND OCEANOGRAPHY ACROSS THE DENMARK STRAIT OVER THE LAST 2000 CAL YR BP: AN ONGOING STUDY**
Andrews, John T; Alonso-García, Montserrat; Belt, Simon; Cabedo Sanz, Patricia; Darby, Dennis; Jaeger, John; Jennings, Anne E; Olafsdottir, Saedis [pg. 1]

11:40 **Discuss the future of the Arctic Workshop & Workshop wrap up**

PM – FRIDAY 9 MARCH 2012

12:00 **LUNCH provided** (Shadow Mountain)

1:30 **End of Meeting - THANKS FOR ATTENDING!**

CHANGES IN SEDIMENT PROVENANCE AND OCEANOGRAPHY ACROSS THE DENMARK STRAIT OVER THE LAST 2000 CAL YR BP: AN ONGOING STUDY

Andrews, John T [1]; **Alonso-García**, Montserrat [2]; **Belt**, Simon [3]; **Cabedo Sanz**, Patricia [4]; **Darby**, Dennis [5]; **Jaeger**, John [6]; **Jennings**, Anne E [7]; **Olafsdottir**, Saedis [8]

[1] University of Colorado; andrewsj@colorado.edu
[2] University of South Florida; montsealonso82@gmail.com
[3] Plymouth University; S.Belt@plymouth.ac.uk
[4] Plymouth University; patricia.cabedosanz@plymouth.ac.uk
[5] Old Dominion University; ddarby@odu.edu
[6] University of Florida; jmjaeger@ufl.edu
[7] University of Colorado; jenninga@colorado.edu
[8] University of Iceland; saediso@hi.is

The area of the Denmark Strait is a "type area" for the generally accepted climatic intervals of the last 2000 cal yr BP, including the Medieval Warm Interval (MWI) and the Little Ice Age (LIA). On the N Iceland shelf, the 2000 cal yr BP interval marks a dramatic change in benthic foraminifera, with the arctic species Elphidium clavata forma clavata, making a dramatic re-appearance. Paleoceanographic proxy data from 5 cores, resampled at 100-yr intervals, from SW, NW, and N Iceland showed a coherent response between a variety of proxies, including ice-rafted minerals, the sea ice biomarker IP25, carbonate weight%, and foraminiferal light stable isotopes (Axford et al., 2011) (Fig. 1). The 1st PCA explains 68% of the variance in the data, and is positively associated with quartz wt% and IP25, and is negatively loaded with carbonate values. Here we extend this analysis across the Denmark Strait to the more polar environment of East Greenland between Scoresby Sund and Kangerlussuaq Trough (~66°-70°N) (Fig. 2) with a multi-proxy approach including 210Pb and 137Cs dating (Jaeger), foraminifera and their light isotopes (Jennings and Olafsdottir), Fe-iron oxide provenance fingerprinting (Darby), lithic counts (Alonso-García), sea-ice biomarkers and total organic carbon content (Cabedo Sanz and Belt), and X-ray diffraction and sediment magnetic mineral composition (Andrews). Data analysis is still ongoing on several of the proxies.

Along the NW and N Iceland shelf, drift-ice is a frequent but not pervasive element in the environment, whereas in contrast, the East Greenland shelf is characterized by an extensive and pervasive cover of sea ice (~October to July ±), including landfast sea-ice, and with numerous tidewater glacier margins contributing icebergs. Kangerlussuaq Trough and Fjord, a focus of the research, is directly influenced by modified Atlantic Water, which forms an Intermediate Water mass linked to the Irminger Current (Jennings et al., 2011). We have extended our research onto the East Greenland and Iceland shelf using a number of high-resolution cores from the PO175, HU93030, JM96-, B997- and MD99- cruises. On the NW/N Iceland shelf we also present data on a series (4) of small 20-cm gravity cores collected in 1997. Chronological control is being based on AMS 14C dates, 210Pb and 137Cs (Smith et al., 2002). Three short giant gravity cores (~20 cm in length) (PO175GKC#7, -8, and –9) in the middle reaches of Kangerlussuag Trough extend back into the middle of the Little Ice Age, whereas on the inner shelf HU93030-019B and MD99-2322 can be combined to present a detailed record of environmental change over the last 2000 cal yr (Fig. 3), which can then be directly compared with data from the MD99-2263 box core (Andrews et al., 2009). Rates of sediment accumulation vary by a factor of 10 between the East Greenland (~0.2cm/yr) versus Iceland (0.02cm/yr) margins across the strait. These rates allow multi-decadal to century-scale resolution of sediment archives. The data for the last ~190 yrs in the PO175GKC cores can be compared with the historical (Schmith and Hanssen, 2003) compilation of the Storis records (ice transported around the southern tip of Greenland and north along the SW/W Greenland margin). The wealth of data that are accumulating for this cross-strait transect will be assessed to answer the following critical questions: 1) are the climate events (based on our proxies) on either side of Denmark

Strait strongly correlated? 2) Can these events be strongly linked to the "standard" LIA, MWI, Dark Ages, and Roman Warm Period intervals? 3) Can we detect significant temporal variations in our proxies that deal with sediment provenance? 4) What are the associations, if any, between sediment and biological proxies?

Andrews, Darby and Jennings supported by NSF-ARC 1107761; Belt and Cabedo Sanz supported by EU FP7 2007/2013 Marie-Curie Actions Grant Agreement No. 238111; Alonso-García supported by NSF (OCE-0961670) and the Comer Science and Education Foundation (CP75)

Andrews, J.T., Belt, S.T., Olafsdottir, S., Masse, G., Vare, L., 2009, Sea ice and marine climate variability for NW Iceland/Denmark Strait over the last 2000 cal. yr BP. The Holocene, v. 19, p. 775-784.

Axford, Y., Andresen, C., Andrews, J.T., Belt, S.T., Geirsdottir, A., Masse, G., Miller, G.H., Olafsdottir, S., Vare, L.L., 2011, Do paleoclimate proxies agree? Statistical comparison of climate and sea-ice reconstructions from Icelandic marine and lake sediments, 300-1900 AD. Journal of Quaternary Science, v. 26, p. 645-656.

Jennings, A.E., Andrews, J.T., Wilson, L., 2011, Holocene environmental evolution of th SE Greenland Shelt north and south of the Denmark Strait: Irminger and East Greenland current interactions. Quaternary Science Reviews, v. 30, p. 980-998.

Schmith, T., Hanssen, C., 2003, Fram Strait ice export during the nineteenth and twentieth centuries reconstructed from a multiyear sea ice index from Southwestern Greenland. Journal of Climate, v. 16, p. 2782-2791.

Smith, L.M., Alexander, C., Jennings, A.E., 2002, Accumulation in East Greenland Fjords and on the continental shelves adjacent to the Denmark Strait over the last century based on 210Pb geochronology. Arctic, v. 55, p. 109-12

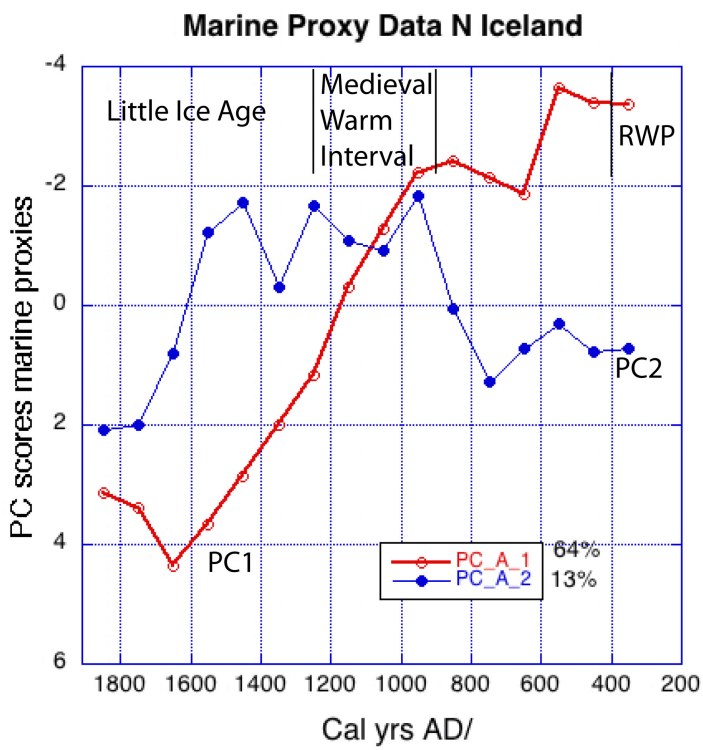

Fig 1. Principal component scores on marine climate proxies from NW/N Iceland (Axford et al., 2011) and standard climatic units.

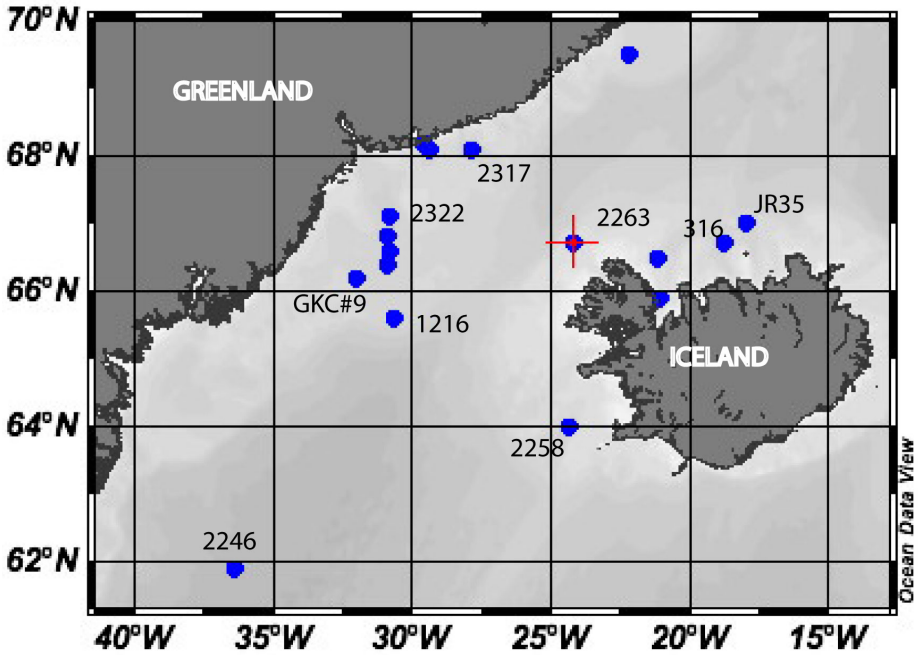

Fig 2. Map of the Denmark Strait area and the location of cores

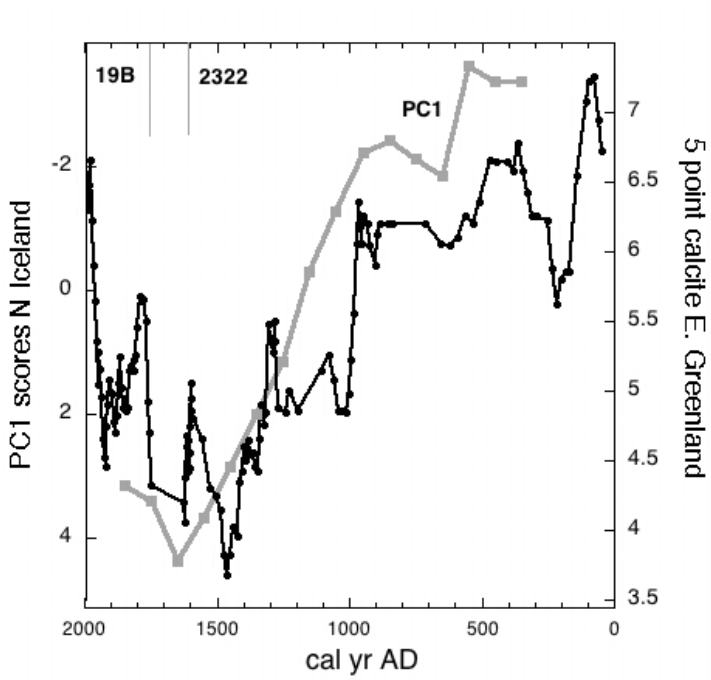

Fig 3. Calcite wt% from a combined HU93030-019B and MD99-2322---there is a short gap between the two records---compared with the 1st axis PC scores from the N Iceland proxies (Fig. 1).

TREE-RING DATING AND GLACIAL STRATIGRAPHY OF THE MID HOLOCENE HISTORY OF WACHUSETT INLET, GLACIER BAY NATIONAL PARK AND PRESERVE, SE ALASKA

Appleton, Sarah N [1]; **Wiles**, Greg C [2]; **Lawson**, Daniel E [3]; **Wilch**, Joe T [4]; **Wiesenberg**, Nick [5]

[1] The College of Wooster; sappleton12@wooster.edu
[2] The College of Wooster; gwiles@wooster.edu
[3] Cold Regions Research and Engineering Laboratory; daniel.e.lawson@usace.army.mil
[4] The College of Wooster; jwilch13@wooster.edu
[5] The College of Wooster; nickthebomb@hotmail.com

Two interstadial, tree ring width chronologies, built with 75 tree cores and cross sections from in situ forests and detrital logs collected from 40 locations in a valley near the base of Mount Wordie in Wachusett Inlet in the East Arm of Glacier Bay National Park and Preserve. Calibrated radiocarbon dating and wiggle matching provides absolute ages for the ring-width series which shows that the trees were likely killed by a series of ice-related sedimentation events approximately 3,300 yr BP and again approximately 4,000 yr BP. Trees are linked stratigraphically to sediment packages indicating the glacial advances of glaciolacustrine, deltaic, glaciofluvial, and glacial diamicts. The 4,000 yr BP chronology spans 570 years, whereas the 3,300 yr BP chronology spans 280 years documenting the duration forest growth and ice-free conditions.

The two ring-width chronologies strongly cross date with a regional tree-ring-width series from Geikie Inlet and Muir Inlet in the East and West Arms, in Glacier Bay respectively. Crossdating over this broad region suggests that the two glacial expansions covered much of the Glacier Bay upper to mid watershed. The added resolution of tree-ring dating reveals ice in the West Arm expanding to the mouth of Geikie Inlet, 30 km southwest of Wachusett Inlet, decades before those within the Mt. Wordie valley. Farther to the north, approximately 15 km, the Muir Inlet glacier expanded several decades following the upper Wachusett Inlet ice. The coupled use of radiocarbon dating with tree-ring-width chronologies adds decadal resolution to the glacial chronology within Glacier Bay National Park and Preserve.

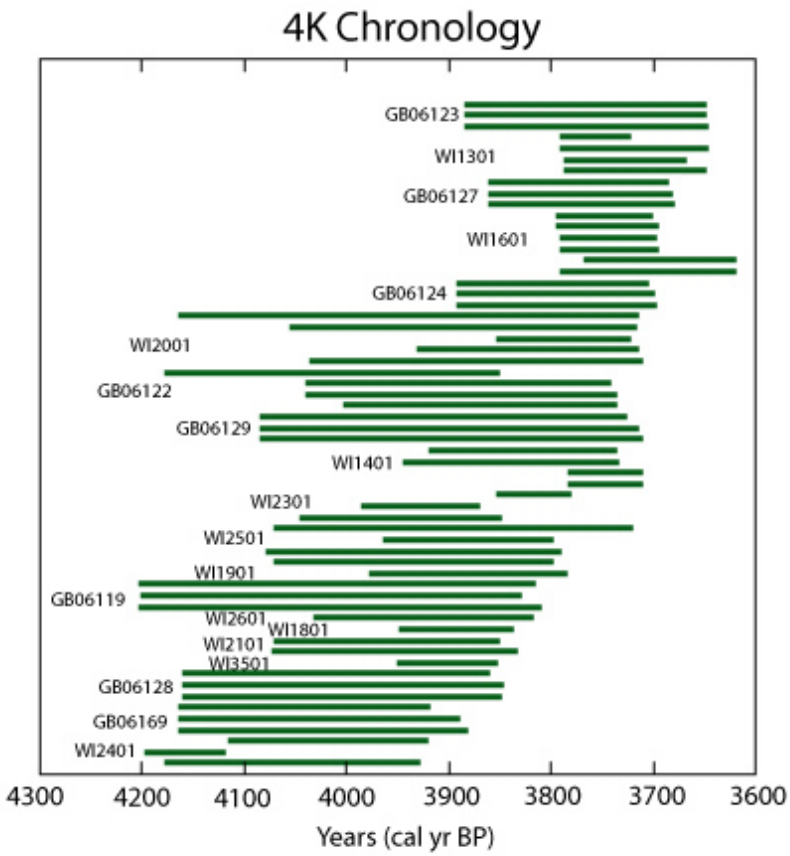

Fig 1. The tree ring chronology of the glacial advance between 3700-3900 cal yr BP. In this robust series several kill dates can be observed noting the advance of the Cushing-Plateau glacier in Wachusett Inlet

Fig 2. A buried forest that was sampled and dates the Wachusett Inlet glacial advance at 3700 cal yr BP. This figure also clearly shows the sediment stratigraphy in the unnamed valley below Mt. Wordie in Glacier Bay National Park and Preserve.

HYDRO-CLIMATE AND SEDIMENT VARIATIONS AT ALLISON LAKE, SOUTH-CENTRAL ALASKA.

Arnold, Megan S [1]; **Kaufman**, Darrell [2]

[1] Northern Arizona University; msa69@nau.edu
[2] Northern Arizona University;

Allison Lake, Alaska is glacier-fed with minerogenic laminations that appear to be varves. The proximity to Valdez (7 km to the north), where a meteorological record extends from 2011-1909, and to Solomon Lake, where a discharge record is available from 2010-1987, enables the physical properties of its varved sediments to be readily correlated with hydro-meteorological records. The purpose of this study is to compare the modern sediment record with hydro-meteorological data in order to classify varve characteristics for the instrumental sedimentary years. Several studies of glacial-fed lakes in a similar climate regime have shown that varve thickness and discharge were strongly correlated (Cockburn and Lamoureux, 2007; Kaufman et al., 2011; Menuous and Clague, 2008).

Allison Lake is 55 m deep with an area of 1.2 km^2. The lake is and situated in a steep-sided trough that was eroded by Allison Glacier, which now terminates 3 km up-valley. Allison Glacier feeds the primary inlet to Allison Lake, which flows through a vegetated braided stream plain (0.23 km^2) before entering the lake. The main outlet is at the northern end where the lake is dammed by bouldery drift-mantled bedrock that is likely a moraine formed during an early Holocene advance or standstill of Allison Glacier. In 1983, the glacier covered approximately 20% of the 17 km^2 watershed.

On the basis of the 102-year-long instrumental record, monthly average precipitation at Valdez peaks during August (15.8 cm) and September (22.2 cm). The inflow hydrograph of Solomon Lake from 2010-1987 indicates that the amount and timing of April – June inflow is controlled by increasing minimum temperatures and subsequent snowmelt (Figure 1), whereas July – October inflow peaks are controlled by precipitation events. Daily discharge of the outflow of Allison Lake was recorded from August 2008 – March 2011, and is strongly correlated with the inflow to Solomon Lake ($r^2 = 0.73$, $p = 0.016$; all p values were adjusted for autocorrelation).

A sediment trap deployed in Allison Lake from August 2009 – July 2010 collected suspended material at 10- or 30-day intervals (Figure 2). Most (80%) of the sediment accumulated from August through November, 2009, with a flux of 5.3×10^{-4} $g/cm^2/day$. Sedimentation decreased by a factor of ten from December through April 2010, while the lake had ice cover. Sedimentation picked up slightly between May and July, 2010. The highest flux of sediment was August 15-24, 2009, with 2.4×10^{-3} $g/cm^2/day$. This interval coincides with the two peak river flow discharges of the year, which occurred on August 16-17, 2009 with a mean daily discharge of 4.8 and 4.0 m^3/s, respectively. On August 16, 2009 5.0 cm of precipitation fell. Although the total 2009 ASO (August, September, October) discharge was less than the total 2010 MJJ (May, June, July) discharge, the incrementing traps indicate that peak annual discharges, which result from autumn precipitation, are the primary control on varve thickness.

Several sediment cores were collected proximal, central, and distal to the inlet in 2006, 2009, and 2010. Age constraints are given by ^{137}Cs and $^{239+240}Pu$ profiles (1963 peak), excess ^{210}Pb, and tephra presumed to be from the August 18, 1992 eruption of Mt. Spurr. Laminated selections in a 2009 core from the central site were correlated with laminations in a 2006 core from the proximal site. The proximal core indicates that the uppermost lamination (which is below a turbidite) at the central site was formed in 2005. Correlations between the central and distal site cores were made with the tephra and isotope age constraints and marker laminations. Based on the age constraints, the distal cores seem to be "missing" laminations; however, some laminations have unusually thick clay layers, suggesting that they might have been deposited during multiple years.

The Solomon Lake discharge record is strongly correlated to Allison Lake discharge and is used for comparison with varve thickness. Over the 18 years of discharge record (1987-2005), varve thickness at the central site is positively correlated with the sum of the three largest daily flows of each month for ASO ($r^2 = 0.38$, $p = 0.004$), ASO total discharge ($r^2 = 0.39$, $p = 0.004$), and JAS total precipitation ($r^2 = 0.46$, $p = 0.001$).

To simulate discharge for years prior to 1987, the meteorological parameter with the strongest correlation with discharge (ASON precipitation $r^2 = 0.39$, $p = 0.001$) is used for correlations with varve thickness. From 1965-2005, varve thickness and ASON precipitation are well correlated ($r^2 = 0.21$, $p = 0.002$). In contrast, from 1964-1909 the correlations are insignificant ($r^2 = 0.08$, $p = 0.03$). The strongest correlation is with total annual precipitation (April-March, $r^2 = 0.19$, $p = 0.001$). We are presently unsure as to what might be the cause of this apparent discrepancy, although turbidites might have eroded layers at the central core site. Work is underway to compare the varve record there with a site more distal to the inflow.

Cockburn, J., Lamoureux, S., 2007, Century-scale variability in late-summer rainfall events recorded over seven centuries in subannually laminated lacustrine sediments, White Pass, British Columbia: Quaternary Research, v. 67, p. 193-203.

Kaufman, C., Lamoureux, S., Kaufman, D., 2011, Long-term river discharge and multidecadal climate variability inferred from varved sediments, southwest Alaska: Quaternary Research, v. 76, p. 1-9.

Menounos, B., Clague, J., 2008, Reconstructing hydro-climatic events and glacier fluctuations over the past millennium from annually laminated sediments of Cheakamus Lake, southern Coast Mountains, British Columbia, Canada: Quaternary Science Reviews, v. 27, p. 701-713.

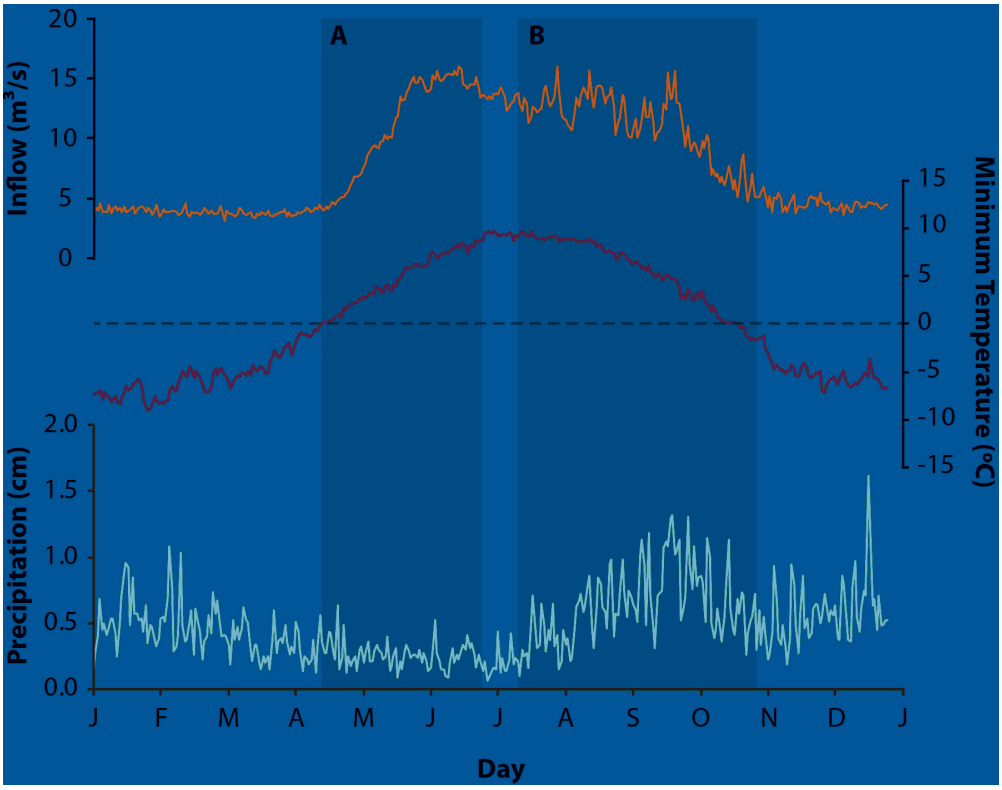

Fig 1. Averages of daily inflow to Solomon Lake, minimum temperature, and daily precipitation from 2010-1986. In April, coinciding with minimum temperatures exceeding 0 oC, inflow begins to increase and peaks in June (gray box A). Inflow is controlled by precipitation events in late summer and autumn months (gray box B).

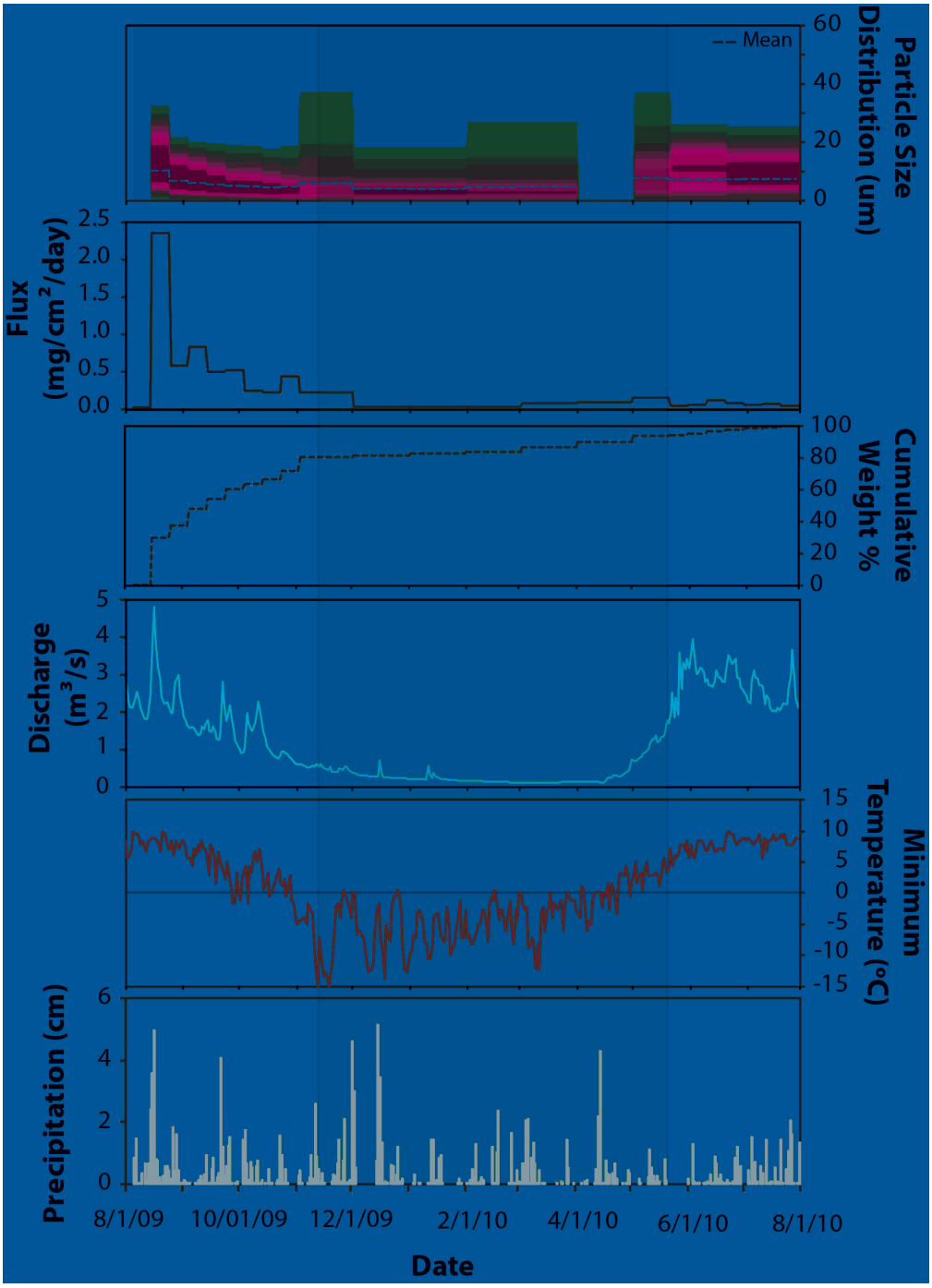

Fig 2. Lake-bottom sediment flux and hydro-meteorological conditions. Sediment flux and mean grain size was greatest August 5-August 14, 2009 coinciding with highest precipitation and discharge peaks. Flux and particle size steadily decreased into the winter, with little sediment entering the trap. Spring discharge increased with minimum temperatures exceeding 0 oC. Gray box highlights presence of lake ice inferred from lake-surface temperature.

WHEN GLACIERS LEFT, AND WHEN THEY CAME BACK: NEW ^{10}BE AGES ON DEGLACIATION AND NEOGLACIATION IN THE BROOKS RANGE, ARCTIC ALASKA

Badding, Michael E [1]; **Briner**, Jason P [2]; **Kaufman**, Darrell S [3]

[1] University at Buffalo; mbadding@buffalo.edu
[2] University at Buffalo; jbriner@buffalo.edu
[3] Northern Arizona University; Darrell.Kaufman@nau.edu

Although well-developed records of ice-sheet retreat from Late Pleistocene maximum positions exist for most of the Arctic, few records of alpine glacier retreat are available. Yet, such records of deglaciation are important because little is known about how Arctic alpine glaciers fit the pattern of deglaciation found elsewhere across the Northern Hemisphere. The Brooks Range, Arctic Alaska, is an exception because it is a vast stretch of Arctic mountains that were glaciated by alpine glaciers and not coved by an ice sheet during the Last Glacial Maximum (LGM). In addition to providing a record of deglaciation since the LGM, the Brooks Range hosts an outstanding sequence of Neoglacial moraines, unique to the Northern Hemisphere. The Little Ice Age (LIA), typically representing the largest late Holocene advance, removes geomorphic evidence of earlier Neoglaciation in most places across the Northern Hemisphere. The Brooks Range contains numerous mid-Holocene moraines that lie downvalley of LIA moraines (Calkin and Ellis, 1980; Ellis and Calkin, 1984), which are currently dated with lichenometry. This detailed record provides a unique opportunity to obtain absolute 10Be exposure dating chronologies on pre-LIA moraines to constrain the initiation of Neoglaciation and the timing of subsequent phases of glacier maxima. In addition, our 10Be chronology will allow us to improve existing lichen growth curves, which might result in broader age refinements of the remarkable chronology of Holocene glaciation in the Brooks Range.

We investigated two valleys, located ~200 km apart in the north-central Brooks Range to determine the timing of deglaciation and to date the oldest Neoglacial moraine to constrain the onset of Neoglaciation. We use cosmogenic 10Be exposure dating, which has yet to be used in the Brooks Range to date deglaciation or Holocene moraines. We sampled boulders on the outermost pre-LIA moraines in two valleys previously dated by lichenometry (Ellis and Calkin, 1984; Lamb, 1984). In addition, we sampled transects of exposed bedrock surfaces along valley bottoms to develop a chronology of deglaciation as glaciers receded into their cirques.

Our first site, the eastern headwaters of Kurupa River valley, hosts three small (<1 km2) modern cirque glaciers (Figure 1). Samples were collected from three boulders on the outermost Holocene moraine fronting Fireweed West glacier (Figure 1,2), estimated by lichenometry to be ~3,300 yr old (Lamb, 1984). Four samples from valley-bottom bedrock were collected down valley of the Holocene moraines, spanning a distance of ~5 km. Our samples collected in Kurupa River valley accompany a companion study (Boldt et al., this volume) of proglacial lacustrine sediment analysis for a high resolution record of Holocene climate and glacier change. At our second site, an unnamed tributary valley to Itikmalak River valley, four samples were collected from the outermost Holocene moraine of Triple East Glacier, previously estimated to be ~4,200 yr old (Ellis and Calkin, 1984). Unsuitable bedrock did not allow for valley-bottom samples to be collected in this valley; however, we collected a transect of valley-bottom bedrock downvalley of present glaciers from a valley ~20 km to the east. At Roche Moutonée Valley (informally named), a tributary to Atigun River valley, ice-sculpted bedrock was sampled at five locations.

At the time of this abstract submission, we have three 10Be ages from the outermost Holocene moraine in Kurupa Valley, which are 2770±110, 2650±70 and 2180±80 yr BP. These ages broadly agree with moraine age estimated from lichenometry. Seventeen additional 10Be ages, from the two sites combined, are expected prior to the Workshop.

Calkin P.E., and Ellis, J.M., 1980, A lichenometric dating curve and its application to Holocene glacier studies in the Central Brooks Range, Alaska: Arctic and Alpine Research, v. 12, no. 3, p. 245-264.
Ellis, J.M., and Calkin, P.E., 1984, Chronology of Holocene glaciation, central Brooks Range,Alaska: Geological Society of America Bulletin, v. 95, p. 897-912.
Lamb, B., 1984, Geomorphology of the Upper Kurupa River Valley system, Brooks Range, Alaska: Master of the Arts Thesis, University at Buffalo, 150 p.

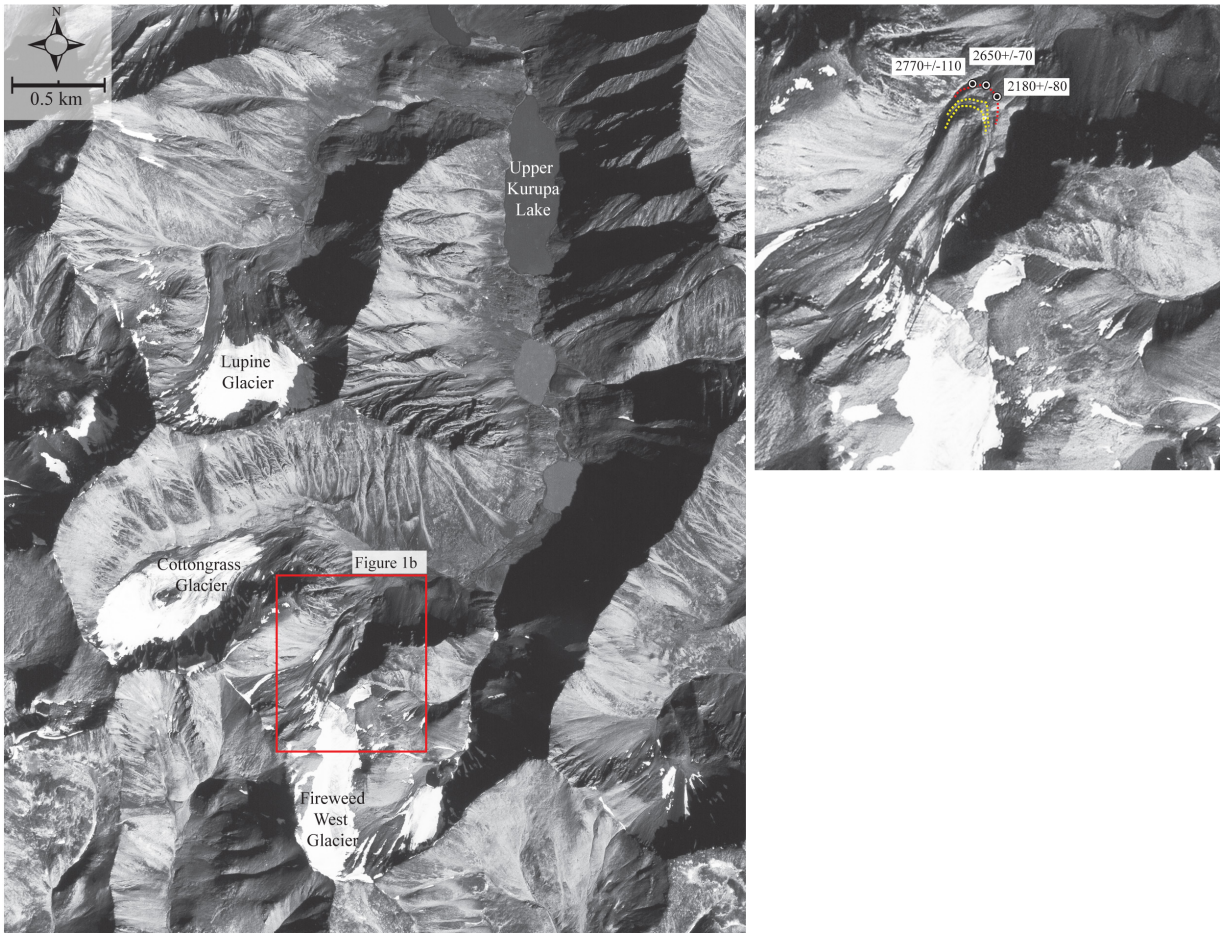

Fig 1. 1982 aerial photograph of the headwaters of Kurupa River valley with remaining glaciers labeled. 10Be exposure dating samples for deglaciation chronology were collected from valley bottom north and south of Upper Kurupa Lake. Moraine complex fronting Fireweed West Glacier where moraine boulder samples were collected. Yellow dashed lines highlight Little Ice Age (LIA) extent and red dashed line shows pre-LIA extent. Three samples were collected from perched moraine boulders on outer-most Holocene moraine, with reported ages shown.

Fig 2. Field photographs of perched moraine boulders on outer-most Holocene moraine fronting Fireweed West Glacier.

ON THE SPATIAL DISTRIBUTION OF GLACIAL EROSION RATES IN THE ST. ELIAS MOUNTAINS, ALASKA

Barker, Adam D [1]; **Hallet**, Bernard [2]; **Headley**, Rachel M [3]

[1] University of Washington; adbarker@uw.edu
[2] University of Washington;
[3] Universität Tübingen;

The rugged mountains of SE Alaska have recently received considerable attention because of the proposed link between climate, tectonics and landscape evolution. In particular, the St. Elias Mountains are an ideal region to study this link where the dominant agent shaping the landscape is glacial ice. The region also exhibits some of the most extreme relief resulting from ongoing crustal convergence coupled with focused, vigorous erosion. Prevailing winds off the northeastern Pacific, together with orographic effects, result in heavy precipitation and, at high altitudes, snow, which sustains the largest temperate glaciers on the planet. These glaciers are particularly erosive where massive amount of ice funnel through relatively narrow valleys. Despite this concept of tectonic:climatic interactions, little is known about the role of glaciers in shaping SE Alaska, and in the crustal evolution in the region. Past exhumation studies have explored potential linkages with climate and the glaciers in the region (Berger et al., 2008) and glaciological studies of individual glacier systems have shed light on the spatial variation in erosion rates within a single valley (Headley et al., submitted); however, there are no broad, orogenic-wide studies to define quantitatively the spatial variation in the erosive potential of the major glacier systems in the region.

Herein we define the likely spatial variation in erosion rates of glaciers throughout the St. Elias Mountains assuming that the rate of erosion scales with the amount of energy available for erosion per unit time and per unit area of the glacier bed. We define an erosion index that scales with the product of the ice flux and glacier surface slope, paralleling what is commonly done in studies of bedrock incision by rivers (e.g., Finlayson et al., 2002). The ice flux is approximated by the balance flux based on mass balance profiles from Zhang et al. (2007) and the regional topography. The resulting map of erosive index shows two hotspots where rates of erosion (and hence uplift) are extremely high. The first hotspot is in the Seward Throat where the Malaspina/Seward glacier system cuts across high topography near Mt St. Elias. The second hotspot is further east, about 10 km north of the Hubbard glacier terminus. This position is geodynamically of special interest because this is where strike-slip motion along the Fairweather fault transitions to convergence across many structures, and is thought to be a region of preferentially weakened crust (Koons et al., 2010). Through a relatively simple approach, we have delineated areas of rapid erosion that can be used to guide geodynamics models of landscape and tectonic evolution.

Berger, A.L., J.A. Spotila, J.B. Chapman, T.L. Pavlis, E. Enkelmann, N.A. Ruppert, and J.T. Buscher, 2008, Architecture, kinematics, and exhumation of a convergent orogenic wedge: A thermochronological investigation of tectonic-climatic interactions within the central St. Elias orogen, Alaska: Earth and Planetary Science Letters,v. 270, p. 13-24.

Finlayson, D.P., D.R. Montgomery, and B. Hallet, 2002, Spatial coincidence of rapid inferred erosion with young metamorphic massifs in the Himalayas: Geology, v. 30, no. 3, p. 219-222.

Headley, R.M., B. Hallet, G. Roe, and E. Waddington, Spatial pattern of glacial erosion rates in the St. Elias range, Alaska, inferred from a realistic model of glacier dynamics: Journal of Geophysical Research - Earth Surface. Submitted Nov. 29, 2011; 2011JF002291

Koons P.O., B.P. Hooks, T. Pavlis, P. Upton, and A.D. Barker, 2010, Three-dimensional mechanics of Yakutat convergence in the southern Alaskan plate corner: Tectonics, v. 29, TC4008, doi:10.1029/2009TC002463.

Zhang, J., U.S. Bhatt, W.V. Tangborn, and C.S. Lingle, 2007, Response of glaciers to northwestern North America to future climate change: an atmosphere/glacier hierarchical modeling approach: Journal of Glaciology, v. 46, p. 283-290.

THE ECOLOGY OF DECAYING ICE-WEDGES: NOVEL HABITATS IN A POLAR DESERT

Becker, Michael S [1]; **Pollard**, Wayne H [2]

[1] McGill University; michael.becker@mail.mcgill.ca
[2] McGill University; michael.becker@mail.mcgill.ca

The Arctic is set to experience greater change due to global warming than lower latitude areas, with significant effects on both the ecology and geomorphology of the region (Kaplan & New, 2006). However, the expected effects of climate change on geocryological processes may vary due to the potential vegetative buffer of the surrounding ecosystem (Schuur et al., 2008). To what extent can an ecosystem influence its own development and environment by mediating the effects of changing climate? Many climate/permafrost models have yet to incorporate the idea of an adaptive ecosystem in response to global warming (Kaplan & New, 2006). The idea of a linear geocryogenic response does not take into account the insulation properties of vegetation that may expand or decrease depending on the reaction of the biotic community to a warming climate. Indeed, the idea that vegetative and geomorphic interactions are large and reciprocal is one not fully stressed in the literature.

The model system to be examined is thaw ponds created by ice-wedge thermokarst on Ellesmere and Axel Heiberg Islands in the Canadian High Arctic. Thaw ponds catalyzed by ice-wedge thermokarst represent a particular type of pond that may expand in frequency and size given predictions for increasing atmospheric temperature. As the tops of ice-wedges are in equilibrium with the permafrost active layer, any increase in ground temperature will result in localized subsidence over the ice-wedge and an increase in available groundwater. As the active layer is shallow in the high arctic, it is unlikely that this groundwater would meet subsurface aquifers, and so draining of the ponds through continued active layer deepening is unlikely. Thus, these thaw ponds should show continued expansion in number and size, resulting in localized pooling of water and nutrients. These novel habitats will have different selective pressures than the surrounding polar desert and may create oases of biodiversity in an otherwise sparse landscape (see Figure 1). Given the rate and intensity of warming, what can we expect for thaw pond spread considering a possible negative feedback cycle with the concurrent spread of vegetation cover?

With new habitats available, the usual scenario described is one where species and ecotypes from more temperate latitudes will advance northward as arctic climatic conditions become more 'hospitable', and these invading species will replace locally adapted arctic-specialists. This view ignores a key alternative – the adaptive phenotypic plasticity of arctic plants will allow them to persist or potentially thrive in response to a warming climate. So will temperate species colonize and outcompete locals in the artic, or will the plasticity of endemic arctic species allow them to persist and restructure their communities? Phenotypic plasticity can allow for plant survival and development in varying environments (Pigliucci et al., 2006), and with sufficient adaptive capacity they may persist in their local environment despite changing pressures (Lindner et al., 2009). Indeed, short-term plasticity can allow for plants to compensate for rapid change (Pigliucci et al., 2006). Hamrick (2004) states that large genetic diversity within a population would improve their ability to rapidly adapt to a new environment, which could pose significant problems for arctic communities given their lower rates of sexual reproduction and lower rates of genetic mixing (Bauert, 1996). Thus, given these low rates in arctic plants it is likely that phenotypic plasticity instead of genetic diversity would allow resident arctic vascular plants to withstand rapid climate change. This native plasticity may be enough to outcompete new colonization by lower-latitude invaders.

Interestingly, the ecotypic differentiation of Arctic plants may mean that certain populations more suited to the new climate will persist, such that native community restructuring occurs and the entire specie is not lost. There is a commonly held belief that there is little genetic diversity among arctic plants because the environment is spatially uniform. This is largely untrue, as the arctic zone has a huge

diversity of microsite climates that produce unique plant habitats that are exposed to their own set of selective pressures (Murray, 1987). This microsite heterogeneity has produced relatively high genetic diversity within even clonal plant populations through diversifying selection (Ellstrand & Roose, 1987). This occasional sexual reproduction in clonal plant species is a vital component of survival (Bauert, 1996), and so coupled with phenotypic plasticity may allow for persistence in the face of rapid change. Thus, the more plastic species in an ecosystem may be able to persist long enough for sexual reproduction, and true evolutionary adaptation, to take place.

The aim of this study is to address three primary hypotheses concerning ice-wedge thermokarst and their resulting thaw ponds: 1) Geomorphic and vegetative interactions are large and reciprocal, where vegetation growth buffers ice-wedges from runaway decay. 2) The ecosystem mediates change in permafrost dynamics of thaw ponds, creating novel environmental selective pressures. 3) High arctic natives will persist in climate change; and local community restructuring will predominate over invasive colonization.

Bauert, M.R., 1996, Genetic diversity and ecotypic differentiation in arctic and alpine populations of Polygonum viviparum: Arctic and Alpine Research, v. 28, p. 190-195.

Ellstrand, N.C., & Roose, M.L., 1987, Patterns of genotypic diversity in clonal plant species: American Journal of Botany, v. 74, p. 123-131.

Hamrick, J.L., 2004, Response of forest trees to global environmental changes: Forest Ecology and Management, v. 197, p. 323–335.

Kaplan, J.O, & New, M., 2006, Arctic climate change with a 2°C global warming: timing, climate patterns and vegetation change: Climatic Change, v. 79, p. 213-241.

Lindner, M., Maroschek, M., Netherer, S., Kremer, A., Barbati, A., J., G.-G., Seidl, R., Delzon, S., Corona, P., Kolstrom, M., Lexer, M.J. & Marchetti, M., 2009, Climate change impacts, adaptative capacity, and vulnerability of European forest ecosystems: Forest Ecology and Management, v. 259, p. 698–709

Murray, D.F., 1987, Breeding systems in the vascular flora of arctic North America: In Urbanska, K. M. (ed.), Differentiation Patterns in Higher Plants. London: Academic Press, p. 239- 262.

Pigliucci, M., Murren, C.J. & Schlichting, C.D., 2006, Phenotypic plasticity and evolution by genetic assimilation: Journal of Experimental Biology, v. 209, p. 2362–2367.

Schuur, E.A.G, Bockheim, J., Canadell, and others, 2008, Vulnerability of permafrost carbon to climate change: implications for the global carbon cycle: BioScience, v. 58, p. 701- 714.

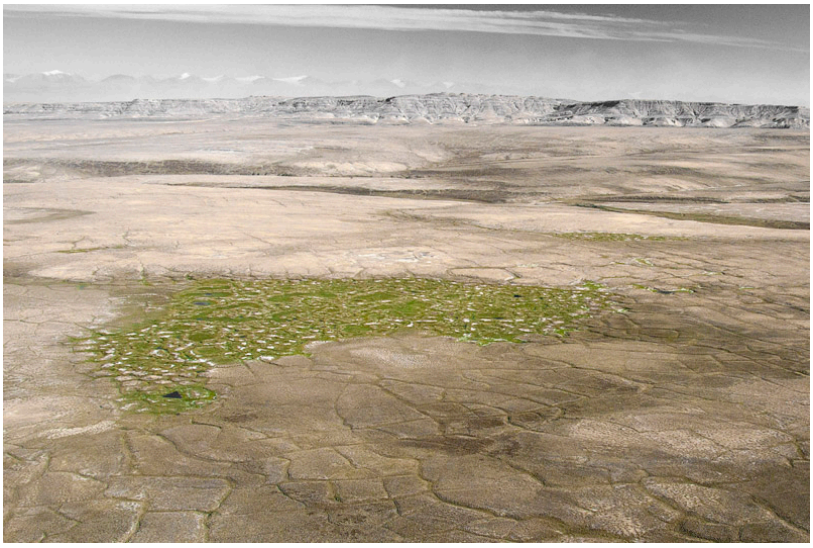

Fig 1. Abundant biomass and diversity resulting from thermokarst in a polar desert.

A HIGH RESOLUTION STUDY OF HISTORICAL CLIMATE CHANGES AND HUMAN IMPACTS ON THE NORTH ATLANTIC - NORTH SEA BOUNDARY: THE SHETLAND ISLANDS CLIMATE AND SETTLEMENT PROJECT

Bigelow, Gerald F. [1]; **Jones**, Michael E. [2]; **Retelle**, Michael J. [3]; **Johnson**, Beverly J. [4]; **Ambrose Jr.**, William G. [5]

[1] Bates College; gbigelow@bates.edu
[2] Bates College; mjones@bates.edu
[3] Bates College; mretelle@bates.edu
[4] Bates College; bjohnso3@bates.edu
[5] Bates College; wambrose@bates.edu

Scotland and its Northern and Western Isles contain many coastal sand environments where humans have lived at different periods, and then abandoned the areas when their aeolian sands remobilized and buried farms, fields and fishing settlements. Thus, today many archaeological sites of different periods have been exposed on beaches and dune systems through marine and aeolian erosion (Griffiths & Ashmore 2011), a process that is anticipated to intensify as sea levels rise with global warming, and as oceanic storms increase in frequency and/or strength in the mid- to high latitudes (ACIA 2004).

Nearly 40 years ago the pioneering climate historian H. H. Lamb proposed that major phases of coastal aeolian sand movements on European coasts, and their succeeding environmental catastrophes, were associated with climate changes, particularly episodes of rapid cooling (1977, 129). He also proposed that the Little Ice Age ca. A. D. 1300-1800 caused the most extensive sand movements in North Sea and North Atlantic regions over the past two thousand years, and that climate-correlated, great storms were key agents in dynamic transformations of coastal sand landscapes (1991).

The Shetland Islands Climate and Settlement Project (Bigelow et al. 2005; Bigelow et al. 2007) is investigating these possible links between decadal trends in Little Ice Age cooling, storminess, and destructive mass mobilizations of sand on beaches and dune systems in the UK's northernmost islands. Shetland's location on the edge of the Eurasian continental shelf, in a position of sensitivity to both North Atlantic Current and North Atlantic Oscillation variability, makes it a prime location for assessing relationships between climate processes, extreme weather events, and coastal vulnerability (Dawson 2007). The islands also contain multiple, aeolian sand environments, and the SICSP is outlining the environmental history of the largest, which is today called Quendale Links. However, until the later 1600s A.D. the Quendale area was also occupied by an agriculturally-rich township called Broo, which was one of the most valuable properties in Shetland. Historical records demonstrate that the Broo Township was completely destroyed by blowing sand by the mid-1700s (Irvine 1987:87). This presentation will provide an update on our project's multidisciplinary research activities that are addressing the questions of when, why and how the sands of Quendale Beach annihilated this early modern community; the possible involvement of Little Ice Age climate change in the process; and how humans responded to the catastrophe.

ACIA 2004 Impacts of a changing climate: Arctic Climate Impact Assessment. New York: Cambridge University Press.
Bigelow, G. F.; Ferrante, S. M; Hall, S. T.; Kimball, L. M.; Proctor, R. E.; Remington, S. L. 2005 Researching catastrophic environmental changes on northern coastlines: a geoarchaeological case study from the Shetland Island. Arctic Anthropology v. 42 (1), p. 88-102
Bigelow, G. F.; Jones, M. E.; Retelle, M. J. 2007 The Little Ice Age, blowing sand and a lost township. The New Shetlander v. 240, p. 6-12.
Dawson, A. 2007 So foul and fair a day: a history of Scotland's weather and climate. Edinburgh: Birlinn.
Griffiths, D.; Ashmore, P. 2011 Aeolian archaeology: the archaeology of sand landscapes in Scotland. Scottish Archaeological Internet Report 48. www.sair.org.uk.
Irvine, J. W. 1987 The Dunrossness story. Lerwick: A. Irvine Printing Ltd.
Lamb, H. H. 1977 Climate: past, present and future. Vol. II. London: Methuen.
Lamb, H. H. 1991 Historic storms of the North Sea, British Isles and Northwest Europe. New York: Cambridge University Press.

Fig 1. An excavated building of the Broo Township, Shetland Islands, after it was cleared of 1.5 to 2 meters of aeolian sand deposits that also destroyed an entire settlement system during the 17th century AD. Photo: G.F. Bigelow

A LACUSTRINE RECORD OF MIDDLE- TO LATE-HOLOCENE GLACIATION FROM KURUPA LAKE, NORTH-CENTRAL BROOKS RANGE, ARCTIC ALASKA

Boldt, Brandon R [1]; **Kaufman**, Darrell S [2]; **Briner**, Jason P [3]

[1] Northern Arizona University; brb257@nau.edu
[2] Northern Arizona University;
[3] University at Buffalo;

Previous reconstructions of Holocene glacier fluctuations in the Brooks Range have focused on mapping and dating moraines (e.g., Elis and Calkin, 1984; Sikorski et al., 2009). While geomorphic research can provide the age and extent of maximum glacier positions, alpine glacier fluctuations are sensitive to minor and continuous changes in moisture balance and temperature that can only be identified in proglacial lake sediment. Therefore, a more continuous glacial record can be derived from an integrated approach that compares independently dated landforms with high-resolution lacustrine records (Bakke et al., 2010). We have dated and analyzed lake sediments that seem to record glacier fluctuations for the last 5500 cal yr BP. This continuous record of Holocene glacier fluctuations in the Brooks Range complements the moraine chronology with an independent approach, and will enable us to incorporate the data into a larger network of proxy climate records that will help to better understand the causes and effects of nonlinearities in Arctic climate variability.

The Kurupa River valley (Figure 1) is a glacial trough in the north-central Brooks Range carved into slightly metamorphosed, siliclastic, quartz-rich conglomerate, sandstone, and shale (Upper Devonian Kanayut Conglomerate) as well as carbonate bedrock (Mississippian Lisburne Limestone). Kurupa Lake is dammed by the terminal moraine of the Itkillik glaciation at the northern range front (Hamilton, 1982). The lake is 29.7 km2, 40 m at maximum depth, and is fed by several tributaries, including rain, snowmelt, and meltwater from eight rapidly disappearing north- to northeast-oriented cirque glaciers in their headwaters (Lamb, 1984). In 1982, these glaciers (n=8) were situated at a mean altitude of 1750 m above sea level (a.s.l.) with an average length of 825 m from headwall to terminus. Holocene moraines located several hundred meters from the modern glacier termini are generally ice-cored with hummocky surfaces and steep front slopes.

The accumulation area ratio (AAR) method for reconstructing paleoglacier equilibrium-line altitude (ELA), which assumes a fixed ratio between the accumulation and ablation area of a glacier, has been successfully applied in Alaska (e.g., Daigle and Kaufman, 2009; Sikorski et al., 2009). We assigned lichen ages to Holocene moraines by fitting Lamb's (1984) original moraine lichen measurements and our new measurements from a subset of moraines to the Brooks Range lichen growth curve of Calkin and Ellis (1980; with modifications by Solomina and Calkin, 2003, and Sikorski et al., 2009). Modern and paleoglacier boundaries were superimposed on a 10-meter/pixel digital elevation model in ESRI ArcGIS. An AAR of 0.55 was applied with raster math to calculate the ELA associated with the former glacier size that was reconstructed from each dated moraine.

Lake sediment cores were collected in July 2010 from Kurupa Lake, the farthest down-valley in a chain of four paternoster lakes. The sediments were photographed with high-resolution line-scan imaging and analyzed for gamma-ray attenuation (bulk density) at 1 cm interval (Figure 2) with a Geotek Multi Scan Core Logger XYZ at the University of Minnesota Limnological Research Center. The age model for the Kurupa Lake core incorporates six AMS radiocarbon ages from macrofossils and a Pu profile (1963 A.D. peak in activity).

The timing and magnitude of cirque glacier advances seem to correspond with variations in sediment bulk density from Kurupa Lake (Figure 3). We hypothesize that bulk density increases with glacier activity because clay and fine silt, characteristic of glacial flour, pack tighter than coarser-grained, non-glacial sediment. This is currently being tested with particle-size analysis of the lake sediments. A continuous density-inferred ELA record for the middle- to late-Holocene was constructed using a

regression model that relates glacier ELA to sediment bulk density. Fifteen moraines from five age groups as well as modern ELA data from seven individual cirque glaciers were included in the reconstruction. The sedimentary bulk density record was smoothed with a 50-year filter because glacier control on sedimentation is essentially constant over shorter time scales (Leonard, 1986). Moraine ages were clustered to the nearest 50-year interval (within the range of age uncertainty) for comparison with the lacustrine record, and the local ELA for each age group was calculated as the mean ELA of paleoglaciers therein. The local ELA of each cluster was paired with the sediment bulk density of corresponding age to produce the second-order polynomial regression (Figure 3). As a result, we can infer glacier size from sediment bulk density.

Our results are similar to other glacier reconstructions for the region that show cirque-glacier advances 1310 to 1860 AD (Little Ice Age), 1.3 ka, and 4.2 ka. An advance at 2.1 ka is inferred from the Kurupa Lake record, but is not obvious in other reconstructions; the 2.1 ka advance may correspond to the 2.9 ka advance described in previous moraine-based studies in the Brooks Range (Ellis and Calkin, 1984). The inferred glacier minima within the last 5.5 ka occurred 4.3 ka, 1060 to 1310 AD (Medieval time), and in the 20th century, with the greatest retreat occurring presently.

Bakke, J.S., Dahl, O., Paasche, O., Simonsen, J.R., Kvisvik, B., Bakke, K., and Nesje, A., 2010, A complete record of Holocene glacier variability at Austre Okstindbreen, northern Norway: an integrated approach: Quaternary Science Review, v. 29, p. 1246-1262.

Daigle, T.A., Kaufman, D.S., 2009, Holocene climate inferred from glacier extent, lake sedimentation, and tree rings at Goat Lake, Kenai Mountains, Alaska: Journal of Quaternary Science, v. 24, p. 33–45.

Ellis, J.M., and Calkin, P.E., 1984, Chronology of Holocene glaciation, central Brooks Range, Alaska: Geological Society of America Bulletin, v. 95, p. 897-912.

Hamilton, T.D., 1982, A late Pleistocene glacial chronology for the southern Brooks Range - stratigraphic record and regional significance: Geological Society of America Bulletin, v. 93, p. 700-716.

Lamb, B., 1984, Geomorphology of the Upper Kurupa River Valley System, Brooks Range, Alaska [Master's Thesis] Buffalo, University of New York, 135 p.

Sikorski, J.J., Kaufman, D.S., Manley, W.F., and Nolan, M., 2009, Winter accumulation at the equilibrium line of Little Ice Age glaciers, Brooks Range, Alaska: Arctic, Antarctic, and Alpine Research, v. 41, p. 138-150.

Solomina, O., and Calkin, P. E., 2003: Lichenometry as applied to moraines in Alaska, U.S.A., and Kamchatka, Russia. Arctic, Antarctic, and Alpine Research, 35: 129–143.

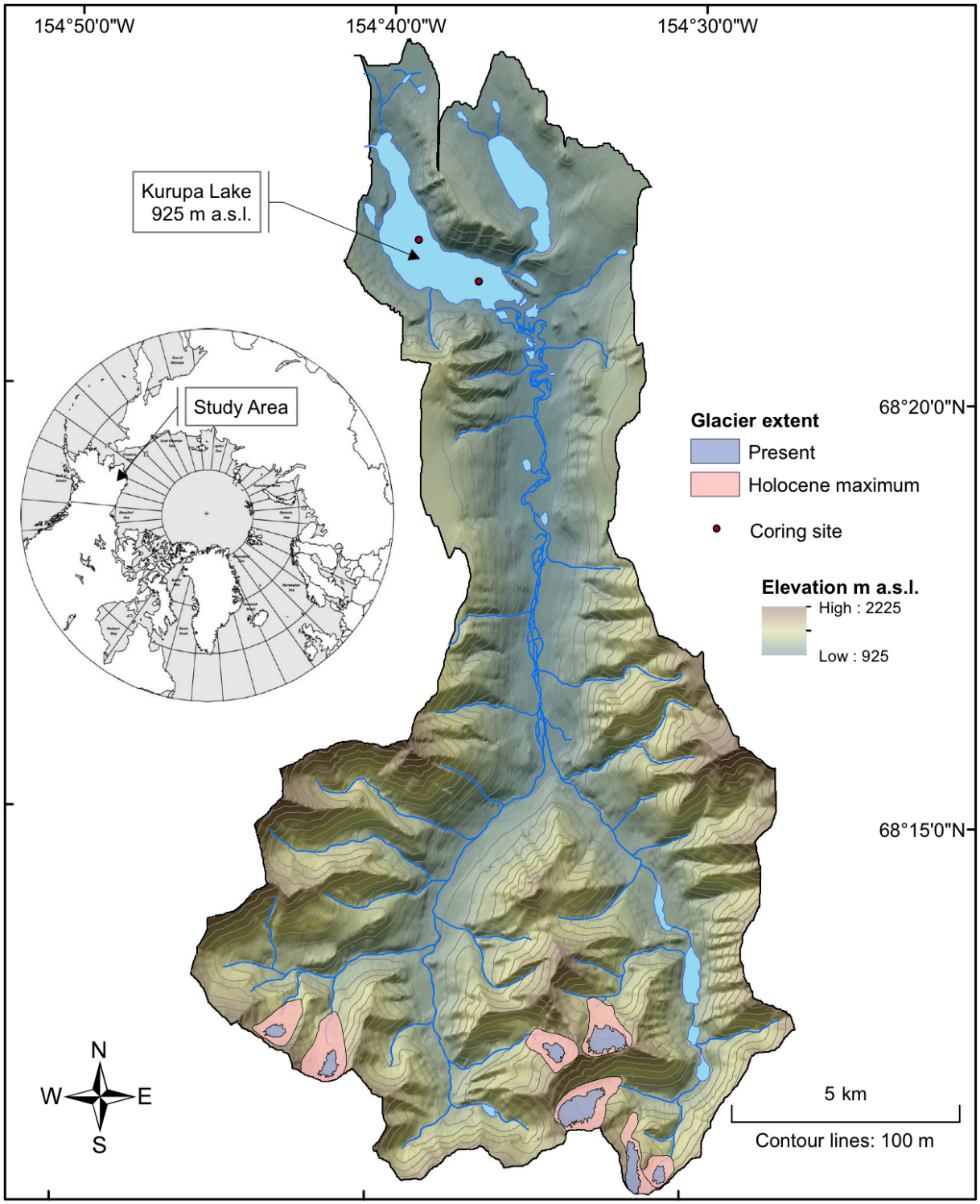

Fig 1. Map of the Kurupa River valley catchment area, showing locations of the coring sites in Kurupa Lake. Present and maximum Holocene glacier extents are indicated for glaciers with discernible lichenometrically dated moraines; based on Lamb (1984), air photographs, and recent fieldwork.

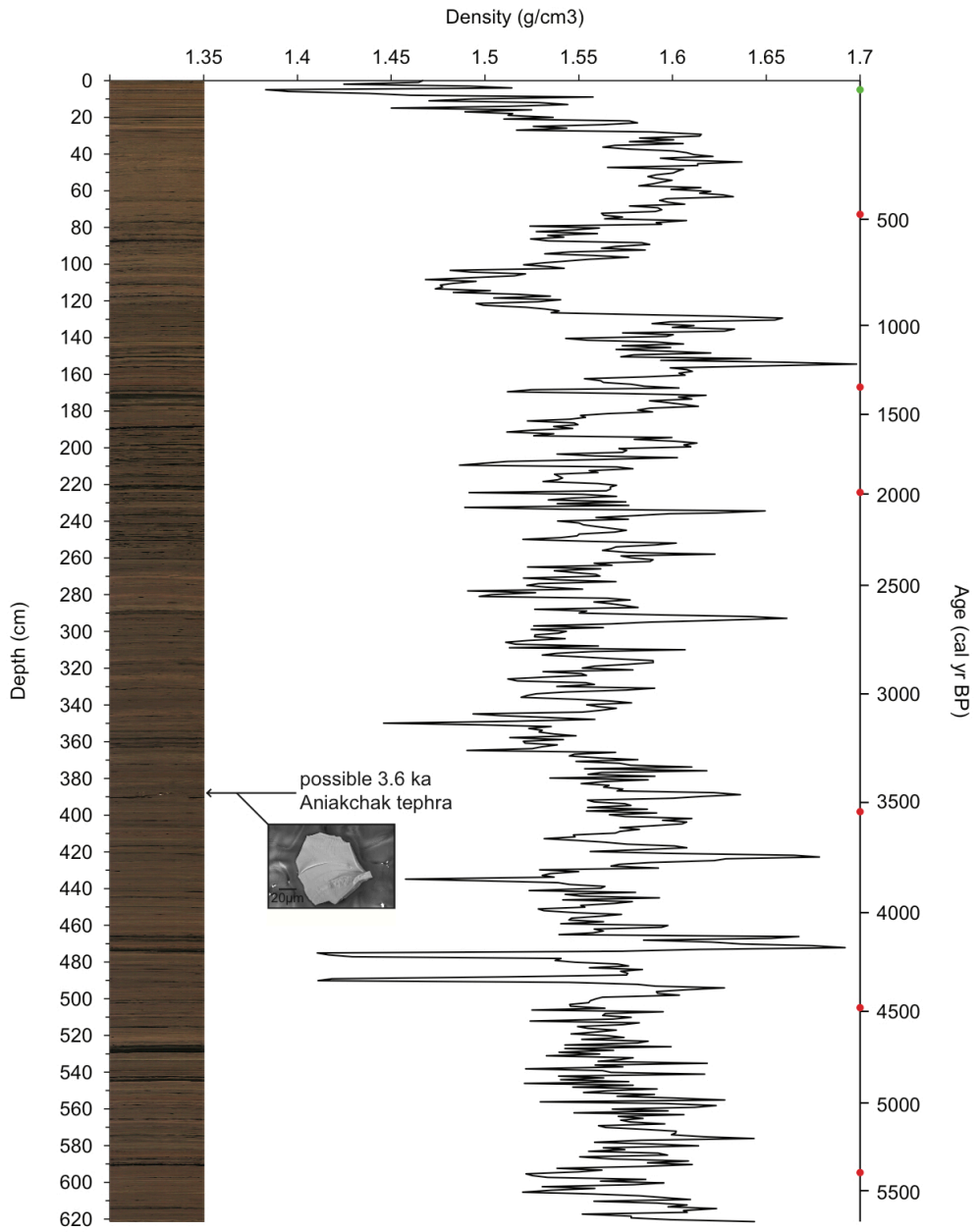

Fig 2. Physical variables from lake core (KU10-2). From left to right: line scan image of the core with depth scale; gamma-ray density; age scale based on cubic spline age-depth model; red circles indicate radiocarbon dates plotted at the weighted mean value of the calibrated ages, green circle indicates 1963 Pu peak.

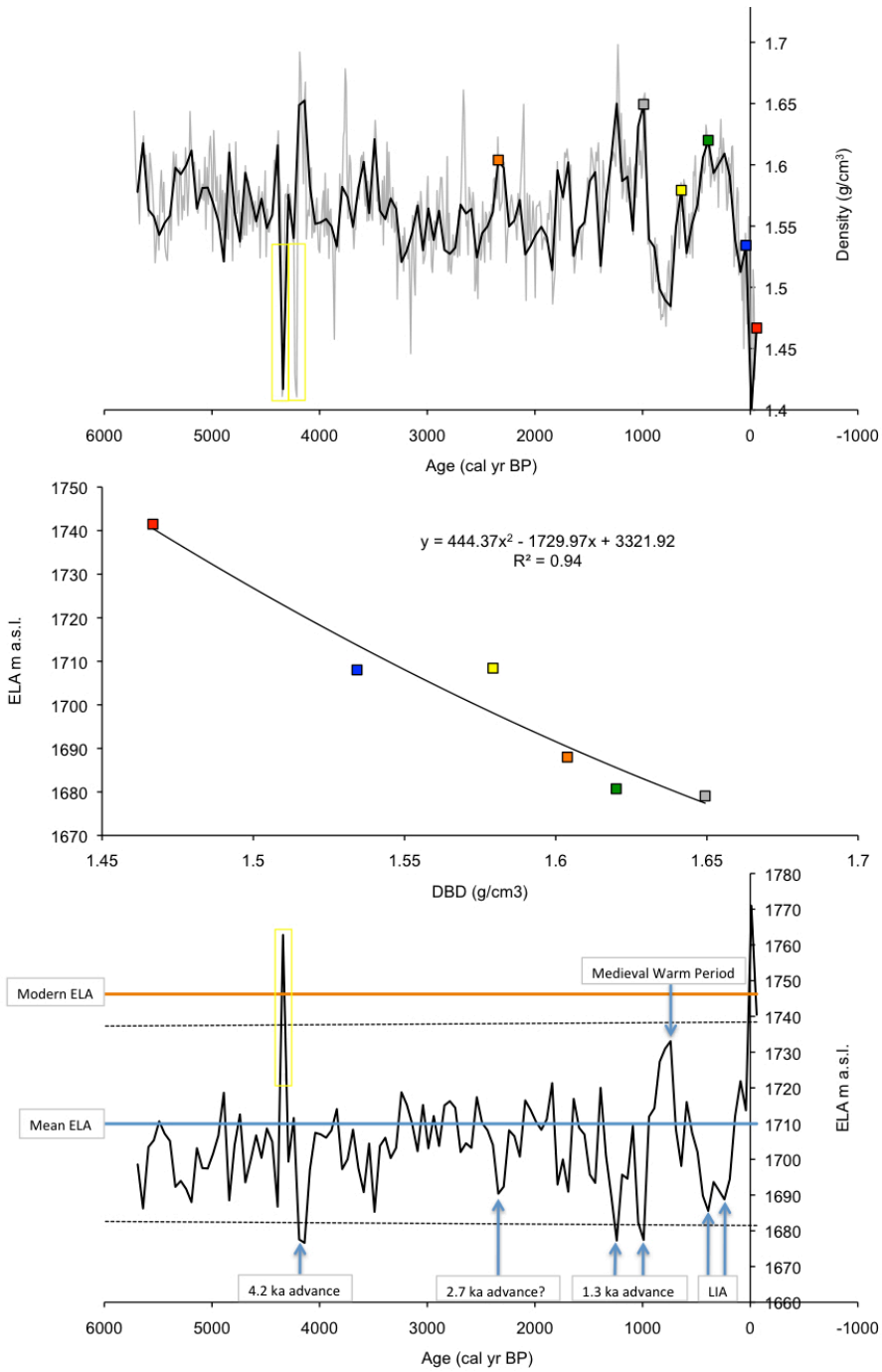

Fig 3. Figure shows the relationship between the density record from Kurupa Lake and Equilibrium Line Altitude (ELA) with estimated ages. (A) Squares indicate periods when the ELA is estimated, either based on historical data and/or lichenometric data. (B) Shows the statistical relationship between periods with known ELA (m a.s.l.) and density values. (C) The regression model is used to model a continuous ELA reconstruction for the middle- to late-Holocene.

WESTERN ARCTIC VULNERABILITY TO CLIMATE VARIABILITY OVER THE PAST 3.6 MYR: A NEW VIEW FROM SEDIMENTS DRILLED AT LAKE EL'GYGYTGYN, WESTERN BERINGIA

Brigham-Grette, Julie [1]; **Melles**, Martin [2]; **Minyuk**, Pavel [3]; , Lake Elgygytgyn Science Team [4]

[1] UMass Amherst; juliebg@geo.umass.edu
[2] Institute of Geology and Mineralogy, University of Cologne, Cologne, Germany; mmelles@uni-koeln.de
[3]; minyuk@neisri.magadan.ru
[4]; juliebg@geo.umass.edu

International Continental Deep drilling (ICDP) at Lake El'gygytgyn (67o30' N, 172 o 05' E; or "Lake E"), recovered lacustrine sediments dating back to 3.58 Ma that now provides the first time-continuous Pliocene-Pleistocene paleoclimate record of different interglacials from the terrestrial Arctic. While discontinuous, spatially diverse Pliocene and Pleistocene marine interglacial records are known from the arctic borderlands at the outcrop scale, the Lake El'gygytgyn record is critically important understanding the landscape response to different forcing factors operating across the Arctic since the mid-Pliocene warm period. The record is important for evaluating the sensitivity of the Arctic region to different forcings and to provide a template of Arctic climate variability that can be compared to other regions. Lake E modeling is framed around suites of sensitivity tests of Beringian climate response to the full range of forcing experienced over the last ~3.5 million years using a nested Global-Regional Climate Model (GCM-RCM). The Pliocene portion of the lake record (~3.58-3.0 Ma; a time when atmospheric CO2 levels may have been in the range of 400 ppm) has nearly twice the sedimentation rate as later Quaternary intervals, partly as a consequence of basin infilling but also presumably due to more rainfall and more active rivers at that time. The sediments are highly laminated in part and might be varved in sections. Studies of spores and pollen from this portion of the core show that the area was once dominated by trees, providing us with the pace of variability in Pliocene Arctic forests, which included species of pine, larch, spruce, fir, alder, and hemlock. Hemlock and tree pine pollen is exceptional for this latitude but the assemblage implies July temperatures nearly 8 degrees warmer than today with ~3 times the annual precipitation. Modeling suggests sustained forests at Lake E in both cold and warm orbits during this interval and restricted ice over Greenland. Extreme warmth in the Mid Pliocene Arctic occurs at the same time ANDRILL results suggest the WAIS was non-existent. The record includes a strong M2 cooling event at ~3.3 Ma to conditions like today, not glacial climates. This has major implications for reinterpreting isotopic shifts during this event in the North Atlantic. Warm interglacial portions of the core investigated so far are those correlative with MIS 5e, 9, 11 and 31 that differ in character, due to orbital forcing and feed backs. The lithofacies can be linked directly to other proxies of climate change and allow us to interpret climatic influences on the watershed as well as changing conditions related to lake productivity, lake ice cover persistence, runoff and clastic input and vegetation in the basin. Multi-proxy evidence shows that interglacials MIS 9, 11 and 31 were remarkably warmer than MIS 5e. A warm MIS 31 at Lake E occurred half a precession cycle after the last time ANDRILL shows direct evidence of the collapse of WAIS. MIS 11, in particular shows surprising similarities to Lake Baikal records and Dome C ice core paleorecords but is remarkably warm. The climate record from Lake E, especially the history of past interglacials, provides a fresh means of testing what controls polar amplification over time.

USING REWORKED BIVALVES AND PROGLACIAL-THRESHOLD LAKES TO CONSTRAIN GREENLAND ICE MARGIN CHANGE DURING THE HOLOCENE: NEW RESULTS FROM UPERNAVIK ISSTRØM

Briner, Jason P [1]; **Håkansson**, Lena [2]; **Bennike**, Ole [3]; **Kaufman**, Darrell [4]

[1] University at Buffalo; jbriner@buffalo.edu
[2] GEUS;
[3] GEUS;
[4] Northern Arizona University;

Knowledge of pre-historic changes of the Greenland Ice Sheet margin is important for determining the sensitivity of the ice sheet to climate change, constraining rates of retreat and advance during past climate excursions, and for evaluating ice sheet models. Our recent investigations in western Greenland have focused on generating reconstructions of ice margin change throughout the Holocene. Traditional glacial geomorphic reconstructions are challenged by the fact that the western Greenland Ice Sheet was less extensive during much of the Holocene than during its historical maximum advance, achieved during the last few centuries. We can partly overcome this challenge by using techniques designed to constrain the time period during which the ice sheet was smaller than its historical maximum extent. To do this, we: (1) use sediments in proglacial lakes beyond the historical moraine that record the ice margin advance into, and retreat out of, the lake catchment area, and (2) date marine fauna (e.g., bivalves) reworked into historical moraines, which provide the times when fjords within the historical limit were previously ice free.

We report new results from Upernavik Isstrøm, northwest Greenland. Upernavik Isstrøm has many similarities to other major Greenland outlet glaciers: velocity on the order of km/yr, discharge on the order of 10 km3/yr, large catchment area, 10s of km of retreat during the 20th century – and, not much is known about its behavior prior to the observational period. We constrain the deglaciation of Upernavik Isstrøm to be ~9500 cal yr BP, based on basal radiocarbon ages from two proglacial-threshold lakes adjacent to the present ice sheet margin. Following this time, the two proglacial lakes have remained ice free until sometime shortly after ~600 cal yr BP, when Upernavik Isstrøm advanced into their catchments, noted by the transition from organic- to minerogenic-rich sediments. Historical imagery indicates that our two study lakes transition back to non-glacial lakes during the last decade. Based on the position of the ice front when the lakes transitioned back to a non-glacial state, we estimate the magnitude of Upernavik Isstrøm's advance during the Little Ice Age to be ~15 km.

We constrain further the duration of mid-Holocene ice sheet retreat by dating bivalves reworked into the historical moraine near our study lakes. Our selection of six bivalves was guided by amino-acid racemization results from a small subset (n = 20) of what was collected (n = hundreds). The ages range from 530±60 to 5070±120 cal yr BP. The youngest bivalve provides a close maximum age for the historical advance of Upernavik Isstrøm, and is similar to the age constraint from the lake sediments of ~600 cal yr BP.

Although this is work in progress, we have learned so far that a combination of techniques can help elucidate the ice margin history of the Greenland Ice Sheet throughout the Holocene. The record from Upernavik Isstrøm so far mimics what we have found at Jakobshavn Isbræ, which also experienced an advance during the Little Ice Age on the order of 10s of km. The deglaciation of Upernavik Isstrøm occurred ~2000 years earlier than that of Jakobshavn Isbræ, which is consistent with prior studies showing the relatively early deglaciation of northwestern Greenland.

STRAIN RATE ESTIMATES ON MOUNT HUNTER, ALASKA: WHAT CAUSES CREVASSING AT AN ICE DIVIDE?

Campbell, Seth W [1]; **Kreutz**, Karl J [2]; **Arcone**, Steven A [3]; **Osterberg**, Erich C [4]

[1] University of Maine/US Army CRREL; seth.campbell@umit.maine.edu
[2] University of Maine; Karl.Kreutz@maine.edu
[3] US Army CRREL; Steven.A.Arcone@usace.army.mil
[4] Dartmouth College; Erich.c.osterberg@dartmouth.edu

Crevasse formation generally occurs when the tensile stress becomes greater than the tensile strength of the ice and the depth of crevasse propagation is theoretically reached when the overburden pressure surpasses the tensile stress. Crevasses have been linked to strain rates that range three orders of magnitude (0.001 and 0.163 a^-1) (Meier, 1958; Hambrey and Miller, 1978; Harper and others, 1998) making it difficult to model related important scenarios such as iceberg calving or fracture propagation. This significant variability results from the temperature dependant non-linear rheological properties of ice and the range of variables, such as water and debris inclusions (as in temperate glaciers) which can influence ice flow dynamics. Unfortunately, most crevasse studies have been conducted in complex conditions on temperate glaciers. Herein, we attempt to minimize some variability by studying strain rates required to form crevasses in cold ice using a polar glacier ice divide which exhibits local crevassing. Secondly, prior research suggests that ice divides represent low strain rate environments which are generally crevasse free. However, our study site, which shows evidence of buried crevasses near the divide, contradicts this assumption making for a unique dynamical situation and interesting case study.

Surface velocities and strain rates were calculated from a network of 38 stakes placed in a grid pattern over the Mount Hunter ice divide, Alaska from May 31-June 12, 2011. We collected radar profiles in a grid pattern over the entire basin to map bed topography and ice depth (with 30, 80, 100 MHz frequency radar) and stratigraphic thickness variations (with 900 MHz frequency radar). To determine accumulation rates, we extracted a 10 m long ice core in 2010 and samples from two 4-m deep snow pits in 2011 for isotope and ion chemical analysis. Our depth-density curve from the ice core compared reasonably well with a curve from a 23.7 m long core extracted from the Kahiltna Glacier (3048 m a.s.l.) in 2008 (approximately 10 km distant).

The ice divide is a relatively small rectangular glacier (1.7 km^2) with the true divide oriented North-South and slightly offset to the west within the field parameters. Ice flows east-west for 600-800 m from the ice divide until it reaches significant ice cliffs where it falls away in semi-regular calving events. Radar profiles collected east to west show crevasses buried 5-20 m below the surface and reaching ~80 m depth, ~100-200 m from, and on both sides, of the ice divide. High vantage points to the north and south of the divide revealed north-south trending continuous, though discrete, snow bridges in these locations suggesting that the buried crevasses are continuous openings extending the width of the study site (N-S), parallel to the ice divide. The snow bridges are also parabolic in shape, mirroring local topography (Fig 1a). The ice divide is high and cold with an -20 C average firn temperature suggesting it is located in the dry snow zone (i.e. avoids melt). With these conditions, it is likely that the basal ice is frozen to the bed making for consistent temporal ice flow velocities. We expect the cold ice and consistent velocities to result in more linear strain rates than that of temperate ice. Also, the close proximity of the crevasses to the divide suggests the current measured strain field represents that which originally initiated the crevasses. We also expect minimal debris inclusion due to the high elevation of the divide and the lack of surrounding rock falls. Each of these observations are consistent with our radar profiles which show surface conformable stratigraphy on either side of the crevasses indicating minimal deformation from ice flow, no evidence of radar signal attenuation via melt, and no random discontinuous reflections which would be expected from rock or entrained debris. Because of the relatively simple conditions and dimensions we suggest that Mt Hunter ice divide is a

good location to model crevasse formation.

We used our field data to constrain the boundary conditions of first order numerical models for estimating strain rates on the surface and at depth. We then compared the model and field strain rates to determine the efficacy of our modeling. Lastly, we compared our results to other crevasse studies, and theorize about their dynamical causes. Our basic modeling consists of a steady state 2D incompressible Navier Stokes flow model developed with COMSOL Multi-Physics version 4.2. The model was represented as a cross section oriented perpendicular to the ice divide. The preliminary model dimensions were 1700 m wide across the ice divide and ranged between 150-250 m in depth. We used a cold ice viscosity (1e14) and the following depth-density equation from the ice core: $\varrho = 343.17*h^{(0.2199)}$

where ϱ is density (kg m^-3) and h is depth (m). We applied a constant density after the depth-density profile reached bubble free ice (917 kg m^-3), a no slip (frozen) boundary at the bed, and open boundaries with normal stress at the left and right boundaries of the model to allow ice flow away from the divide.

Our field data indicates a maximum strain rate of 0.002 a^-1 which is close to the minimal published strain rate required for crevasse initiation (which ranges from 0.001 to 0.163 a^-1). However, our current numerical model suggests higher strain rates, well within the three orders of magnitude needed to generate crevasses. The model also indicates the locations of the highest strain rates being in regions of the observed crevassing. We suggest that the primary driving force to ice flow, surface slope, is enhanced by a frozen bed, which leads to a rotational moment of flow away from the divide. Secondly, the icefalls on either side of the divide appear to be approximately the height of the ice thickness measured with GPR. Therefore, we suggest that these cliffs create a situation of minimal resistance to flow (much like a glacier calving front), generating significant tensile stresses. However, the high tensile strength of the cold and dry ice likely allows this stress to propagate toward the center of the ice divide until a critical stress threshold is eventually reached causing fractures to occur. In other words, besides the frozen bed and tensile strength of the up-glacier ice and firn, there is no resisting force holding the ice up at the icefall edge. We suggest that the combined frozen bed and steep icefalls create an overall unique dynamical situation.

The discrepancy between our field and model strain rates is of obvious concern. A number of potential reasons exist for this discrepancy (field or model related) and we are continuing to improve our numerical models and perform sensitivity analysis to the different input variables. The buried nature of the crevasses is also interesting. We are still attempting to determine whether these crevasses initially formed at depth or on the surface and were subsequently buried by accumulation (Nath and Vaughan, 2003). Our current basic numerical models are inadequate for answering this question.

Meier. M.F., 1958, The mechanics of crevasse formation: International Association of Scientific Hydrology Publication 46 General Assembly of Toronto 1957 - Snow and Ice, p. 500-508

Hambrey, M.J. and F. Miller. 1978. Structures and ice deformation in the White Glacier, Axel Heiberg' Island, Northwest Territories, Canada: Journal of Glaciology, v. 20(82), p. 41- 66.

Harper, J.T., Humphrey, N.F., Pfeffer, T.W. 1998. Crevasse patterns and the strain rate tensor: a high-resolution comparison: Journal of Glaciology, v. 44(146), p. 68-76.

Nath, P.C., and Vaughan, D.G. 2003. Subsurface crevasse formation in glaciers and ice sheets Journal of Geophysical Research, v. 108 No. B1, 2020, doi:10.1029/2001JB000453, p 1-12.

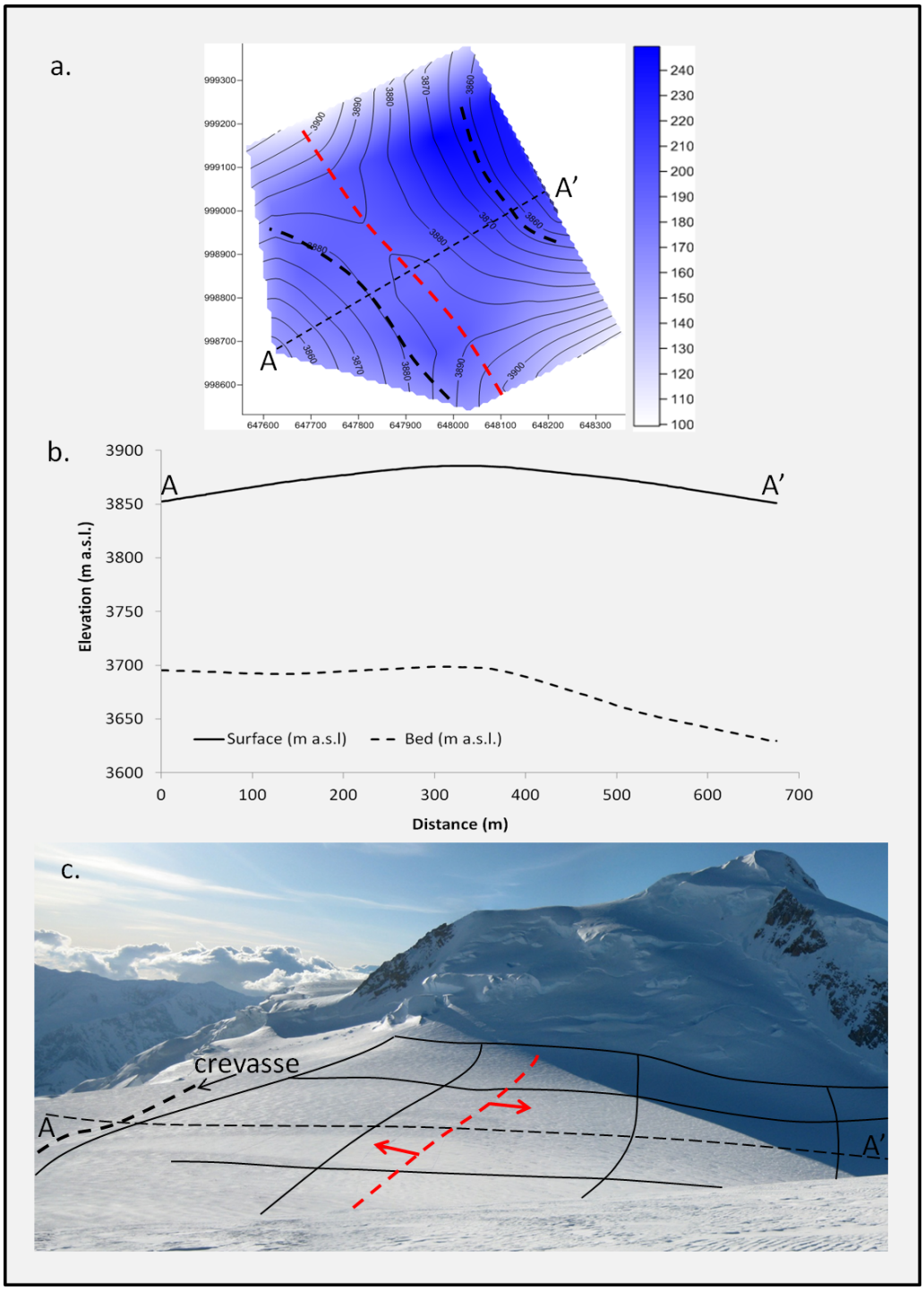

Fig 1. (a) Surface topography (contours) and ice depth in meters (blue color) of the Mount Hunter ice divide (red dotted line) with approximate crevasse locations (black dotted lines). A-A' represents the surface topography and ice depth plotted in (b). (c) An oblique photo of the study site looking north showing approximate radar profile locations (black solid lines), ice divide (red dotted line-arrows) and cross section used for numerical model and for (b) (A-A'; black dotted line).

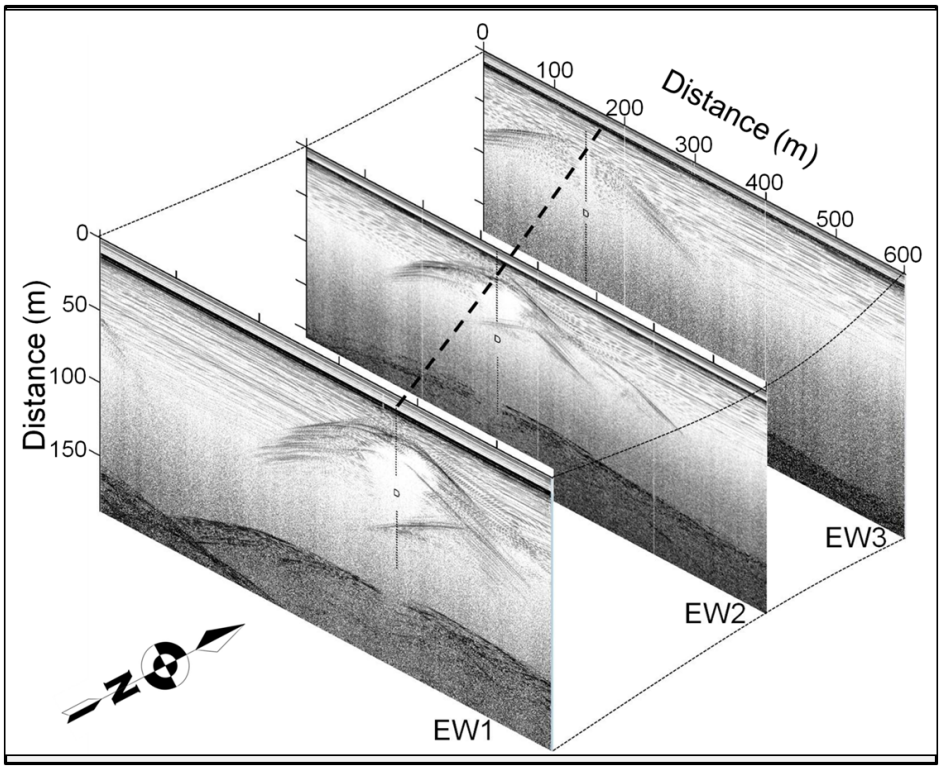

Fig 2. Three 80 MHz un-migrated radar profiles collected across the Mount Hunter ice divide, each of which cross a crevasse (open spaces with no internal layering encased by hyperbolic reflections) and which are surrounded by surface conformable stratigraphy. Dotted black line suggests a continuous crevasse between profiles.

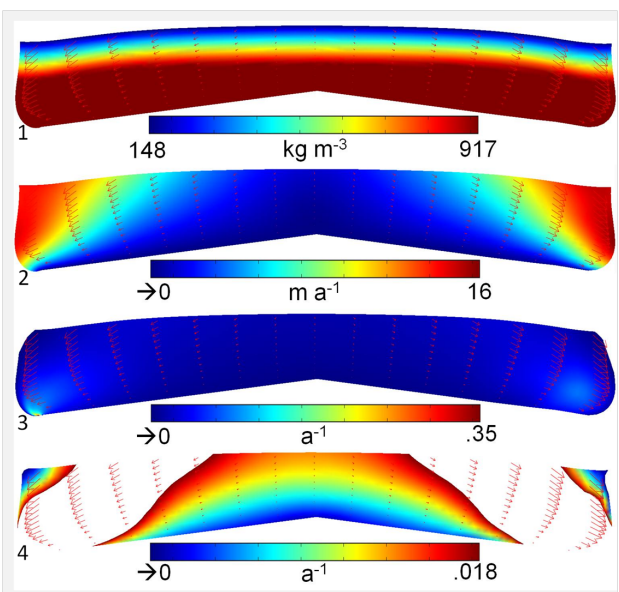

Fig 3. Numerical models showing (1) density profile, (2) velocity profile, (3) strain rate (4) and strain rate with a lower range showing strain concentrations (maroon-red) immediately left and right of the ice divide. Boundary conditions include a frozen bed and open boundaries with normal stress on the left and right walls of the model.

USING CLAY MINERALOGY TO ANALYZE SEDIMENT SOURCES, KRONEBREEN AND KONGSVEGEN GLACIERS, SVALBARD, NORWAY

Ceperley, Elizabeth G [1]; **Brigham-Grette**, Julie [2]; **Powell**, Ross [3]; **Swanson**, Susan [4]

[1] Beloit College; ceperlee@beloit.edu
[2] UMass-Amherst; juliebg@geo.umass.edu
[3] Northern Illinois University; ross@geol.niu.edu
[4] Beloit College; swansons@beloit.edu

This project aims to analyze the spatial distribution of sediment deposited by Kronebreen and Kongsvegen glaciers located in northwestern Svalbard, Norway. Kronebreen and Kongsvegen glaciers form a 6 km long calving margin at the head of Kongfjorden. There are two main sediment sources that deposit glacial sediment into the fjord. The first is an upwelling plume formed from a subglacial stream located in the north-central part of the study area, and the second is a delta formed from a glacial stream on Kongsvegen glacier, located in the southern part of the study area (Figure 1). The focus of this project is to analyze the clay mineralogy of the fjord floor sediments in order to delineate the sediment sources.

Box core samples were collected using a wire-winch system attached to a boat. Sediment was dried and sieved to separate the sand from the silt and clay fraction. The sediment collected near the delta is darker in color and contain a wider range of grain sizes. X-Ray Diffraction is being used as a diagnostic tool to identify the clay minerals present in the samples. Initial results suggest that the sediment sources have differing compositions and that the sources mix gradationally in front of the ice margin.

The processes occurring in this system could be applied to understand tidewater glaciers located is less accessible locations. Results from this project can be tied with sediment core data in order to understand the relative strength and magnitude of sediment sources of retreating tidewater glaciers.

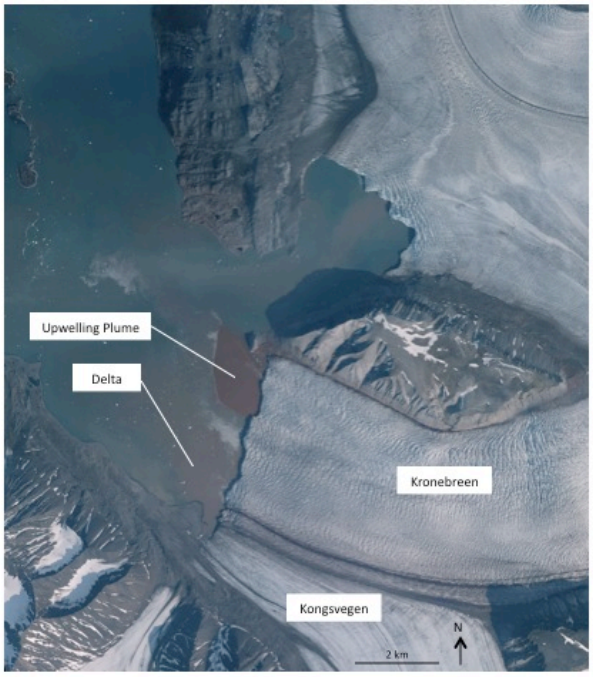

Fig 1. Location of Upwelling Plume and Delta, Kongsfjorden, Svalbard.

VOLCANIC, ANTHROPOGENIC, AND CLIMATIC INFLUENCES ON HOLOCENE ECOSYSTEM DYNAMICS USING MULTIPLE PROXY ANALYSES OF A LAKE SEDIMENT CORE FROM VESTRA GÍSLHOLTSVATN, SOUTHWESTERN ICELAND

Christensen, Celene L [1]; **Miller**, Gifford H [2]; **Geirsdóttir**, Áslaug [3]

[1] University of Colorado/INSTAAR; celene.christensen@colorado.edu
[2] University of Colorado/INSTAAR; gmiller@colorado.edu
[3] University of Iceland; age@hi.is

Volcanic eruptions, climate change and anthropogenic influences have significant impacts on both terrestrial and lacustrine ecosystem dynamics. Icelandic lakes act as reservoirs preserving continuous records of environmental change via the inflow of terrigenous sediment and organic matter and intermittent tephra deposition. In 2008 an 8.35m sediment core was taken from Vestra Gíslholtsvatn, a lake located in southwestern Iceland capturing the Holocene record. An age model was constructed using tephra chronology constraining the last 10.3 ka. A multiple proxy approach including: sedimentation rate, organic matter concentration, biogenic silica, and stable isotopes δ15N and δ13C, was used in an attempt to discern changes in local ecosystem dynamics. These include active volcanism, anthropogenic influence, and ultimately climate change throughout the Holocene. Organic matter in the sediment indicates little biologic activity prior to approximately 11 ka, at which point the lake began a slow recovery, which was halted by the eruption of the Saksunarvatn tephra at 10.3 ka, followed by a restart of ecosystem recovery. Recovery took from approximately 10.3 ka to 8.1 ka. The age model shows a stable sedimentation until settlement at 872 AD, at which point the sedimentation rate increased dramatically. This increase is likely due to land use changes, as Vestra Gíslholtsvatn is located in an agricultural region. High resolution sampling of C, N, δ13C, and δ15N were conducted surrounding 5 tephra layers in the core in attempt to better interpret ecosystem changes following volcanic events.

ROUGHNESS OF GLACIALLY ABRADED BOULDERS MEASURED WITH USE OF HANDYSURF E35-B ELECTRONIC PROFILOMETER AND ITS POTENTIAL FOR RELATIVE DATING: A CASE OF FLÁAJÖKULL MORAINES (SE ICELAND)

Dąbski, Maciej [1]

[1] University of Warsaw, Faculty of Geography and Regional Studies, Department of Geomorphology; mfdbski@uw.edu.pl

The aim of the study was to register roughness variability of glacially abraded rock surfaces with use of Handysurf E35-B electronic profilometer (Carl Zeiss, Accratech/Seimitsu), and therefore to i) test a new potential tool of relative dating of young glacial landforms, and ii) obtain information on initial stages of weathering of basalts in cool maritime climate of SE Iceland. Experimental sites were designed on previously dated moraines of Fláajökull glacier in SE Iceland (Dąbski 2002, 2007, 2011) – Figure 1.

The profilometer is equipped with a skidded pick-up with a built-in stylus which can register rock surface roughness down to a few micrometers. The diamond stylus tip is pressed against the studied surface with a constant force and run along a demanded profile (a distance up to 12.4mm long). Roughness elements are calculated based on the evaluation length of the roughness profile, which consists of five elementary segments (sampling length, referred to as a cut-off value), to produce roughness parameters (Ra, Rz, Rzmax, Rsm). The profilometer is equipped with a micro-processor, LCD display and a light portable printer enabling quick print-outs of magnified surface roughness profiles (Fig. 2).

Surface roughness is expressed by following parameters: Ra – arithmetic mean deviation of roughness profile (integral of the roughness profile function divided by the sampling length); Rz – "ten point height of irregularities" (average vertical distance between peaks and valleys); Rzmax – maximum height of irregularities; Rsm – mean width of the profile elements (wavelength).

Fifteen boulders were chosen for the roughness measurements on each of 6 experimental sites designed on Fláajökull moraines deposited since LIA maximum. Boulders were carefully selected as they had to meet following requirements: 1) all boulders were grey basalts of tertiary age; 2) they had clear signs of glacier abrasion – tests were done on glacially polished surfaces; 3) studied surfaces faced glacier (cold stoss-sides, exposition N, NW); 4) they were large enough in order to allow for complimentary Schmidt hammer tests (boulders smaller than 30x30x30cm were omitted). These requirements significantly limited the number of possible measuring surfaces, but were crucial for the study. All abraded surfaces were first optically analysed in order to find the smoothest possible places (free of lichens, without any glacial striae or gauge). Measurements were done in 3 places on each of the boulder (45 measurements in each experimental site). Skidding distance was set for 4mm and a cut-off value for 0,8mm.

Measurement of roughness was supplemented by weathering rind thickness measurements and Schmidt hammer rebound values (R) obtained from the same boulders. Thin sections of rock samples were analysed under optical microscope and scanning electrone microscope in order to determine mineral content and texture of the boulders.

The study revealed that there is a significant diversification of roughness between rock surfaces within a single experimental site (Fig. 3), which was to expected considering very high sensitivity of the instrument. Nevertheless, gradual increase in all roughness parameters within younger part of the glacier foreland, ice-free since c. 1932 AD (Fig.3), is clearly observed. Boulders on older moraines exhibit relatively constant, elevated values of Ra, Rz and Rzmax. There is a significant decrease in the wavelength parameter (RSm) between sites exposed in 1932 and 1907 AD. This shows that: i) either RSm value does not depend on weathering duration or ii) weathering processes lead to sudden

shortening of roughness wavelength after 80 years of operation (the study was performed in 2011 AD).

Increase in roughness of glacially abraded basaltic surfaces is accompanied by significant increase in weathering rind thickness, especially within younger moraines, and decrease in Schmidt hammer rebound values (Fig. 3).

Previous studies on roughness of glacial landforms proved usefulness of the method elaborated by McCarroll (1992) and McCarroll and Nesje (1993, 1996) in diversification between landforms created during LIA and those from the onset of Holocene. The Handysurf E35-B electronic profilometer can be, under specific petrographic conditions, successfully used in studies on relative age of glacier landforms developed since LIA maximum. Furthermore, it allows to get an insight into initial stages of weathering deterioration of basaltic surfaces under cool maritime climatic conditions. Roughness increase-in-time of basalts probably results from a complex weathering processes including chemical decomposition of plagioclases and pyroxenes.

Acknowledgements

I would like to thank Aleksander Tittenbrun for help during field-work. This study is a part of a more comprehensive investigation of Fláajökull, Heinabergsjökull and Skalafelsjökull forelands funded by the National Science Centre in Poland, project N N306 034440.

Dąbski, M., 2010, A commentary to 'Asynchronous Little Ice Age glacial maximum extent in southeast Iceland' by Chenet et al. (Geomorphology 114 (2010) 253-260); a case of Fláajökull: Geomorphology, v. 120, p. 365-367.

Dąbski, M., 2007, Testing the size-frequency-based lichenometric dating curve on Fláajökull moraines (SE Iceland) and quantifying lichen population dynamics with respect to stone surface aspect: Jökull, v. 57, p. 21-35.

Dąbski, M., 2002, Dating of the Fláajökull moraine ridges, SE – Iceland; comparison of the glaciological, cartographic and lichenometrical data: Jökull, v. 51, p. 17-24.

McCarroll, D., 1992, A new instrument and techniques for the field measurement of rock surface roughness: Zeischrift für Geomorphologie, v. 36, p. 69-79.

McCarroll, D., Nesje, A., 1993, The vertical extent of ice sheets in Nordfjord, western Norway: measuring degree of rock surface weathering: Boreas, v. 22, p. 255-265.

McCarroll, D., Nesje, A., 1996, Rock surface roughness as an indicator of degree of rock surface weathering: Earth Surface Processes and Landforms, v. 21, p. 963-977.

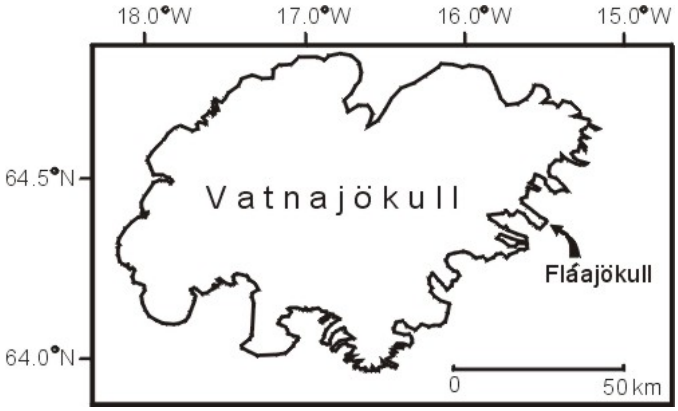

Fig 1. Location of the study site

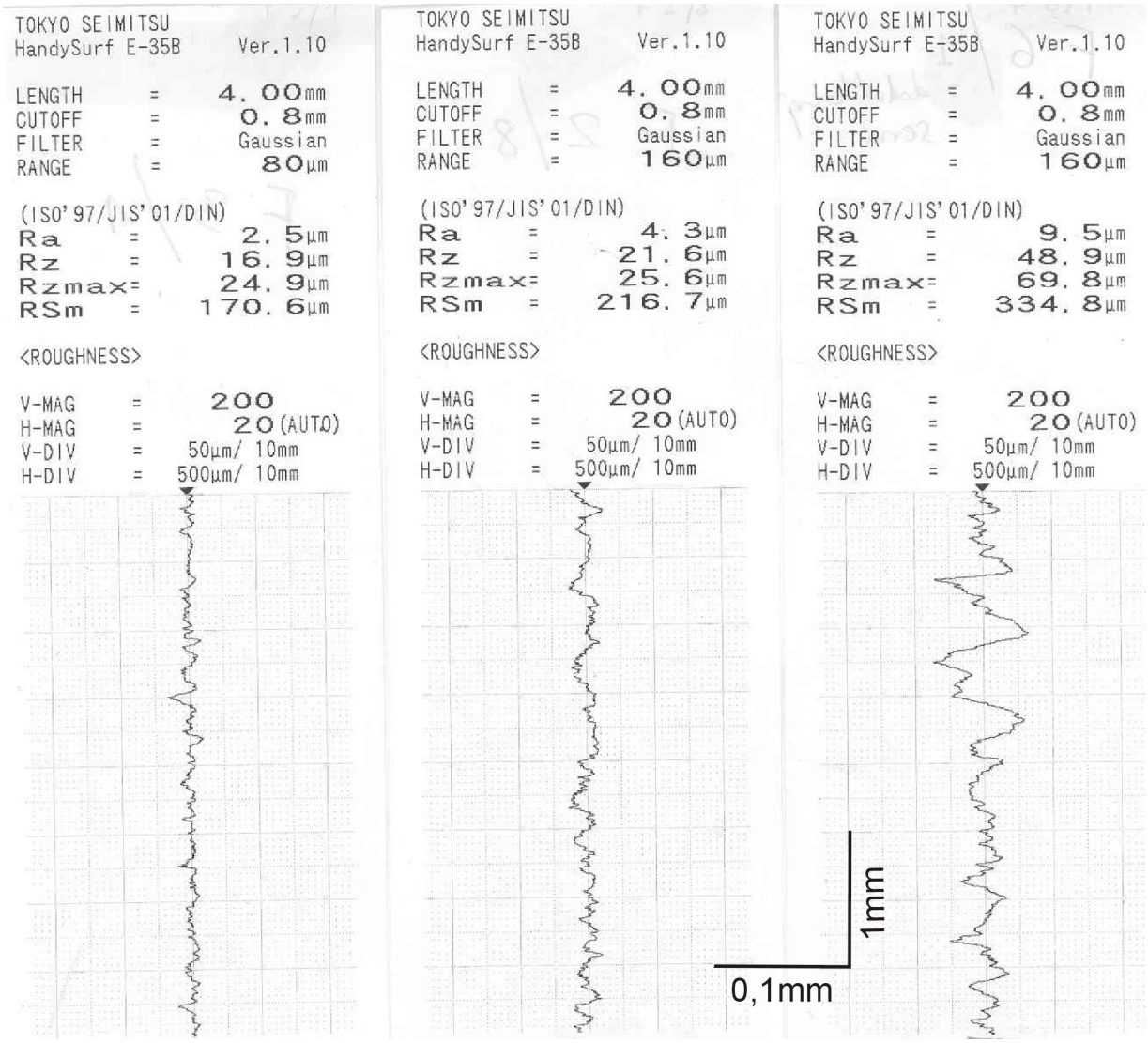

Fig 2. Print-outs of roughness curves of selected basaltic surfaces

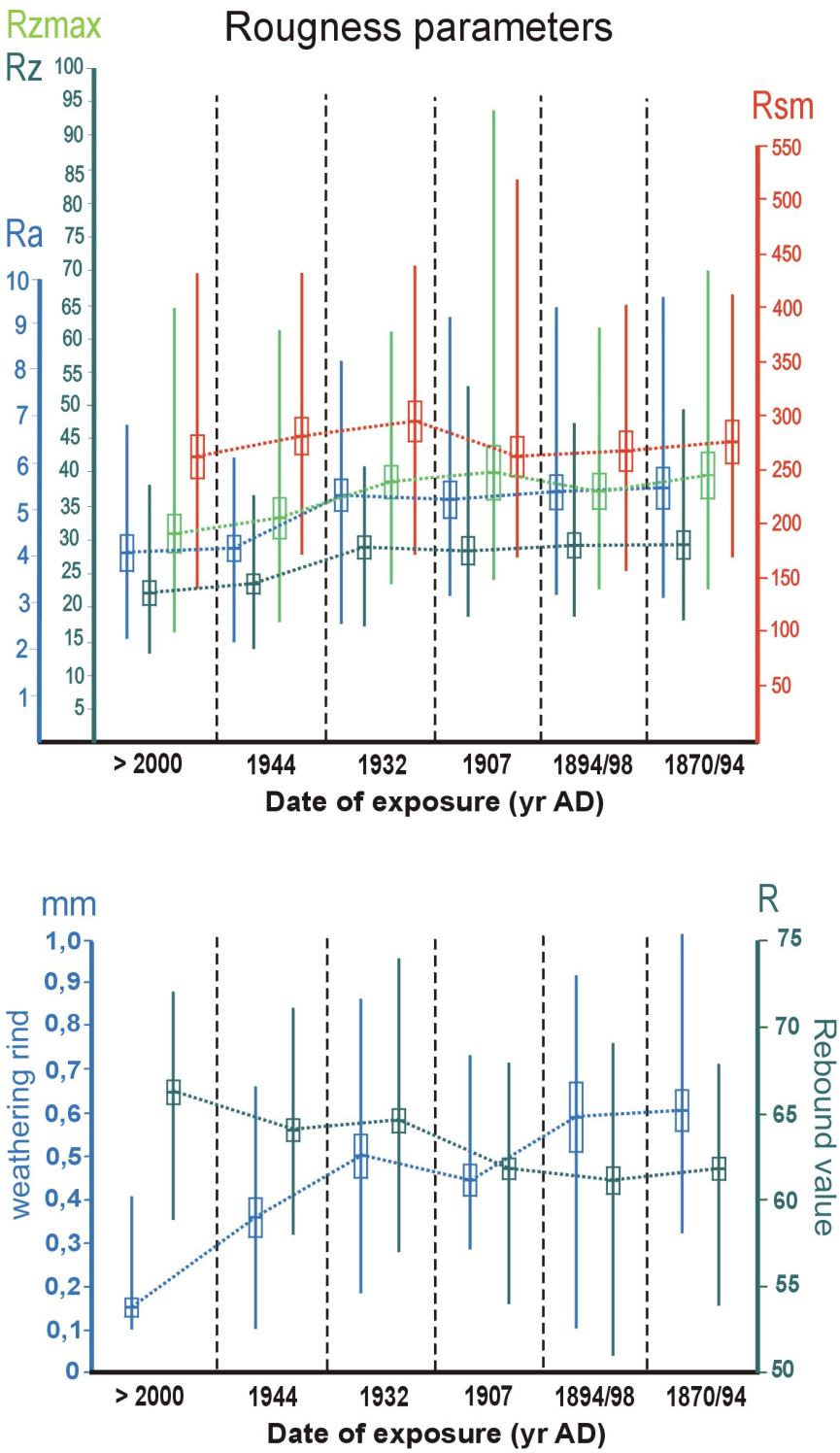

Fig 3. Upper diagram - roughness parameters (Ra, Rz, Rzmax, Rsm) obtained at experimental sites of different age; lower diagram – corresponding weathering rind thickness and Schmidt hammer R values; the diagrams show maxima, minima and means (the latter connected by dashed lines) together with 95% confidence intervals

THE IMPACT OF GLACIAL EROSION ON NORTHERN SHIELDS

Ebert, Karin [1]; **Hall**, Adrian M [2]; **Kleman**, Johan [3]

[1] Stockholm University, Sweden; karin.ebert@natgeo.su.se
[2] University of St Andrews, UK;
[3] Stockholm University, Sweden;

The long-term geomorphic evolution of shield surfaces is poorly understood, especially of glaciated shields where saprolites and correlative sediments have been removed by glacial erosion. We know the rough picture of land uplift and erosional unloading during the Cenozoic (e.g. Hendriks et al., 2007) and we know of the existence of stepped surfaces on the shield (Ebert et al., 2011). However for further studies of the long term geomorphology of glaciated shields, we first need to assess the patterns and depth of glacial erosion on the shield bedrock landforms in order to reconstruct the preglacial land surface (cf. Ebert et al., 2011).

Large scale topography controls ice inception on that surface and influences ice dynamics during glaciation. Large-scale relief is a trigger for selective erosion and for ice streaming (Figure 1) and bed materials affect the ice flow and the composition of tills. Yet the quantitative impact of glacial erosion on shield bedrock is barely known.

The patterns of erosion, deposition and redistribution of loose material on the shield surface are well known (Kleman et al., 2008). The interesting question is if the bedrock surface of the northern shields only was the surface for redistribution, largely unaffected, or if the surface itself was modified and to what degree?

A detailed and convincing quantification of removal of bedrock by ice does not exist. Studies show that the ice erosional impact can be modest (e.g. Sugden, 1976; Lidmar-Bergström, 1997; Ebert and Hättestrand, 2010). However these are results of regional studies and wider studies of the northern shields are desirable, with the final aim of a quantification of the glacial erosional removal of bedrock for entire cratons.

Field investigations on the basis of identification of promising field localities in a digital elevation model (DEM), and in combination of GIS-analysis of combinations of the DEM with databases of bedrock geology and tectonics, are a new and powerful tool to identify patterns of glacial erosion over large areas and eventually to quantify the depths of glacial erosion on glaciated shield surfaces.

The presentation will show current results for northern Fennoscandia and future possibilities to assess patterns and quantities of glacial erosion in glaciated shield areas, with a focus on DEM-analysis.

Ebert, K., Hättestrand, C., 2010,The impact of Quaternary glaciations on inselbergs in northern Sweden: Geomorphology, v. 115, p. 56-66.

Ebert, K., Hättestrand, C., Hall, A.M., Alm, G., 2011, DEM identification of macroscale stepped relief in arctic northern Sweden: Geomorphology, v. 132, p. 339-350.

Hendriks, B., Andriessen, P., Huigen, Y., Leighton, C., Redfield, T., Murrel, G., Gallagher, K., Nielsen, S.B., 2007, A fission track data compilation for Fennoscandia: Norwegian Journal of Geology, v. 87, p. 143-155.

Hirvas, H., 1991, Pleistocene stratigraphy of Finnish Lapland: Bulletin of the Geological Survey of Finland, v. 345, p. 1-123.

Kleman, J., Stroeven, A.P., Lundqvist, J., 2008, Patterns of Quaternary ice sheet erosion and deposition in Fennoscandia and a theoretical framework for explanation: Geomorphology, v. 97, p. 73-90.

Lidmar-Bergström, K., 1997, A long-term perspective on glacial erosion: Earth Surface Processes and Landforms, v. 22, p. 297-306.

Sugden, D.E., 1976, A case against deep erosion of shields by ice sheets: Geology, v. 4, p. 580-582.

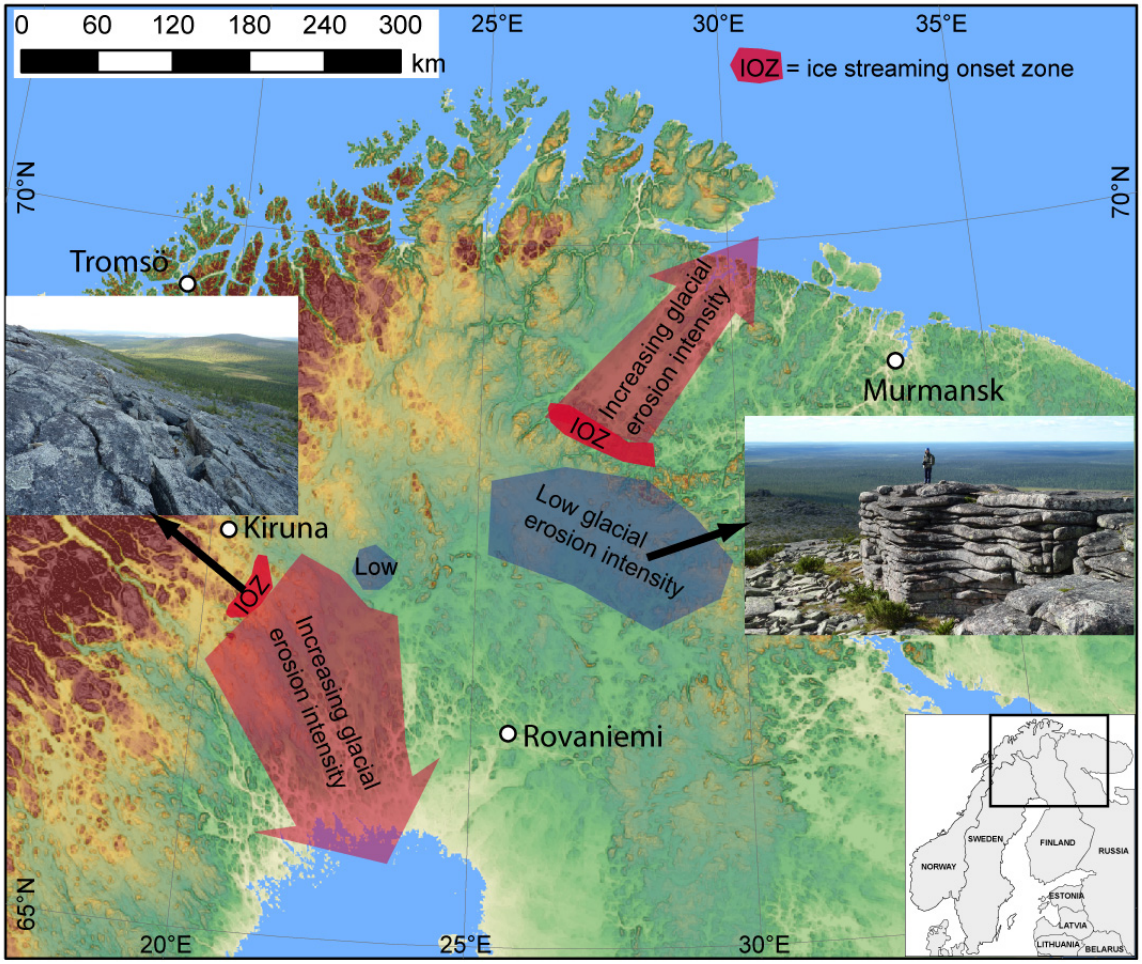

Fig 1. Sketch of areas of strong and low glacial erosion intensity in northern Fennoscandia. Glacial erosion intensity inferred from the bedrock morphology in the DEM, in the field (inset photos), and from literature (e.g. Hirvas, 1999; Ebert and Hättestrand, 2010). Ice streaming onset zones demarcate areas of abrupt changes between glacially streamlined and non-streamlined bedrock terrain (Ebert and Hättestrand, 2010).

COUPLED ICE SHEET/CLIMATE SIMULATIONS OF GREENLAND EVOLUTION IN HIGH-CO_2 CONDITIONS: SENSITIVITY TO MODELLED POLAR AMPLIFICATION

Fyke, Jeremy G. [1]; **Weaver**, Andrew J. [2]; **Eby**, Michael [3]

[1] Los Alamos National Laboratory; fyke@lanl.gov
[2] University of Victoria;
[3] University of Victoria;

Large ice sheets are sensitive to atmospheric CO_2 concentrations. In order to contribute to understanding of future Greenland Ice Sheet (GIS) evolution, we developed and used a coupled ice sheet/climate model to simulate the climate/GIS system for multiple millennia under elevated CO_2. The climate model consists of the University of Victoria Earth System Climate Model; the ice sheet model is PSUI; the coupled model is described in Fyke et al. (2011).

When initialized with a stable present-day GIS and reasonable surface mass balance distribution and run forward using default model parameters and present-day orbital conditions, a suite of model simulations simulated a basic limit on GIS existence between 2 and 3 times preindustrial atmospheric concentrations of CO_2: at 3x PAL CO_2 all ice was lost over several thousand years while below this concentration the ice sheet was diminished but not completely melted. However, an additional matrix of sensitivity experiments highlighted the large range of long-term ice volume evolutions (and thus sea level rise) to realistic perturbations to parameters and processes within the model. This presentation focuses on the role of polar amplification. By directly controlling the amount of simulated polar amplification (via anomaly-based alterations to atmospheric heat diffusivity) we were able to 'tune' the model to reproduce the range of polar amplifications found in the ensemble of IPCC AR4 AOGCMs. This range of polar amplifications resulted in a large range of cumulative GIS volume losses, and times taken to achieve given volume decreases. For example, volume loss at 3x PAL CO_2 ranged from 20% to 90% after 4 kyr, and the time taken to achieve a 20% reduction in volume differed by a factor of 4.

These findings suggest that future GIS-derived eustatic sea level rise will be strongly regulated by the combination of processes that determine the realized magnitude of polar amplification in preindustrial-to-future climate change (Serreze and Barry, 2011). These climate-side processes will need to be well modelled in coupled ice/climate models in order to reduce ensemble mean uncertainty in long term predictions of GIS-based sea level rise. To this end, we suggest that reducing polar amplification uncertainty in GIS-related sea level rise may come largely from model/data comparisons of polar amplification during previous warm climate states (Miller et al., 2010).

Fyke, J.G, Weaver, A.J., Pollard, D., Eby, M., Carter, L. and Mackintosh, A., 2011, A new coupled ice sheet/climate model: description and sensitivity to model physics under Eemian, Last Glacial Maximum, late Holocene and modern climate conditions: Geoscientific Model Development, v. 4, p. 117–136.

Miller, G.H., Alley, R.B., Brigham-Grette, J, Fitzpatrick, J.J., Leonid Polyak, L., Serreze, M.C. and White, J.W.C., 2010, Arctic amplification: can the past constrain the future?: Quaternary Science Reviews, v. 29, p. 1779–1790.

Serreze, M.C. and Barry, R.G., 2011, Processes and impacts of Arctic amplification: A research synthesis: Global and Planetary Change, v. 77, p. 85-96.

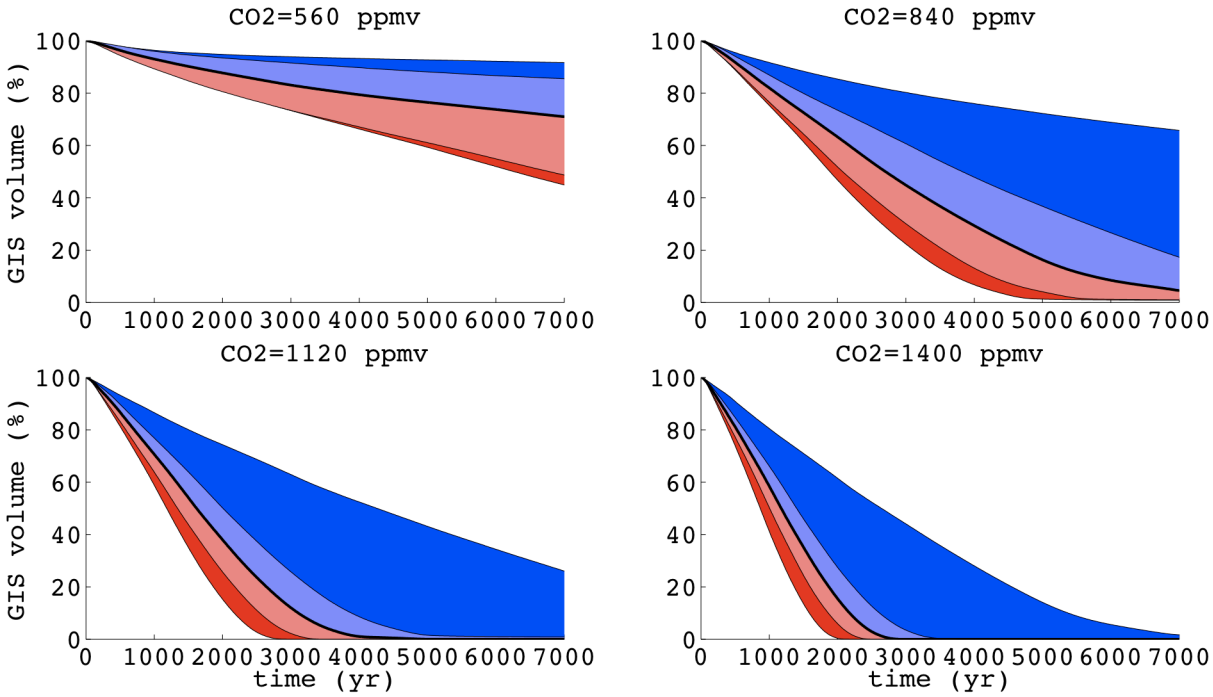

Fig 1. GIS volume changes over time, from 2-5x PAL carbon dioxide, for perturbed surface albedos (pale shading) and perturbed polar amplifications (solid shading).

PALEOMAGNETIC SYNCHRONIZATION AND LAND – SEA PALEOCLIMATIC CORRELATIONS FROM ICELAND

Geirsdottir, Aslaug [1]; **Miller**, Gifford H. [2]; **Olafsdottir**, Saedis [3]; **Larsen**, Darren [4]

[1] Insti of Earth Sciences, University of Iceland; age@hi.is
[2] INSTAAR, University of Colorado Boulder; gmiller@colorado.edu
[3] Insti of Earth Sciences, University of Iceland; saediso@hi.is
[4] INSTAAR, University of Colorado Boulder; djlarsen@gmail.com

The correlation between land and sea is one of the main challenges in paleoclimatic research. This is particularly important when comparing high-resolution terrestrial and marine archives where accurate dating of records is also essential. Accurate and precise dating of high-resolution records has been the limiting factor in both high-latitude lake sediment and shelf records. Lake sediments are difficult to date due to high flux of soil derived "aged" carbon, and reworking of terrestrial macrofossils. In Iceland, comparisons between radiocarbon dates and varves or known tephra layers have shown that the difference between them can be several hundred years. In the marine environment radiocarbon dating on shell material has been the most successful method, but a changing ocean reservation correction (delta R) is a large remaining uncertainty. Whereas a wealth of information is available on the variability of marine environments, high-resolution data from terrestrial environments are yet relatively scarce. Few precise correlations of environmental change in terrestrial and marine settings exist.

Fjords along the coast of Iceland are directly linked to the North Atlantic Ocean, but are also influenced by adjacent lands. To analyze the effects of short-term climatic change on terrestrial environments and to correlate terrestrial and marine signals of environmental change, we have analyzed high sedimentation-rate cores from lacustrine, fjord and marine shelf archives, each with relatively high-resolution paleoclimate proxies, and detailed, well-preserved, Paleomagnetic Secular Variations (PSV) records. The PSV records are combined with independently dated tephras and radiocarbon dates from optimal settings allowing synchronization of these records. Proxy data from the fjord core Jökulfirðir, NW Iceland, the coastal lake Haukadalsvatn, W Iceland, and the glacial lake Hvítárvatn, central Iceland, together with a reference curve from the shelf north of Iceland follow the general insolation forcing trend of the Holocene. However, peak warmth in all records lags behind the 11 ka primary insolation peak. The delay in peak warmth suggests that the early Holocene marine climate is strongly influenced by freshwater discharge from the decaying Laurentide Ice Sheet. The terrestrial records show a clear stepwise perturbation between 8.7 ka and 7.9 ka indicating increased landscape instability and soil erosion. This is not as clear in the marine record which seems to lag the terrestrial record by approximately 100 to 200 years. All proxy data in all environments reflect a sharp transition out of the 8 ka event and the shift to peak summer warmth by 7.9 ka, but the transition out of the HTM occurs in a stepped manner similar to the perturbations around 8.0 ka centered at ca. 6.0 ka in the terrestrial records followed by a subsequent irreversible climate shift at ca. 5.4 ka. The fjord and marine record also indicates a stepwise transition but again delayed by 100 to 200 years compared to the terrestrial record. An abrupt cooling related to the Little Ice Age is observed in all records starting at approximately 0.7 ka.

The synchronized shelf, fjord and lacustrine climate events in early and middle Holocene underscore that the terrestrial climate is essentially a slave to marine conditions at a millennial scale rather than responding directly to the early Holocene increased insolation. The land, however, appears to be leading at centennial and shorter time scales. Whether this difference in leads and lags is actually within the uncertainty of the PSV correlation or due to differences in resolution between archives calls for higher resolution studies of both archives.

LATE WEICHSELIAN ICE SHEET CONFIGURATION IN NORTHWEST SPITSBERGEN, FROM 10BE DATING AND LITHOLOGICAL STUDIES OF ERRATIC BOULDERS AND BEDROCK

Gjermundsen, Endre F [1]; **Briner**, Jason P [2]; **Salvigsen**, Otto [3]; **Akçar**, Naki [4]; **Kubik**, Peter W [5]; **Gantert**, Niklas [6]; **Hormes**, Anne [7]

[1] The University Centre in Svalbard; endreg@unis.no
[2] University at Buffalo; jbriner@buffalo.edu
[3] University of Oslo; otto.salvigsen@geo.uio.no
[4] University of Bern; akcar@geo.unibe.ch
[5] Swiss Federal Institute of Technology; kubik@phys.ethz.ch
[6] The University Centre in Svalbard; niklas.gantert@gmx.de
[7] The University Centre in Svalbard; anne.hormes@unis.no

We used cosmogenic 10Be dating and lithological studies of boulders and bedrock to reconstruct the configuration and deglaciation history of the Late Weichselian ice sheet in Northwest Spitsbergen, Svalbard. Investigations of erratic boulders on the northern and southern extremity of our study area point to a local ice dome in Northwest Spitsbergen. Our reconstruction fits well with the hypothesis of a complex multi-dome-ice-sheet-configuration over Svalbard and the Barents Sea during the Late Weichselian glaciation, with numerous drainage basins feeding fast ice streams, separated by slow flow, possibly cold based, inter-ice-stream areas (Landvik et al 2005, Ottesen et al 2007, Ottesen and Dowdeswell, 2009, and Alexandersson et al 2011).

Lithological studies of erratic boulders on the flat, low-elevation peninsulas Mitrahalvøya and Reinsdyrsflya indicate one common source region - the Smeerenburgfjord complex, consisting primarily of migmatites. The lithology of these boulders points towards a main ice dome covering the Smeerenburgfjord complex in the central part of Northwest Spitsbergen with drainages to the north-northeast along Liefdefjorden and southwards along Krossfjorden. 10Be ages from 7 well spread erratic boulders from Reinsdyrflya range from 11.2±0.8 ka to 21.6.1±1.7 ka (average 14.7±1.1 ka), indicating an active ice stream on Reinsdyrflya during LGM and complete deglaciation prior to the Holocene. Three high elevation (687-836 m asl) erratic boulders, two on Auriviliusfjellet (18.5± 1.3 and 20.3±1.1 ka) and one on Kaffitoppen (21.8± 1.4 ka) suggest that the center of this local ice dome was at least 300 m thicker than the ice coverage in the area at present. Several bedrock samples (10Be) from vertical transects on mountains in the area also give insight into the ice configuration and its deglaciation, however, partial inheritance cannot be excluded at these sights.

Our results are the first to suggest a separate ice-dome over Northwest Spitsbergen during the Late Weichselian with drainage in all directions. Our data also suggests that deglaciation started very early (> 20 ka ago) and that the duration of maximum ice occupancy during the Late Weichselian therefore was very short.

Alexanderson, H., Landvik, J.Y. Ryen, H.T. 2011, Chronology and styles of glaciation in an inter-fjord setting, northwestern Svalbard: Boreas, Vol. 40, p. 175–197.

Ottesen, D., Dowdeswell, J.A., Landvik, J.Y., Mienert, J., 2007, Dynamics of the Late Weichselian ice sheet on Svalbard inferred from high-resolution sea-floor morphology: Boreas 36, p. 286–306.

Landvik, J.Y., Ingólfsson, Ó., Mienert, J., Lehman, S. J., Solheim, A., Elverhøi, A. & Ottesen, D. 2005, Rethinking Late Weichselian ice-sheet dynamics in coastal NW Svalbard: Boreas, Vol. 34, p. 7–24.

Ottesen, D. and Dowdeswell, J.A. 2009, An inter-ice-stream glaciated margin: Submarine landforms and a geomorphic model based on marine-geophysical data from Svalbard: GSA Bulletin, v. 121; no. 11-12; p. 1647-1665.

TRACING GROWING DEGREE-DAYS AND CO_2 CONCENTRATION USING *BETULA GLANDULOSA* LEAF CUTICLE CHARACTERISTICS

Holmquist, James R [1]; **Wagner-Cremer**, Friederike [2]

[1] University of California, Los Angeles; JamesHolmquist@ucla.edu
[2] University of Utrecht; F.Wagner@uu.nl

Previous paleoclimatic studies have exploited *Betula* leaf cuticle characteristics to reconstruct two important annual climate parameters: growing degree-days and atmospheric [CO_2] (Wagner-Cremer et al. 2010). However, *Betula glandulosa*, a North American dwarf birch, has not been investigated for either of these functional relationships. In this study we used *B. glandulosa* leaves from Canadian herbaria to calculate cell undulation index (UI) and stomatal index (SI). We hypothesized that undulation index would correlate positively with growing degree days above 5 degrees C (GDD_5) and that SI would correlated negatively with CO_2 concentration. The initial epidermal cell analysis identified two morphotypes with significantly different epidermal cell areas. Each morphotype has a distinct but significant positive correlation with GDD5. SI's of the leaves analyzed in this study were unresponsive to recent increases in [CO_2]. It is possible that a response limit to increasing [CO_2] has been reached in modern birch samples. Further investigation of *B. glandulosa* SI for reconstructing [CO_2] will require the use of subfossil leaf material, or a more extensive herbarium study. This is the first study to investigate the possibility of using microphenological proxies to reconstruct GDD_5 and [CO_2] in the North American subarctic, an area where knowledge of past climate change is crucial for anticipating future plant productivity and soil Carbon fluctuations.

Wagner-Cremer, F., Finsinger, W. and Moberg, A., 2010. Tracing growing degree-day changes in the cuticle morphology of Betula nana leaves: a new micro-phenological palaeo-proxy. J. Quaternary Sci., v. 25. p. 1008–1017.

TWO-STEP DEGLACIATION OF THE UMANAK TROUGH, WEST GREENLAND

Jennings, Anne E [1]; **Sheldon**, Christina [2]; **Andrews**, John T [3]; **Hogan**, Kelly [4]; **Dowdeswell**, Julian A [5]; **Ó Cofaigh**, Colm [6]; **Kilfeather**, Aoibheann [7]

[1] University of Colorado; anne.jennings@colorado.edu
[2] University of Colorado and University of Aarhus; christina.sheldon@colorado.edu
[3] University of Colorado; andrewsj@colorado.edu
[4] Scott Polar Research Institute, University of Cambridge; kah55@cam.ac.uk
[5] Scott Polar Research Institute, University of Cambridge; jd16@cam.ac.uk
[6] Durham University; colm.ocofaigh@durham.ac.uk
[7] Durham University;

Sediment cores, TOPAS acoustic profiles, and swath bathymetry data collected during cruise JR175 of RRS James Clark Ross in 2009 in the Umanak Trough, West Greenland, provide evidence for a two-step deglaciation of the trough. Swath bathymetry data show that the Greenland Ice Sheet extended to the shelf edge via an ice stream in the Umanak fjord-trough system during the Last Glacial Maximum (LGM) (O'Cofaigh et al., subm; Dowdeswell et al., in prep). The main objective of the study was to document the timing and rate of ice retreat and the role of the West Greenland Current (WGC) in initiating or sustaining ice retreat. Core sites with a till (or glacigenic debris flow on the adjoining continental slope) to glacial-marine boundary within reach of the 6-m limit of the vibrocores were selected on the basis of TOPAS high-resolution acoustic profiles. Four vibrocores were collected along a transect from the trough-mouth fan on the continental slope (VC46), outer-shelf moraines (VC45, VC43), to the mid-shelf landward of a large grounding-zone wedge (GZW) (VC42). Sediment core data used to determine changes in environmental conditions from the LGM to the early Holocene included lithofacies analysis from x-radiography and visual core descriptions, IRD stratigraphy (ice-rafted detritus counts from x-radiographs), quantitative x-ray diffraction mineralogy to document changes in sediment provenance, and foraminiferal assemblage analyses. Radiocarbon dates on foraminifers and molluscs constrained the timing of events interpreted in the cores. At the LGM, the Umanak Ice Stream delivered glacigenic debris flows to the trough-mouth fan on the continental slope (VC46). Debris flow deposition at the site of VC46 ceased prior to ice retreat from the shelf edge. Seventy centimeters of bioturbated mud containing very little IRD overlie the debris flows and contain foraminiferal faunas consistent with West Greenland Current Atlantic Water impinging on the slope. The onset of deglaciation of the shelf is marked by an abrupt increase in sedimentation rate on the slope inferred from flame structures marking the onset of pebbly mud at 198 cm in VC46. This transition coincides with high percentages of the glacial-marine indicator species, Elphidium excavatum clavata. The pebbly mud interval ends at 120 cm with a buff-colored detrital carbonate (DC) unit 1-cm thick. The DC unit has a date of 14.07 cal kyr BP and is associated with a large influx of Atlantic fauna. Shelf-edge core VC45 penetrated to the top of the till forming the shelf-edge moraine. A date of 14.72 cal kyr BP on glacial marine foraminifers in pebbly mud only 5 cm above the top of the till closely constrains the timing of ice retreat from the shelf edge. This age likely coincides with the onset of pebbly mud deposition at 198 cm in VC46. The massive pebbly mud in VC45 ends at 100 cm with a buff-colored detrital carbonate unit 1-cm thick, identical to that dated to 14.07 cal kyr in VC46. The overlying bioturbated mud in VC45 has low IRD content and a chilled Atlantic Water fauna indicative of relatively high productivity. A date of 13.86 cal kyr BP from only 5 cm above the DC event indicates ice distal conditions were established by this time and that deglaciation was initiated and completed during the Bølling Interstadial. A second phase of deglaciation is indicated by a return to very high IRD counts above the bioturbated mud in both VC46 and VC45. We infer from stratigraphic correlations to a date in VC43 that the onset of this high IRD interval is c. 11.35 cal kyr BP. A 40-m high GZW identified from TOPAS acoustic profiles forms a bathymetric high on the mid shelf that

separates outer and inner bathymetric depressions of the Umanak Trough (Dowdeswell et al., in prep). We infer that retreat from this GZW is the source of the renewed IRD deposition in VC45 and VC46. VC42 located c. 85 km landward of the moraine contains a till to proximal glacial-marine sequence that represents continued landward retreat from the mid-shelf moraine. Core MSM343520, located between the mid shelf moraine and VC42, has a closely constraining deglacial age of 10.9 cal kyr BP (McCarthy, 2011). We infer that deglaciation of VC42, 32 km to the east of MSM343520, must be close to McCarthy's 10.9 cal kyr BP age. The foraminiferal fauna in stratified glacial-marine sediments of VC42 contain a peak in chilled Atlantic Water foraminifers suggesting that West Greenland Current Atlantic Water was present during the initial early Holocene retreat from the moraine. Farther up in the section, species indicative of glacial meltwater replace the Atlantic fauna.

Dowdeswell, J.A., Hogan,K.A., Ó Cofaigh,C., Fugelli,E.M.G., Evans, J., R. Noormets, R., in prep. Late Quaternary ice flow in a West Greenland fjord and cross-shelf trough system: submarine landforms from Rinks Glacier to Umanak Trough.

McCarthy, D.J. 2011. Late Quaternary ice-ocean interactions in central West Greenland. Doctoral thesis, Durham University. Available at Durham E-Theses Online: http://etheses.dur.ac.uk/868/

Ó Cofaigh, C. , Andrews, J.T., Jennings, A.E., Dowdeswell, J.A., Kilfeather, A.A., and Hogan, K.A., submitted. Glacimarine lithofacies, provenance, and depositional processes on a West Greenland trough-mouth fan. Journal of Quaternary Science.

SEDIMENTARY AND GEOCHEMICAL EVIDENCE OF RECENT MARINE TRANSGRESSION IN THE SEDIMENTS OF A HYPERSALINE COASTAL BASIN, SHELLABEAR LAKE, MELVILLE ISLAND, NORTHWEST TERRITORIES

Kathan, Kasey [1]; **Lamoureux**, Scott [2]; **Dugan**, Hilary [3]

[1] Queen's University; kmkathan@gmail.com
[2] Queen's University; scott.lamoureux@queensu.ca
[3] University of Illinois;

In the Arctic, research has focused on understanding the processes of lacustrine isolation from marine water due to isostatic rebound. However, very little work has focused on understanding the impacts of marine transgression on lacustrine systems. Understanding the lacustrine evolutionary processes of salinity development and its relationship to marine transgression is an important component of understanding the potential future impacts of climate change and particularly, related eustatic sea level rise on Arctic coastal lake systems.

Shellabear Lake (unofficial name; 74°50'N, 113°30'W, 0.59 km2) is a hypersaline (56 PSU) seasonally-isolated marine basin on Melville Island in the western Canadian High Arctic. The primary inflow to the basin is nival runoff from the 17 km2 catchment. The basin is at sea-level and currently connected to the ocean by a ~1 m deep outlet, which is obstructed by snow and ice between the months of October and June. The lake is located to the west of the current zero isobase and within the region of current transgression due to fore-bulge collapse (Lajeunesse and Hanson, 2008; Tarasov and Peltier, 2004). The development of hypersalinity within the basin is thought to be through a process of the accumulation of brine rejected during ice formation from sea water and has been modeled to have occurred rapidly after the initiation of tidal connection (Dugan and Lamoureux, 2011).

Three surface gravity cores were recovered from the basin in 2009 from depths ranging between 25 and 27m. The location of these cores range from inflow proximal to inflow distal and all are laminated for the majority of the record with the distinct exception of the most recent sediments. All cores were split and thin-sectioned for stratigraphic interpretation and detailed grain size (1mm resolution) analysis. Cores were analyzed for geochemistry using μXRF (ITRAX™ Core Scanner) at a 0.1 mm resolution to capture stratigraphic geochemical variability. Age control for the most recent sediments is constrained by 210Pb profiles from one of the cores.

The uppermost five centimeters of the sediment cores are characterized by a shift from reduced laminated sediments at depth into massive oxidized sediments with a number of reduced laminations capping the sequence (Figure 1). As the basin is currently anoxic at depth, these sediments are believed to indicate a period of previous ventilation from which the lake has relatively recently recovered. 210Pb results indicate that the base of this ventilation transition was during the early 20th century and that the return to laminated reduced sediments at the top of the sequence was within the last decade.

The geochemical signatures indicate that the units related to the recent ventilation event are significantly influenced by variability in the redox sensitive elements (Fe, Mn) and indicators of salinity change (Br/Cl, Croudace et al., 2006). As Fe has a lower redox potential than Mn, low values of the Fe/Mn ratio indicate higher levels of oxygenated bottom water conditions. Each of the cores presents Fe/Mn minima at the center of the rust-red colored unit of the uppermost sediments (~3.5 cm depth). However, the most distal and shallowest core, indicates a brief Fe/Mn excursion prior to the basin wide ventilation with a period of high variability following. This core also has a notable early shift in Br/Cl that is not present in the deeper and more proximal cores

These and other geochemical indicators have led us to interpret the following sequence of events. 1. The lake basin remained meromictic following isolation from marine influence upon coastal isostatic uplift as indicated by the accumulation of rhythmic, reduced laminations. The duration of this phase is

open due to the short surface cores in this study. 2. Initial tidal connection to the basin occurred as irregular storm surges. These events would introduce oxygenated marine water to the meromictic lake basin with the marine waters entering as mesopycnal flows and mixing with the hypolimnion of the lake through diffusive processes. The shallowest, marine-proximal site would be most sensitive to the salinity changes associated with this marine intrusion as indicated by the early shift in the Br/Cl ratios. The early excursion in Fe/Mn at the marine-proximal shallow core site indicates that these initial phases of ventilation were not sufficient to penetrate to the deepest portion of the basin and were likely limited in spatial and temporal extent. 3. Upon further transgression, full seasonal tidal connection was established with the lake basin. Oxygenated marine waters would be introduced to all depths within the basin as the system mixed with dense (saline and cold) marine waters. This ventilation phase results in the prominent low Fe/Mn values and visible oxidized iron in the sediment. 4. With the establishment of seasonal tidal exchange, subsequent brine rejection during seasonal sea ice formation forms hypersaline plumes which accumulate in the basin. As these plumes are formed in the surface waters, they initially may deliver oxygen to the hypolimnion during the winter months during periods of tidal isolation. However, over time, the accumulation of hypersaline waters at depth progressively limits the degree of vertical brine mixing, resulting in the uppermost presence of the reduced laminations and elevated Fe/Mn values.

The stratigraphy and geochemical profile of Shellabear Lake supports the modeled results of Dugan and Lamoureux (2011) indicating that given the appropriate conditions, hypersalinity can develop in a seasonally isolated marine basin within a short period of time, potentially within the last decade at Shellabear Lake.

Croudace, I.W., Rindby, A., Rothwell, R.G., 2006, ITRAX: description and evaluation of a new multi-function X-ray core scanner: from: Rothwell, R.G. 2006. New Techniques in Sediment Core Analysis: Geological Society, London, Special Publications 267, p. 51-63.

Dugan, H.A., Lamoureux, S.F., 2011, The chemical development of a hypersaline coastal basin in the High Arctic: Limnology and Oceanography 56, p. 495-507.

Lajeunesse, P., Hanson, M.A., 2008, Field observations of recent transgression on northern and eastern Melville Island, western Canadian Arctic Archipelago: Geomorphology 101, p. 618-630.

Tarasov, L., Peltier, W.R., 2004, A geophysically constrained large ensemble analysis of the deglacial history of the North American ice sheet complex: Quaternary Science Reviews 23, p. 359-388.

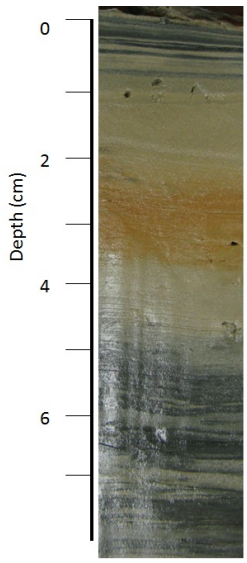

Fig 1. Uppermost sediments from core 09SB04, an inflow proximal core from 26m water depth, with the characteristic shift in sediment preservation within the top 5 cm.

A COMPARISON OF TWO LAKE SEDIMENT RECORDS ON ADAK ISLAND, ALASKA AND THE POTENTIAL FOR A RECONSTRUCTING PRECIPITATION TO 2 KA

Krawiec, Anne C. [1]; **Kaufman**, Darrell S. [2]; **Vaillencourt**, David A. [3]

[1] Northern Arizona University; ack62@nau.edu
[2] Northern Arizona University; darrell.kaufman@nau.edu
[3] Northern Arizona University; davev@nau.edu

The central Aleutian Islands are a largely unexplored area for paleoclimate reconstructions in subarctic latitudes of the North Pacific. This study focuses on the biogenic silica (BSi) content and its dilution by mineral-matter input as recoded in sediment cores from Heart Lake and Andrew Lake on Adak Island, Alaska. Andrew Lake is located 10 km northeast of Heart Lake on Adak Island. Andrew Lake is much larger (8.4 km2) and deeper (25 m) compared with Heart Lake (0.25 km2 and about 8 m deep). Andrew Lake is fed directly from steep volcanic mountain streams, whereas Heart Lake has a complex catchment including two larger lakes upstream. Sediment cores were collected from the lakes in the summers of 2009 and 2010. Age models were developed based upon radiocarbon dating of macrofossils and the 1963 spike in plutonium activity. In addition, a lead profile was analyzed for the last 200 years on the Andrew Lake surface core. Tephra thicknesses, assumed to be deposited instantaneously, were subtracted from the sediment depth for the age modes. Surface cores that include the sediment/water interface were spliced onto their respective long cores using the tephra beds for correlation. In addition, the Heart and Andrew lake cores were correlated based on tephrostratigraphy. Each core was sampled contiguously at 2 mm (annual to 3-year resolution) for the instrumental period, and at 1 cm intervals (near-decadal resolution) for the last 2000 years. Samples were analyzed for BSi by wet-alkaline extraction, as outlined in Mortlock and Froelich (1989).

Both records show similar downcore trends in BSi, dry bulk density (DBD), and sedimentation rate during the last 2000 years, except for the period between 750 and 1350 AD during which BSi and sedimentation rate trends diverge (Figure 1). BSi content is a function of aquatic primary production, dilution by clastic sediment, and preservation of silica tests (Wetzle, 2001). Microscopic observation shows intricately detailed diatom tests throughout the core indicating that preservation of tests does not contribute to downcore variability. Aquatic primary production typically responds to sunlight, water temperature, and nutrient availability (Wetzle, 2001). The available climate data from Adak (1942-1996; National Climate Data Center) show little seasonality (<10 °C between winter and summer), nearly continuous cloud cover, and winter temperatures normally too high for lake ice to develop. Therefore sunlight and temperature likely have little influence on production, as suggested in the lack of significant correlations between BSi and temperature during any season. Strong winds (daily average = 24 km/hr) promote re-suspension of lake bottom nutrients. During the past 2000 years, BSi flux varied less than mineral flux at both Heart and Andrew lakes (Heart Lake: BSi = 0.47 ± 0.27, mineral = 1.5 ± 1.1 g/cm3/yr; Andrew Lake: BSi = 0.61 ± 0.41, mineral = 2.5 ±1.5 g/cm3/yr). BSi and mineral flux calculations for both lakes are largely controlled by the sedimentation rate, which has the highest variability and lowest resolution of the three parameters especially for Andrew Lake (Figure 2).

Rather than production, we interpret downcore changes in BSi % as fluctuations in the amount of clastic sediment delivered to the lake by streams. This interpretation is supported by the inverse correlation between total annual precipitation (averaged for a three-year period centered on the BSi-sample age) and BSi % at both Heart and Andrew lakes (Heart Lake: r2 = 0.37; p = 0.03 (all p values adjusted for autocorrelation); n = 15; Andrew Lake: r2 = 0.47; p = 0.02; n = 15) (Figure 2). Much of the 1500 mm/yr average precipitation falls in storms with greater than 19 mm (0.75 inches), which causes overland flow and increased sedimentation into the lakes. This effect is amplified at Heart Lake, where the lake size to catchment ratio is much lower. In fact, comparing BSi content to the number of days per year with > 19 mm of precipitation strengthens the correlation with BSi % at Heart Lake (r2 =

0.51, p = 0.02), while remaining significant at Andrew Lake (r2 = 0.33, p = 0.06).

BSi % at Heart Lake correlates inversely with spring (March, April, May; MAM) precipitation (r2 = 0.40; p = 0.02) and number of days per spring season with > 19 mm of precipitation (r2 = 0.60, p = 0.02). In addition to runnoff directly from storms in MAM, this precipitation also induces snowmelt from the upper elevations of the catchment. This coupled with reduced groundcover prior to the seasonal growth of grass increases soil erosion and sedimentation into the lake. This differs slightly for Andrew Lake where BSi % does not significantly correlate with MAM precipitation, but does correlate with spring storm / snowmelt days with greater than 19 mm of precipitation (r2 = 0.43, p = 0.09).

We applied the inverse relation between spring precipitation and BSi % to reconstruct a near-decadally resolved record of spring precipitation at Heart and Andrew lakes. Both records suggest high precipitation compared with the record mean at 0 AD, tapering to dryer conditions at 700 AD. The records from the two lakes diverge between 1350 and 700 AD. Both records show increased precipitation relative to the record mean and conditions similar to present during the last 200 years.

Mortlock, R.A., and Froelich, P.N., 1989, A simple method for the rapid determination of biogenic opal in pelagic marine sediments, Deep-Sea Research, Part A: Oceanographic Research Papers, v. 36, p. 1415-1426.
Wetzel, R. G., 2001, Limnology: Lake and River Ecosystems, 1006 pp. Academic Press, San Diego, Calif.

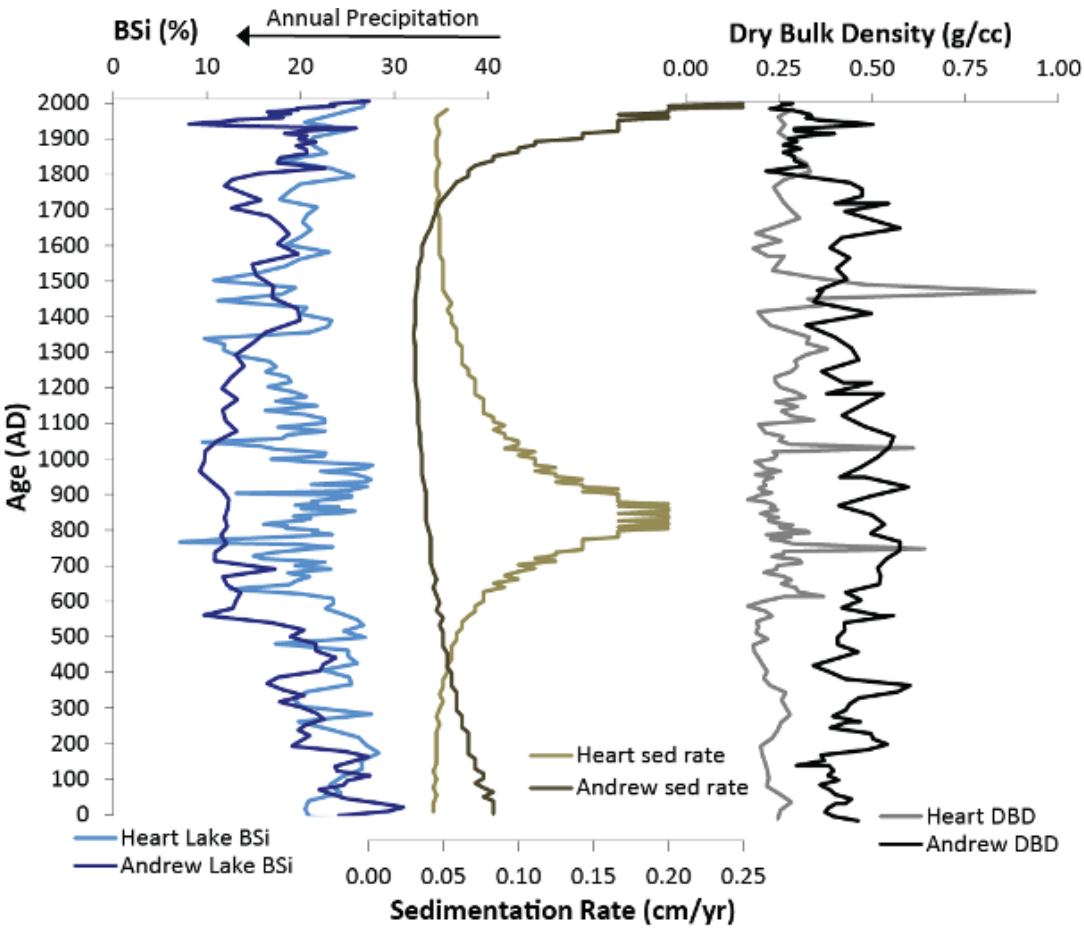

Fig 1. BSi, Sedimentation rate, and DBD comparisons between Heart and Andrew Lakes for the 2000-year record

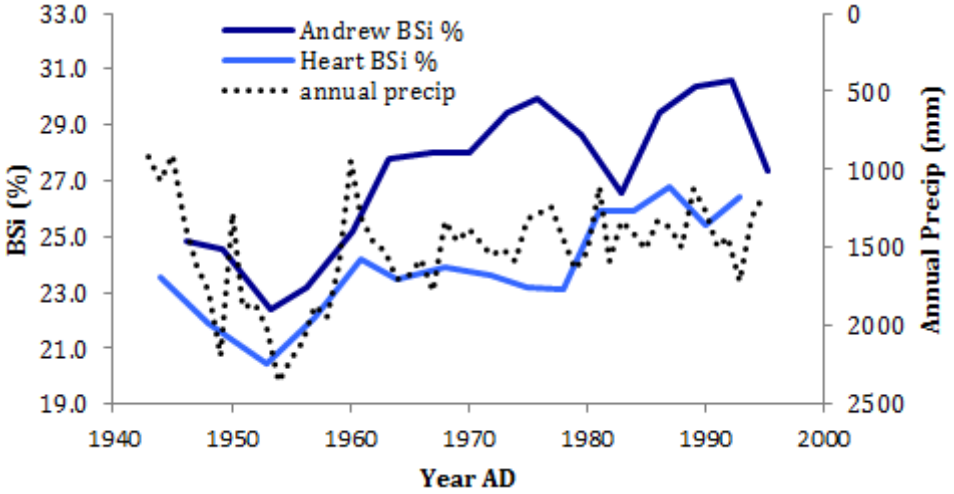

Fig 2. Heart and Andrew Lake BSi content for the instrumental record period with sum annual precipitation in millimeters

DEVELOPING K-5 AND PUBLIC OUTREACH PRODUCTS FOR ALASKAN GLACIOLOGY AND SEA LEVEL USING THE iPAD APP PLATFORM

Kreutz, Noah [1]; **Plourde**, Joshua [2]; **Campbell**, Seth [3]; **Kreutz**, Karl [4]; **Wanamaker**, Alan [5]

[4] Presenting Author

[1] Asa Adams Elementary School; karl.kreutz@maine.edu
[2] University of Maine;
[3] University of Maine;
[4] University of Maine;
[5] Iowa State University;

The relationships among atmospheric chemistry, climate, glaciers, and sea level are arguably among the most important scientific issues facing society. Communicating the complexity inherent in various research approaches to these issues is challenging, particularly to groups with little or no direct experience with glaciology. The recent introduction of the iPad platform, and in particular its use in education, presents new opportunities for content delivery in highly interactive ways. Here we describe recent work designing software and content for iPad apps, centered around our work in Denali National Park and the Gulf of Maine, initially with two focus groups: grades K-5, and climbers/general public visiting Denali National Park, Alaska. Our goal at the Arctic Workshop is to stimulate discussion with colleagues that can better inform our content collection efforts during the coming Alaskan summer field season, and software development over the coming year.

Our initial effort with app development is centered around changes in the Gulf of Maine climate and oceanography during the last millennium, with a component of sea level included. The Holocene sea level history of the Gulf of Maine is dynamic, responding both to eustatic sea level rise and isostatic rebound. K-5 students in Maine most often do not recognize this, but in fact are often surrounded by evidence of dramatically different sea level during the last deglaciation and Holocene (e.g., marine deposits and fauna, glacial moraines and other deposits). Therefore, we are working on an iPad app that integrates components of the existing Maine Ice Age Trail (http://iceagetrail.umaine.edu/) with interactive maps and diagrams that can be manipulated to show the evolution of Holocene sea level and changes in the Maine landscape in a dynamic time sense. Research techniques involve schlerochronology, or the use of accretionary hard parts in organisms, to reconstruct past changes in ocean temperature, salinity, and circulation patterns. All of this will be geared for the K-5 level, tested in the classroom (Asa Adams Elementary, Orono, Maine), and of course ultimately be available to educators, students, and the general public through iTunes.

The sea level theme that will be prevalent in the initial Gulf of Maine app development will be carried into our second effort, to develop an app focusing on glaciology and in particular the relationship between climate, Alaskan glacier change, and sea level. This app will feature a K-5 student narrator (the first author) to provide commentary, tangible student field experience, and demonstration of classroom activities. For example, several glaciologists have used Flubber-based experiments in classroom settings to demonstrate various basic glaciological concepts. We envision at least one interactive map that will allow students to scroll through time (from the LGM to today) to see how sea level change has affected global coastlines, as well as a predictive tool that explains different possible future sea level scenarios.

Our third planned app will focus on the West Buttress route on Denali, and be geared towards mountaineers using the route as well as the general public visiting Denali National Park. We intend to make an interactive map of the West Buttress route that interfaces our glaciological research on the Kahiltna Glacier with that of other colleagues. In particular, we seek to educate climbers and public on basic issues such as ice thickness, velocity, mass balance, and local meteorology. We envision a climber or interested visitor being able to pick a spot along the route (or established campsite), and pull up various glaciological information and associated educational material.

NON-LINEAR HOLOCENE CLIMATE EVOLUTION IN THE NORTH ATLANTIC: A HIGH-RESOLUTION, MULTI-PROXY RECORD OF GLACIER ACTIVITY AND ENVIRONMENTAL CHANGE FROM HVÍTÁRVATN, CENTRAL ICELAND

Larsen, Darren J [1]; **Miller**, Gifford H [2]; **Geirsdóttir**, Áslaug [3]; **Ólafsdóttir**, Sædís [4]

[1] University of Colorado/INSTAAR; darren.larsen@colorado.edu
[2] University of Colorado/INSTAAR;
[3] University of Iceland;
[4] University of Iceland;

Iceland is well situated to monitor North Atlantic Holocene climate variability and terrestrial sites there offer the potential for well-dated, high-resolution, continuous records of environmental change and/or glacier activity. Laminated sediments from the proglacial lake Hvítárvatn provide a continuous record of environmental change and the development of the adjacent Langjökull ice cap for the past ~10.2 ka. Replicate lake sediment cores, collected from multiple locations in the basin, are placed in a secure geochronology by splicing a varve chronology for the past 3 ka with a tephra-constrained, paleomagnetic secular variation derived chronology for older sediments. Multiple proxies, including sedimentation rate, bulk density, ice-rafted debris, sediment organic matter, biogenic silica, and diatom abundance, allow annual to multi-decadal resolution and reveal a dynamic Holocene terrestrial climate. Following regional deglaciation of the main Iceland Ice Sheet, summer temperatures were high enough that mountain ice caps had already melted, or were contributing insignificant sediment to the lake. Pronounced increases in sedimentation rate, sediment density, and the influx of terrestrial organic matter, between 8.5 and 7.9 ka suggest early Holocene warmth was interrupted by two distinct pulses of cold summers leading to widespread landscape destabilization and possibly glacier growth. The Holocene thermal maximum (HTM; 7.9 to 5.5 ka) was characterized by high within-lake productivity and ice-free conditions in the watershed. Neoglaciation is recorded as a non-linear transition toward cooler summers, landscape destabilization, and the inception and expansion of Langjökull beginning ca. 5.5 ka, with notable increases in ice-cap size and landscape instability at 4.2 and 3.0 ka. The past two millennia are characterized by the abrupt onset of sustained cold periods at ca. 550 and 1250 AD, separated by an interval of relative warmth from ca. 950 to 1150 AD. The greatest Holocene extent of Langjökull occurred in the nineteenth century and is coincident with peak landscape instability, followed by ice recession throughout the twentieth century.

PROPAGATING ATMOSPHERIC PATTERNS ASSOCIATED WITH SEA ICE MOTION THROUGH THE FRAM STRAIT

Liptak, Jessica [1]; **Strong**, Courtenay [2]

[1] University of Utah; jessica.liptak@utah.edu
[2] University of Utah; court.strong@utah.edu

The Fram Strait is the primary conduit of sea ice export in the Arctic. Ice motion, in turn, largely depends on atmospheric forcing, which is often measured in terms of storm tracks and standing-wave teleconnections such as the North Atlantic Oscillation (NAO). While storm tracks and teleconnection patterns contain information about the mean pressure and wind fields, they do not fully capture the variability associated with moving features like synoptic-scale cyclones. Thus, Hilbert complex empirical orthogonal function (HEOF) analysis is used to examine the variations in daily Fram Strait sea ice export that are associated with with propagating phenomena.

HEOFs of zonal and meridional components of the surface wind field obtained from NCEP-NCAR Reanalysis (Kalnay et al., 1996) are calculated from 60◦-90◦N for winters during 1979–2006. Following Tsukernik et al. (2010), an index of Fram Strait sea ice export is defined using the meridional component of the surface wind. Since the phase of each HEOF is arbitrary, a phase shift is applied such that the temporal correlation between the propagating pattern and the sea ice export index is consolidated entirely into the real domain. As a result, the real part of the HEOF depicts a phase with the clearest statistical relevance to Fram Strait sea ice export.

The leading two HEOFs of surface wind account for 25% of the variance in the wind field. Following the application of the phase shift, the real parts of the first and second HEOFs explain 7% and 10% of the variance in Fram Strait sea ice export, respectively. Both HEOFS depict patterns representative of the passage of synoptic-scale cyclones where sea ice export is strongest when a downstream cyclonic circulation enhances northwesterly flow through the Fram Strait. Correlation maps between the surface wind and sea ice export represent a combination of the two storm tracks captured by the HEOFS with northwesterly flow from the pole through the Fram Strait between a cyclonic circulation in the Barents Sea and an anticyclonic circulation centered over northwestern Greenland.

Kalnay, E. et al., 1996, The NCEP/NCAR 40-year reanalysis project: Bulletin of the American Meteorological Society, v.77,p.437–470.

Tsukernik, M., C. Deser, and R. Tomas, 2010, Atmospheric forcing of Fram Strait sea ice export: a closer look: Climate Dynamics, v.35, p.1349-1360.

MARINE EVIDENCE FOR A GLACIAL ICE STREAM IN AMUNDSEN GULF, CANADIAN ARCTIC ARCHIPELAGO.

MacLean, Brian [1]; **Blasco**, Steve [2]; **Bennett**, Robbie [3]; **Lakeman**, Tom [4]; **Hughes-Clarke**, John [5]; **Kuus**, Pim [6]; **Patton**, Eric [7]

[1] Geological Survey of Canada, Atlantic; Brimacle@nrcan.gc.ca
[2] Geological Survey of Canada, Atlantic; sblasco@nrcan.gc.ca
[3] Geological Survey of Canada, Atlantic; rbennett@NRCan.gc.ca
[4] University of Alberta; tlakeman@ualberta.ca
[5] University of New Brunswick; jclarke@unb.ca
[6] Geological Survey of Canada, Atlantic; pkuus@NRCan.gc.ca
[7] Geological Survey of Canada, Atlantic; epatton@NRCan.gc.ca

The study area lies at the southwestern end of the Northwest Passage adjacent to the Beaufort Sea. It comprises Amundsen Gulf, Dolphin and Union Strait and Coronation Gulf. High resolution multibeam sonar imagery and sub-bottom profiles of the seabed have been acquired by ArcticNet and Ocean Mapping Group, University of New Brunswick on transits through these waterways for the past decade. Studies of these data revealed a variety of seabed features including glacial sole marks or flutings, drumlins, a moraine, ice-contact strata, current scours, iceberg scours, bedrock outcrops and discontinuous sediment deposits of variable thickness.

The presence of glacial ice streams in channels of the Canadian Arctic Archipelago was postulated by earlier workers based on various parameters including regional morphologies (Denton and Hughes, 1981), satellite imagery (Clark and Stokes, 2001; Stokes et al., 2005), satellite imagery and limited marine data (Stokes et al., 2006; Des Angelis and Kleman, 2007) and from marine data (MacLean et al., 2010). A glacial ice stream in Amundsen Gulf was interpreted by Stokes et al. (2006) from a study of satellite imagery and limited marine data.

The pattern of sole marks or glacial flutings on the seabed in Amundsen Gulf now evident from extensive multibeam imagery, and ice flow patterns identified on the adjacent mainland and islands by Dyke and Prest (1987), Sharpe (1992) and Kerr (1994) confirm that an ice stream of the Laurentide Ice Sheet occupied Amundsen Gulf, Coronation Gulf, Dolphin and Union Strait and parts of the adjacent terrestrial areas during the Last Glacial Maximum, 26,500-19,000 calibrated years BP. Part of the northwestward-flowing ice stream was deflected around the Colville Mountains on Victoria Island and rejoined the main ice stream in Amundsen Gulf by way of Prince Albert Sound.. The grounded ice stream extended northwestward to the margin of the inner shelf in the Beaufort Sea at a depth of 450 m. Retreat from that maximum position began prior to 13,000 cal yr BP (Scott et al., 2009).

The bathymetry of Amundsen Gulf and known extent of the ice stream on land indicates the ice was at least 700 m thick in the gulf. Thick, multi-sequence deposits of ice-contact sediments in the northwestern part of Amundsen Gulf suggest that a number of ice retreats and re-advances occurred in that region. A series of moraines at the northwestern end of the gulf mark temporary positions of the ice stream front during final retreat. Early stages of ice retreat may have been associated with meltwater discharge under the ice stream as evidenced by current erosion associated with some of the sole marks or glacial flutings. Melting at the leading edge of the ice stream resulted in calving of icebergs and the generation of keel-scour marks in the seabed. Retreat of the ice was relatively rapid as indicated by generally sparse deglacial glaciomarine sediment in Amundsen Gulf. Based on terrestrial radiocarbon dates the retreating ice front had reached eastern Amundsen Gulf by about 12,000 cal yr BP (10.7 14C ka BP, Sharpe 1992; Kerr, 1994, 1996).

A later ice re-advance trending to the west and west-southwest formed extensive drumlin fields on southern Victoria Island (Sharpe, 1992; Stokes et al. (2006). This event is also evident in northwestern Coronation Gulf, in Dolphin and Union Strait, and on the adjacent mainland where those trends are superimposed on the earlier northwesterly ice flow features (St-Onge and McMartin, 1987). The lack of Holocene sediments draping the sole marks or flutings, and outcrops of exposed bedrock and glaciomarine sediment indicates very low sedimentation rates in most areas of Amundsen Gulf since ice retreat.

CLIMATE INDUCED CHANGES OF THE TREE-LINE ECOTONE IN THE POLAR URALS AND IMPACTS ON LAND-SURFACE PROPERTIES

Mazepa, Valeriy [1]; **Ivanov**, Valeriy [2]; **Shiyatov**, Stepan [3]

[2] Presenting Author

[1] Institute of Plant and Animal Ecology, Ural Branch Russian Academy of Sciences, Yekaterinburg, Russia; mazepa@ipae.uran.ru
[2] Department of Civil and Environmental Engineering, University of Michigan, Ann Arbor, U.S.A.; ivanov@umich.edu
[3] Institute of Plant and Animal Ecology, Ural Branch Russian Academy of Sciences, Yekaterinburg, Russia; stepan@ipae.uran.ru

The Arctic region has been warming over the last 30 years and the process has been accelerating at unprecedented rates over the last decade (Serreze et al., 2000). This climate transformation has triggered a number of changes in terrestrial ecosystems that are characterized by a high sensitivity to the climate change. Recent studies indicate an occurring expansion of trees and shrubs into tundra areas across the polar regions of Alaska, Canada, and Russia. As shrubs and trees increase in abundance and size, they modify the thermal, hydrological, and microbial regimes of the soil. There is a need to better understand how changes of these regimes will impact ecosystems in future as well how they will affect global climate processes through feedback mechanisms. For instance, positive feedbacks associated with higher heat capacity of thawing soils and decreasing surface albedo because of a larger tree cover could amplify atmospheric heating and can further accelerate Arctic climate change.

This study focuses on climate-induced changes in the forest and forest-tundra ecosystems of mountainous areas in the Polar Urals (Russia) and the associated land-surface feedback mechanisms. In this area, climate change in the second half of the 20th century led to increases in air temperature and rainfall, which caused one of the rapidest recorded expansions of woody vegetation into tundra areas. Specifically, the study site is a part of the Polar Urals Monitoring Observatory managed by the Institute of Plant and Animal Ecology of the Ural Branch of the Russian Academy of Sciences. It is located on the eastern slope of the Urals range (200-350 m a.s.l.) in the Sob' River watershed underlain by continuous permafrost, (~66°46′ N, ~65°25'E, Fig. 1). Within a studied alpine ecotone, vegetation belts are classified as follows (in the upslope direction): alpine taiga, "subgoltsy", alpine tundra, and cold goltsy desert (Mazepa et al., 2011). Larch (Larix sibirica) forest-tundra communities prevail in the timberline ecotone, while open larch forest and larch forest with Siberian spruce (Picea obovata) and birch (Betula tortuosa) occur in the lower part of the area (Shiyatov et al., 2005). Average frost-free period is approximately 64 days, leading to short growing seasons that last from mid-June to early August. Based on the long-term meteorological record at a nearby station (Salekhard), over the past

~90 years (1920–2004) mean summer temperatures (JJA) have increased by 0.9°C and mean winter temperatures (DJF) by 1.2°C, as compared to the 1883-1920 period. Over the same interval, mean summer precipitation has increased from 146 to 178 mm, while as winter precipitation has grown from 67 to 113 mm (Mazepa and Devi, 2007). Correspondingly the upper boundaries of the areas of sparse tree growth, open forests, and closed forests shifted both on slopes exposed to strong westerly winds and in the areas where summer temperatures are the main limiting factors (Shiyatov et al., 2005, 2007, 2009; Fig. 2). The 80-100 m upward expansion of single trees and forests was accompanied by a marked increase in the vertical and radial tree growth, crown density, and productivity of tree stands (Mazepa, 2005; Mazepa and Devi, 2007).

Eleven altitudinal transects 300-1100 m long and 20-80 m wide were developed for long-term monitoring of spatiotemporal dynamics of alpine forest-tundra and forest-meadow communities starting in early 1960s (Mazepa, 2005). This study focuses on the earliest ecotone transect (Fig. 3), where monitoring program started in 1960. In order to quantitatively assess changes in the composition, structure, and spatial distribution of the forest-tundra communities, three census campaigns of 1960-62, 1999, and 2011 produced detailed mappings of locations of all alive and dead trees, and measurements of their essential allometric and geometric characteristics such as height, crown size, diameter at breast height, etc. In total, measurements of 1494, 1851, and 1985 trees were obtained during the three respective census periods. Analyses of the temporal change of land-surface conditions at the tree scale are presented. Changes of effective surface albedo, shading factors, and radiative characteristics of the area are estimated. The transect domain area has been digitized for further representation in a physically-based model of heat-moisture dynamics of natural vegetated systems. Spatio-temporal modeling of energy and water dynamics will be carried in future. Current instrumentation program of the site will inform model parameterizations.

Mazepa, V.S., 2005, Stand density in the last millennium at the upper timberline ecotone in the Polar Ural Mountains: Canadian Journal of Forest Research, v. 35, p. 2082–2091.

Mazepa, V.S. and N.M. Devi, 2007, Development of multi-stemmed life forms of Siberian larch as an indicator of climate change in the timberline ecotone of the Polar Urals: Russian Journal of Ecology, v. 38(6), p. 440–443.

Mazepa, V.S., S.G. Shiyatov, and N.M. Devi, 2011, Climate-Driven Change of the Stand Age Structure in the Polar Ural Mountains, in Climate Change - Geophysical Foundations and Ecological Effects, ISBN 978-953-307-419-1, p. 377-402, ed. by J. Blanco and H. Kheradmand, InTech.

Serreze, M. C., J. E. Walsh, F. S. Chapin, T. Osterkamp, M. Dyurgerov, V. Romanovsky, W. C. Oechel, J. Morison, T. Zhang, and R. G. Barry, 2000, Observational evidence of recent change in the northern high-latitude environment: Climatic Change, v. 46, p. 159-207.

Shiyatov, S.G., M.M. Terent'ev, and V.V.Fomin, 2005, Spatiotemporal Dynamics of Forest–Tundra Communities in the Polar Urals: Russian Journal of Ecology, v. 36(2), p. 69–75 (translated. from Ekologiya, v. 2, p. 83–90. (In Russian).

Shiyatov, S.G., M.M. Terent'ev, V.V. Fomin, and N.E. Zimmermann, 2007, Altitudinal and Horizontal Shifts of the Upper Boundaries of Open and Closed Forests in the Polar Urals in the 20th Century: Russian Journal of Ecology, v. 38, p. 223–227.

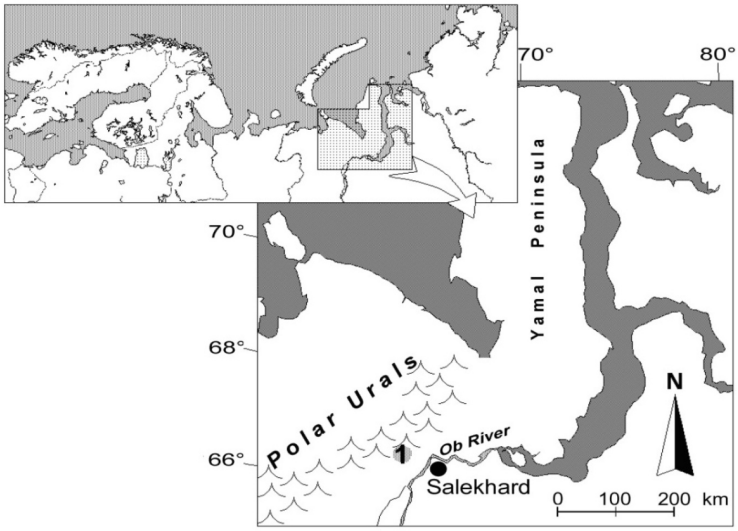

Fig 1. Location of the study area (1) in the Polar Urals region.

Fig 2. Expansion of dense and open larch forests on banks of the Kerdomanshor River, 1962-2004.

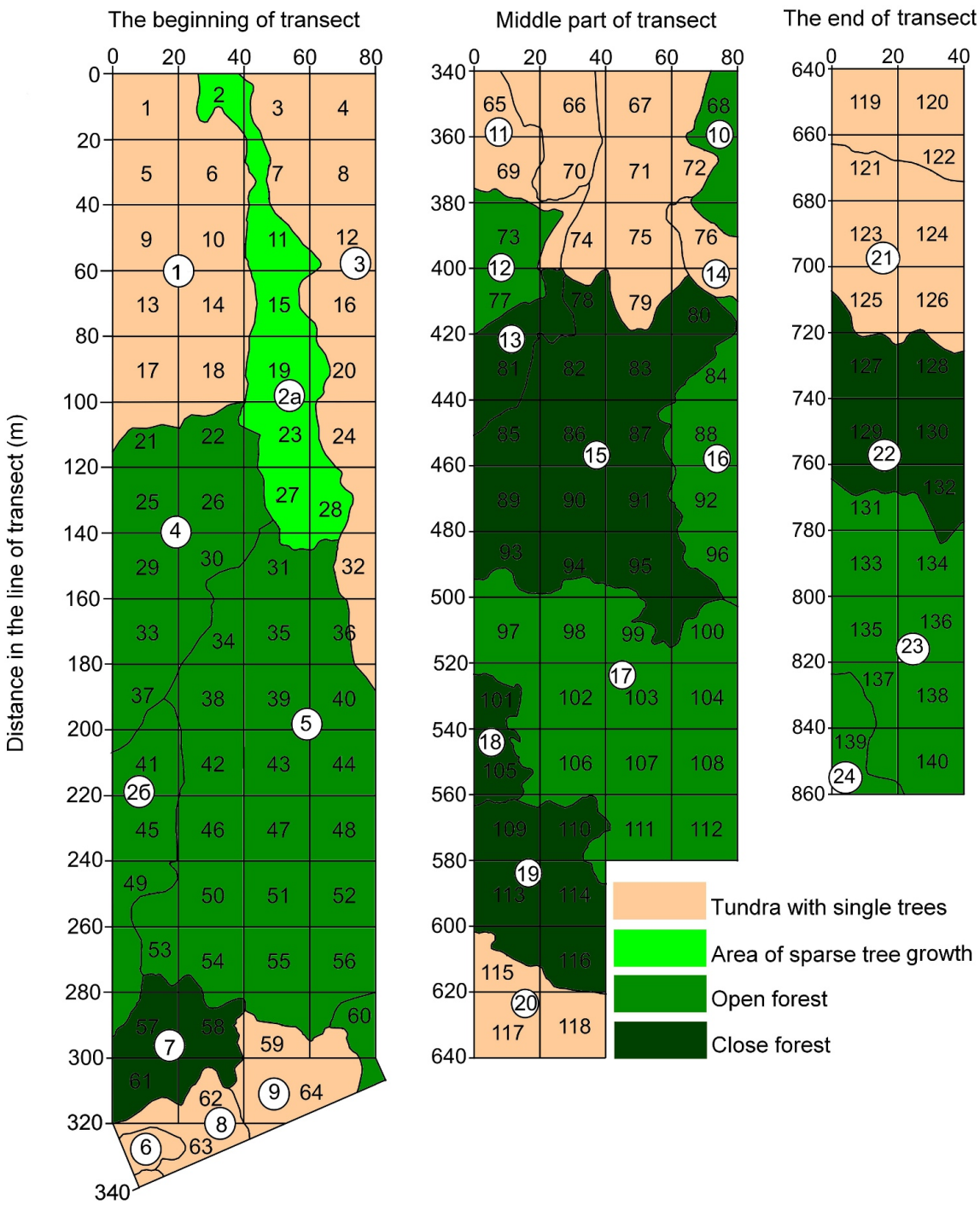

Fig 3. A schematic of the monitored ecotone transect. Numbers indicate individual monitoring polygons.

FJORD-FLOOR SEDIMENTOLOGY AND GEOCHEMISTRY AT THE KRONEBREEN GLACIER, SVALBARD, NORWAY: APPLYING PALEOCLIMATIC TECHNIQUES IN A GLACIMARINE SETTING

McGregor, Daren A [1]; **Brigham-Grette**, Julie [2]; **Powell**, Ross [3]

[1] Colby College; damcgreg@colby.edu
[2] UMass-Amherst; juliebg@geo.umass.edu
[3] Northern Illinois University; ross@geol.niu.edu

During the present period of significant climate flux, scientists are attempting to understand and constrain the way in which Earth responds to these changes, as well as what these changes mean for life on the planet. The polar regions (the Arctic and Antarctic) are particularly sensitive to climatic perturbations, and they house extensive evidence of the impact that warming has had in the past, from changing ocean chemistries to the relationship between glacial retreat and fluctuations in sea level.

As part of an NSF-supported Research Experience for Undergraduates, a group of students traveled to Ny-Alesund, Svalbard, Norway in the summer of 2011 to conduct individual research projects relating to sedimentology and climate studies. Svalbard is an archipelago in the North Atlantic Ocean with a variety of terrains that makes it conducive to studying different aspects of the Holocene geologic record. Sediments throughout the archipelago capture Holocene and modern proxies for past climate fluctuation. This summer's project was based in Kongsfjorden, a northwest-trending fjord with two actively retreating tidewater glaciers (Kronebreen and Kongsvegen) at its head. Rapid sedimentation rates in Kongsfjorden during glacial retreat have resulted in a high-resolution record of the past few decades.

This individual research project (as part of an ongoing senior thesis) seeks to analyze sediment-core geochemistry from the sediments on the floor of Kongsfjorden in a chronostratigraphic framework, using a variety of analytical techniques. This poster presents a multidisciplinary application of X-ray fluorescence, total organic content, Cs-137 and Pb-210 radioisotopic dating, and other methods of sediment core analysis to infer paleoclimatic states.

FRESHWATER RUNOFF AND MASS TRANSFER FROM THE GREENLAND ICE SHEET AT KANGERLUSSUAQ, WEST GREENLAND

Mikkelsen, Andreas B [1]; **Hasholt**, Bent [2]; **Overeem**, Irina [3]; **Hudson**, Ben [4]; **Nielsen**, Morten H [5]

[1] University of Copenhagen, DGG; abm@gei.ku.dk
[2] University of Copenhagen, DGG; bh@geo.ku.dk
[3] University of Colorado, INSTAAR; Irina.Overeem@Colorado.edu.com
[4] University of Colorado, INSTAAR; bdhudson@gmail.com
[5] Technical University of Denmark, ARTEK; mhn@byg.dtu.dk

Major parts of the landscapes in Northern hemisphere are formed by the erosion and transport of material caused by the moving ice, or by melt water inside the ice sheets. Fluvial transport is the major mechanism operating outside of the glaciers and exports substantial amounts of material from glaciated catchments towards the ocean, rendering measurements of sediment transport in proglacial rivers of central interest, see e.g. Strahler & Strahler (1992). However, measurements in the present watercourses in such areas provide no information about the fluvial transport during glaciation periods and e.g. the time needed to develop an outwash plain. Therefore, we need to measure in active proglacial rivers in order to understand the formation of such landscapes. The Greenland Ice Sheet (GrIS) is the only large ice sheet present on the Northern Hemisphere where such land forming processes can be studied. A typical cross section of the GrIS and the proglacial landscape is located at Kangerlussuaq, as shown in Figure 1.

One of the objectives of this study is to describe the yearly patterns (2007 to 2012) of water runoff and sediment delivery from the GrIS to the fjord, and compare those with delivery and erosion from other glaciated areas. Finally, the results from this segment of GrIS have been upscaled to the entire GrIS. Results from 2007 to 2010 are presented here and details can be found in Hasholt et al. (2012).

The water discharge is necessary in order to determine the sediment transport. We assume that it is possible to establish a robust stage/discharge relationship at the gauging location, because of a solid rock sill across the valley.

The instantaneous sediment transport is found by multiplying the sediment concentration with the water discharge at a certain time. The entire water column is homogeneously mixed, because of high velocities (up to 10 m/s) and strong turbulence at the monitoring site. The sediment concentration is found by using data from automatic sensors recording every 20 minutes, where these are calibrated by water samples. If no data from these are available, typically at low water stages in spring and autumn, water samples have been used to interpolate a time series. If no water samples are available a relation between the water discharge and sediment concentration, a Q/C-relation, have been used.

The catchment area on 9743 km^2 is derived from a digital elevation model (DEM) by using the ArcGIS spatial analysis tool. This is used to calculate: runoff (mm), sediment delivery ($t/km^2/y$) and erosion rates (mm/y).

The average runoff from the catchment was 377 mm. If the all water is assumed to originate from the GrIS part of the catchment, wich is a fair assumption due to the very dry proglacial area, the average runoff values are then 401 mm. If related to the ablation area alone, the average runoff value is ~1700 mm. The average specific sediment load (delivery) from the catchment area was 744 $t/km^2/y$ equal to an average effective erosion of 0.28 mm/y. If all sediment is assumed to originate from the GrIS part of the catchment, the corresponding average value is respectively: 792 $t/km^2/y$ and 0.30 mm/y. The average annual sediment load could, if distributed evenly, deposit a layer with a thickness of ~16 mm on the bottom of the deep inner basin of the Kangerlussuaq fjord from Watson River alone. If only grain sizes less than 20 μm are assumed to reach the fjord, as indicated by Lund-Hansen et al. (2010), the annual sediment load equals ~9 mm/y.

If the specific sediment yield documented by the current study is assumed to represent the average

sediment yield from the entire GrIS, the sediment output from the GrIS can be estimated to ~1350 × 10^6 t/y. Compared to the estimated total suspended sediment flux from the entire world on 20000 × 10^6 t/y by Milliman & Syvitski (1992), using this estimate Greenland makes up ~7 % of the total, even though the area of Greenland only covers 1 % of the worlds total land area. However, not all this sediment will reach the oceans, because part of it will be trapped in lakes, on flood plains and in the fjords.

Jökulhlaups (sudden drainage events of glacial lakes) deliver less than 1 % of the total annual sediment load to the fjord. Therefore it is probably not possible to identify layers originating from jökulhlaups in the sediment deposits at the bottom of the fjord. The transport of dissolved material is on average 0.4 % of the total transport of matter (sediment + solutes), confirming that mechanical denudation (glacial erosion) is the most important denudation factor within the Watson River catchment.

This presentation will sum up some of the findings made in this study and highlight new research questions that have evolved during the process. Examples on new are:

- How do the hysteresis patterns of the river and adjacent fjord system behave?
- Can the sediment plumes found in proglacial fjord such as Kangerlussuaq be described in a sufficient physical way, so that the properties of such plume obtained from remote sensing can be related to the river discharge where no discharge measurements are available?
- Compare the river discharge to drainage events of supraglacial lakes in order to see if that can give information on the in/sub glacial drainage systems.
- Closing the water balance in the catchment by 1) constraining the precipitation especially the snow accumulation during winter time and 2) determine the catchment area from subsurface topography, instead of surface topography, if sufficient data becomes available.
-

Hasholt, B., Mikkelsen, A. B., Nielsen, M. H. & Larsen, M. A. D., 2012, Observations of Runoff and Sediment and Dissolved Loads from the Greenland Ice Sheet at Kangerlussuaq, West Greenland, 2007 to 2010. Zeitschrift für Geomorphologie. Submitted.

Lund-Hansen, L. C., Andersen, T. J., Nielsen, M. H., & Pejrup, M., 2010, Suspended Matterm Chl-a, CDOM, Grain Sizes, and Optical Properties in the Arctic Fjord-Type Esturary, Kangerlussuaq, West Greenland During Summer. Estuaries and Coasts, 33: 1442-1451.

Milliman, J. D. & Syvitski, J. P. M., 1992, Geomorphic/tectonic control of sediment discharge to the ocean: the importance of small mountanous rivers. Journal of Geology, 100: 325-344.

Strahler, A. H. & Strahler, A. N., 1992, Modern Physical Geography. John Wiley & Sons, Inc., New York, 638 pp.

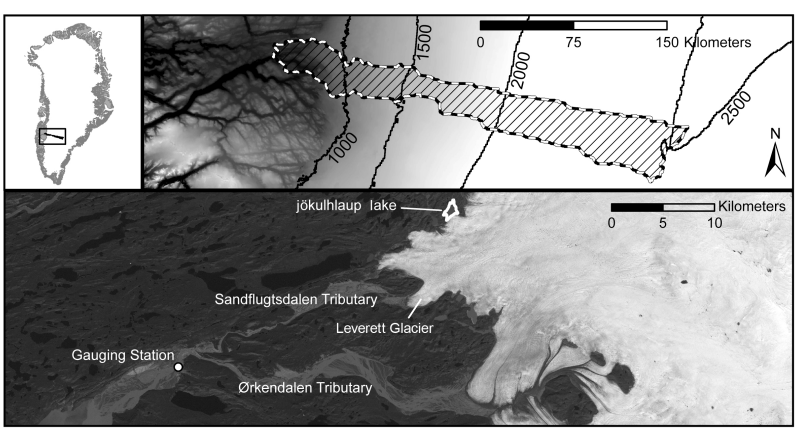

Fig 1. The study area and the catchment of the Watson River, Kangerlussuaq (9743 km²). The location is marked with a square on the index map in the upper left corner. The entire catchment, as determined from a digital elevation model, is shown in the upper right part together with 500 m height interval contours for the ice surface. At the bottom there is a Landsat 7 image showing the proglacial part together with the location of the hydrometric station and other relevant locations.

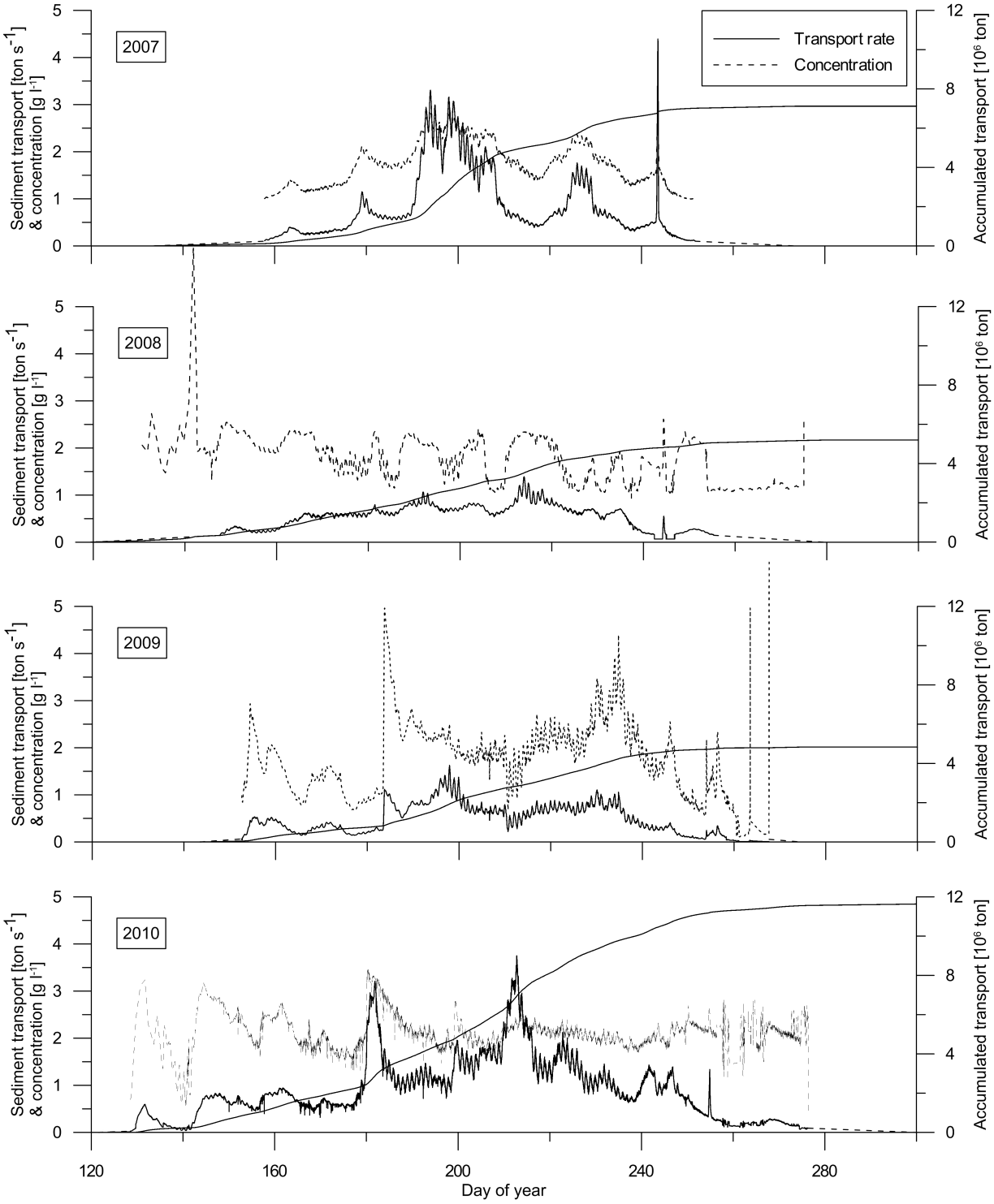

Fig 2. The sediment transport and the concentration for the period 2007 to 2010. The dashed lines, which are connected to the sediments transport rate, indicate estimated values due to low discharges before and after the peak discharge season. The peaks in spring and autumn are probably related to sediment transported in ice.

SIGNAL OF PERSISTENT MULTIDECADAL VARIABILITY IN WINTERTIME SEA-ICE RECORDS: LINKAGES TO THE ATLANTIC MULTIDECADAL OSCILLATION

Miles, Martin [1]; **et**, al. [2]

[1] Uni Research / Bjerknes Centre; martin.miles@uni.no
[2] Several institutions;

Recent satellite observations suggest an arctic sea ice–climate system in rapid transformation, yet its long-term modes of variability is poorly known. Here, we integrate and synthesize an extensive set of multicentury historical records of arctic–subarctic sea ice, supplemented with high-resolution paleo proxy sea-ice records. To identify patterns of multidecadal variability of sea ice, we evaluated a number of long historical and paleo proxy data and selected altogether seven historical sea-ice records spanning the subarctic–arctic Atlantic, from the Labrador Sea to the Barents Sea (Fig. 1), supplemented with two high-resolution paleo proxy sea-ice records: a terrestrial record calibrated for Greenland Sea ice extent and a marine record from north of Iceland. These paleo records are co-located with two of the historical records, thereby providing independent evidence of any signals in the historical records. In contrast to the recent multiproxy reconstruction of summer sea ice (Kinnard et al., 2011), most of the records here reflect conditions in the cold season (winter–spring), when decadal-to-multidecadal climate variability (e.g., the Early Twentieth Century Warming (ETCW)) is most pronounced in the Arctic.

The most salient feature to emerge from the time-series analysis is the presence of pervasive multidecadal variability, upon which interannual-to-decadal fluctuations are superposed. Four key aspects should be noted: (i) Less sea ice is generally seen in the 20th century; however, the changes are far from the monotonic recent negative trend indicated from hemispheric datasets - a common characteristic amongst several of the records is sharply reduced sea ice at the onset of the ETCW, which heralded the termination of the Little Ice Age in the region. The most reduced sea ice before the 20th century occurred in the late 16th and mid-to-late 17th century, as seen in both the Icelandic historical sea-ice and Western Nordic Seas proxy records. (ii) Multidecadal variability is apparent in all of the records (except for Baltic Sea, which is predominated by interannual variability). The wavelet-filtered signals have predominately 60–90 year time scales, which are most pronounced in the Greenland Sea. The multidecadal fluctuations amongst the records are essentially consistent in their periods and in phase (except for the Barents Sea). (iii) The multidecadal signal are persistent in all records where it is found – in no cases does the signal disappear or dissipate through time, although being only quasi-periodic rather than deterministically periodic, the signal naturally varies in amplitude and periodicity. The persistence of the signal through the centuries and longer strongly suggests that the multidecadal oscillation is a robust feature and thus must have an underlying physical mechanism. (iv) Multidecadal signals are strongest in the Greenland Sea region and weaker on either side, i.e., Newfoundland record and the Eastern Nordic Seas (Barents Sea). Further, this is consistent with model simulations of multidecadal climate-system variability that suggest the Greenland Sea to be a key region.

Covariability between sea ice and the Atlantic Multidecadal Oscillation (AMO) is clearly evident during the instrumental record, including an abrupt change during the early 20th century warming (ETCW). Similar behaviour through previous centuries is evident from comparison of longer historical records and paleo proxy reconstructions of sea ice and the AMO, demonstrating that arctic sea ice is a dynamic climate-system component intrinsically and robustly linked to Atlantic multidecadal variability. Further, we extend the analysis to include a cross-comparison with some newly published climate and sea ice reconstructions: the 1,450 year summer sea ice record (KInnard et al., 2011), a 1000-year series of winter surface air temperature variations in Svalbard and northern Norway

reconstructed from ice-core data (Divine et al., 2011), and new sea-ice proxy records from Greenland waters.

Divine, D., et al., 2011, Thousand years of winter surface air temperature variations in Svalbard and northern Norway reconstructed from ice core data, Polar Research, 30, 7379, DOI: 10.3402/polar.v30i0.7379.

Kinnard, C., et al., 2011, Reconstructed changes in Arctic sea ice over the past 1,450 years. Nature, 479, 509–512, doi: 10.1038/nature10581.

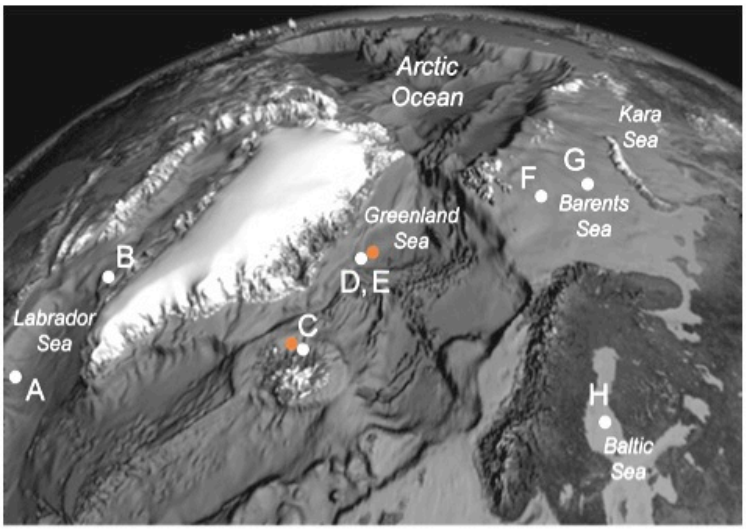

Fig 1. Approximate locations of the historical and paleo proxy wintertime sea-ice time series used in this study. White dots signify the seven historical records, and brown dots signify the two paleo proxy records.. Bathymetry and topography are shown in relief. Selected arctic marginal seas are indicated.

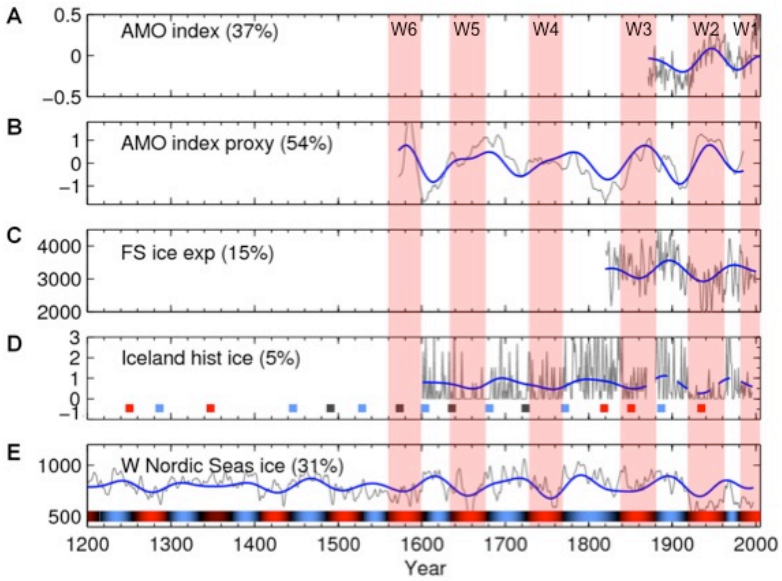

Fig 2. Linking multidecadal fluctuations in sea ice to North Atlantic SSTs. Original non-smoothed time series (gray) and multidecadal 50–120 year component (blue) reconstructed from wavelet decomposition: (A) AMO index, not de-trended, i.e., North Atlantic SST anomaly. (B) AMO proxy index, not de-trended, 10-year running average. (C) Fram Strait ice export (km^3) reconstructed from historical arctic ice extent along SW Greenland. O series (light red shading).

(D) Icelandic sea-ice severity index (1600–1870) and sea-ice incidence index (1880–2000) (sigma units). (E) Western Nordic Seas sea-ice extent (10^3 km^2) proxy reconstruction. The squares in D indicate sea-ice conditions from a marine core sea-ice proxy off North Iceland, with anomalies larger than ±1 s.d. in blue (positive) and red (negative). The color bar in (E) indicates periods of relatively less (red) and more (blue) ice, inferred from the multidecadal wavelet filter; the less-icy warm periods are projected onto the other sea-ice and AM

UNPRECEDENTED RECENT SUMMER WARMTH IN ARCTIC CANADA

Miller, Gifford [1]; **Refsnider**, Kurt [2]; **Lehman**, Scott [3]; **Southon**, John [4]

[1] INSTAAR; gmiller@colorado.edu
[2] Prescott College; kurt.refsnider@colorado.edu
[3] INSTAAR; scott.lehman@colorado.edu
[4] University California Irvine; jsouthon@uci.edu

Average temperatures across the Arctic have increased in recent decades, with documented reductions in sea ice, glaciers, and snowcover. Because the instrumental record in the Arctic is relatively short and limited spatially, placing the recent warming in a longer perspective requires secure reconstructions of past summer temperatures. Radiocarbon dates on rooted plants exposed by recent ice-cap retreat document when the region was last as warm as present. 147 dates on entombed vegetation show that recent summer temperatures in the eastern Canadian Arctic now exceed those of any half-century in at least 37,000 years, including peak warmth of the early Holocene, when solar energy in summer was 9% greater than at present, suggesting that anthropogenic contributions to the atmosphere have led to unprecedented recent warming.

CLIMATE ADAPTATION IN LANDSCAPES AND SEASCAPES OF NORTHERN NORWAY: CHALLENGES AND OPPORTUNITIES

Ogilvie, Astrid E [1]; **Amundsen**, Helene [2]; **Hovelsrud**, Grete K [3]

[1] INSTAAR; Astrid.Ogilvie@colorado.edu
[2] CICERO; helene.amundsen@cicero.uio.no
[3] Nordland Research Institute; grete.hovelsrud@nforsk.no

This presentation will describe a new interdisciplinary project based in northern Norway. Both terrestrial ("landscapes") and marine ("seascapes") systems will be considered in this comparative study of inland and coastal sites. The overarching goal of the project is to document, compare and interpret key linkages between physical and human systems in the context of global and local climate and social change. The purpose of the study hinges on the fact that changes in Arctic regions are occurring extremely rapidly in both social and environmental spheres, with the two inextricably linked (see, e.g. the Arctic Monitoring and Assessment Program (AMAP) http://www.amap.no/; and http://arcticcoasts.org/). The recent persistent warming has caused dramatic changes in the Arctic, with continued loss of sea-ice extent, ice sheet and glacier mass, reduced snow extent and duration, increasing permafrost temperatures linked to the higher Arctic air temperatures, and a general "greening" of the Arctic (www.arctic.noaa.gov/reportcard/). Thus, as sea ice and glaciers diminish at an alarming rate, indigenous peoples and stakeholders note the effect on their way of life both of changes in seasonality and market forces. Both Arctic and non-Arctic nations are eagerly assessing the potential for the acquisition of natural resources such as oil and gas, and the possibility of new shipping routes in high northern regions have far-reaching implications for coastal communities, as well as for global politics. Ecotourism is booming (see, e.g., Smith, 2010), with many implications for northerly communities, currently in transition, with the old ways of pursuing a livelihood disappearing fast.

Climatic and environmental changes will thus impact both terrestrial and marine systems with implications for agriculture and other types of land use, as well as with regard to the distribution and migration of key commercial fish stocks (ACIA, 2005). This is of particular relevance for Norway, where both terrestrial and marine sectors are traditionally extremely important. The RegClim project has developed downscaled climate-change projections for northern Norway for the period 2071-2100, based on climate data for the period 1969-90 (RegClim, 2005). The climate models and downscaled scenarios project higher average temperatures throughout the year, but with most warming in the winter. Increased precipitation has already been observed, and is expected to increase further (Førland, et al., 2007). In addition to this, the Norwegian follow-up to the ACIA report, entitled NorACIA, outlines expected changes in climate as well as impacts on both the natural world and human societies, and considers what adaptations are feasible and/or desirable.

Far-reaching changes are also occurring in socio-economic spheres. Some of these changes are due to expanding oil and gas activities, combined with an increasing outmigration of younger residents. A further change is the growing emphasis on tourism in many northerly regions. In northern Norway these tend to be largely nature-based activities drawn from both the marine and terrestrial sectors, and include boating, whale watching, fishing, angling and hiking. In 2001, tourism and outdoor recreation accounted for 10% of added value, and the multiplying effect of tourist spending added an additional 30—40% output value to the economy (Dybedal, 2003). Numbers of visitors fluctuate from year to year, but on the whole are on the increase.

Two research projects which will form a springboard for the new study are: Community Adaptation and Vulnerability in Arctic Regions (CAVIAR) led by Grete Hovelsrud; and Northern Narratives: Social and Geographical Accounts from Norway, Iceland and Canada (NORSAGA) led by Astrid Ogilvie. Both these interdisciplinary international projects were endorsed International Polar Year (IPY) projects, combining social and natural science.

For this new project five municipalities in have been chosen for special study. These are Lyngen, Bardu, Kvæfjord, Lenvik and Skjervøy. These were chosen because of their varying emphases on primarily terrestrial or marine economies, with most of them having a mix of both. The Lyngen municipality has around 3,200 residents, and covers an area of 810 km2. The main economic activity in the coastal villages here centres on the fisheries, but agriculture may be said to be of prime importance. There is a major emphasis on tourism in this region. Bardu has a population of around 4,000 and an area of approximately 2,704 km2. Bardu is an inland and mountain community with an emphasis on agriculture and forestry, and has a growing tourism industry. It has an interesting history in that it was established in 1791 when many people settled here from Gudbrandsdal and Østerdal after damage caused by the great flood (Storofsen) of 1789. Bardu is also the location of Norway's largest military garrison, the major employer in the municipality. Kvæfjord has a population of just over 3,000 and an area of approximately 513 km2. Its primary economic emphasis is on agriculture and farming. Lenvik is situated partly on the mainland, and partly on the island of Senja. It has the largest population of our study municipalities, with a total of approximately 11,300, and a total area of 892.51 km2. Both fisheries and agriculture are important. Skjervøy has a population of approximately 2,900, and a total area of 464.6 km2. The main industries are fishing and boat building. Tourism is also important not least because it is serviced by the Hurtigruten coastal steamer.

In the context of the far-reaching changes now occurring, the primary research goal of this project is to understand past, present and potential future linkages between climate processes and social adaptations in northern Norway. In short, we seek to understand the interaction of societies with climate and the environment, and the feedbacks involved. Broader research goals focus on: i) how communities in northern Norway perceive climate change; ii) how these communities perceive changes from traditional livelihoods to a focus on tourism; iii) the interactions between contemporary governance systems in fisheries and coastal-community viability in northern Norway; iv) specific effects on indigenous peoples; v) how changes in our study areas mirror changes in Iceland.

To further the goals of the research the project will use tools and methods from the disciplines of: anthropology; meteorology; climatology; marine biology; human geography, and human ecology. The data to be used are: contemporary socio-economic data; systematic instrumental climate data; and data drawn from ethnographic interviews of local stakeholders. In particular, the project will build on recent research on community adaptation to climate change in the Arctic and the north (Hovelsrud et al., 2011).

An important methods component of the project will be the incorporation of local knowledge from fishers, farmers, stakeholders and local people in the chosen research areas. The project is fortunate in that much groundwork has been done in exploring ways of connecting local knowledge and western science (see e.g., Berkes, 1999;Krupnik et al., eds., 2010). Local knowledge is often described more specifically as "Traditional Ecological Knowledge" (TEK). This refers to local indigenous and/or traditional culturally meaningful and embedded perceptions and categories of environmental change, stability and variability. Incorporating TEK in scientific research is mutually beneficial and enriching. It can provide valuable information important to scientific research, and enable researchers to communicate better and to share scientific findings. However, it may be noted that the gathering of TEK can be complex and context bound. There is no single way to do it, and many perspectives are involved. The project will also draw on systems theory in order to focus on agents of change in social-ecological systems (SES) and will also make use of the concepts and methods of panarchy to explore transformations in human-ecological systems. Panarchy provides a theoretical framework for understanding sustainability that integrates SES with economic, ecological and social aspects at various time scales (see, e.g. Gunderson and Holling, 2002).

ACIA, Arctic Climate Impact Assessment. 2005, Impacts of a Warming Arctic: Arctic Climate Impact Assessment. Cambridge University Press, New York. ARCTIC REPORD CARD UPDATE, 2011, www.arctic.noaa.gov/reportcard/.

AMAP, Arctic Monitoring and Assessment Program (AMAP). http://www.amap.no. Retrieved 5 February 2012.

Berkes, F. 1999, Sacred Ecology: Traditional Ecological Knowledge and Resource Management. Philadelphia, Taylor and Francis.

Dybedal, P. Fylkesvise økonomiske virkninger av reiseliv i Finnmark, Troms, Nordland og Nord-Trøndelag, Economic impacts of tourism in counties in northern Norway, Oslo, TØI rapport 640-2003.

Førland, E.J., Alfnes, E., Amundsen, H., Asvall, R.P., Benestad, R., Debernard, J. et al., 2007. Climate change and natural disasters in Norway. An assessment of possible future changes. met.no report 6-2007. met. no. Oslo, Norway, 120 pp.

Gunderson, L.H. and Holling, C.S. (eds), 2002, Panarchy: Understanding Transformations in Systems of Humans and Nature. Island Press, Washington and London.

Hovelsrud, G.K., Poppel, B., van Oort, B. and Reist, J.D. 2011, Arctic societies, cultures and peoples in a changing cryosphere. Ambio 40, 100-110. DOI 10.1007/s13280-011-0219-4.

Krupnik, I., Aporto, C., Gearheard, S., Laidler, G., Kielsen Holm, L. 2010, SIKU: Knowing Our Ice: Documenting Inuit Sea Ice Knowledge and Use. Springer, Netherlands – Dordrecht.

RegClim. 2005, RegClim: Norges klima om 100 år: Usikkerheter og risiko. Oslo: met.no.

LAND ICE AND SEA LEVEL: UPDATE

Pfeffer, W. Tad [1]

[1] University of Colorado; wtpfeffer@gmail.com

Recent developments in observations and modeling improve our ability to assess present-day and predict future land ice contributions to sea level rise. Among the most recent assessments, a newly published GRACE gravity study (Jacob et al, 2012) puts the net global land ice contribution for the period 2003-2010 to sea level at 1.48 ± 0.26 mm/yr; another recent study (Cazenave and Llovel, 2010) estimated the land ice contribution to be 2.40 ± 0.45 mm yr/yr for the period 2003-2007. It is unresolved whether the difference is due to improvements in measurement techniques, actual recent changes in loss rates, or both. In any case, glacier and ice cap loss rates are seen to have significant variability in time, owing to their smaller size and faster response time than ice sheets. I review the recent observations of land ice loss rate assessments and current efforts to project sea level rise in the future.

Cazenave, A., and W. Llovel. 2010. Contemporary sea level rise. Annual Review of Marine Science 2:145–173.
Jacob, T.; J. Wahr; W. T. Pfeffer; and S. Swenson, Recent contributions of glaciers and ice caps to sea level rise. 2012 Nature, doi:10.1038/nature10847

FORAGING ECOLOGY AND SUMMER FEEDING GROUNDS OF BOWHEAD WHALES (BALAENA MYSTICETUS) IN THE EASTERN CANADIAN ARCTIC

Pomerleau, Corinne [1]; **Ferguson**, Steven H [2]; **Lesage**, Veronique [3]; **Winkler**, Gesche [4]

[1] Université du Québec à Rimouski (UQAR) and Fisheries and Oceans Canada - Institute of Ocean Sciences; corinne.pomerleau@dfo-mpo.gc.ca
[2] Fisheries and Oceans Canada - Freshwater Institute; steve.ferguson@dfo-mpo.gc.ca
[3] Fisheries and Oceans Canada - Institut Maurice Lamontagne;
[4] Université du Québec à Rimouski (UQAR) - Institut des Sciences de la Mer;

The Eastern Canada - West Greenland (EC-WG) bowhead whale (Balaena mysticetus) population is slowly recovering from the commercial whaling of the 19th and 20th centuries. However, bowhead whales are still at risk of extinction because of a combination of biological characteristics (e.g., low natural growth rate and long interbirth interval) and identified threats (e.g., climate change, predation and human activities). The analysis of stable isotope ratios, particularly those of carbon (δ13C) and nitrogen (δ15N), in tissues of predators and their preys, is a tool commonly used in feeding ecology to study trophic structure of ecosystems. In this study, our objective was to identify the main prey species and diet composition of the EC-WG bowhead whale population. We examined the foraging ecology of bowhead whales by comparing δ13C and δ15N isotopes ratios of whales (n = 190) with those of various potential zooplankton prey species collected across the Canadian Eastern Arctic during the IPY-Canada's Three Oceans project 2007-2009. Stable isotope ratios varied among zooplankton species as well as spatially within species. A Bayesian stable isotope mixing model (SIAR v 4.0) was used to calculate the proportional contributions of various sources (zooplankton) to the diet of bowhead

whales. These results were compared to fatty acid signatures of bowhead whale blubber samples and to stomach contents from four bowhead whales harvested between 1994 and 2008 in the Canadian Arctic. Our study established that bowhead whale's diet varied among groups of individuals but not between males and females, which suggest cultural specialization within bowhead whales. The isotopic model discarded Davis Strait and Disko Bay as potential foraging areas for bowhead whales, at least in spring and summer. Lancaster Sound, Baffin Bay and the Gulf of Boothia were the three main areas used by bowhead whales for summer feeding. Bowhead whales fed mainly on large arctic calanoid copepods (C. hyperboreus, C. glacialis, M. longa), mysids, euphausids and chaetognaths. Thus, the strong dependence of the only endemic arctic mysticete species on arctic zooplankton may leave them vulnerable to the predicted latitudinal shift in prey species composition as a result of the ongoing warming trend.

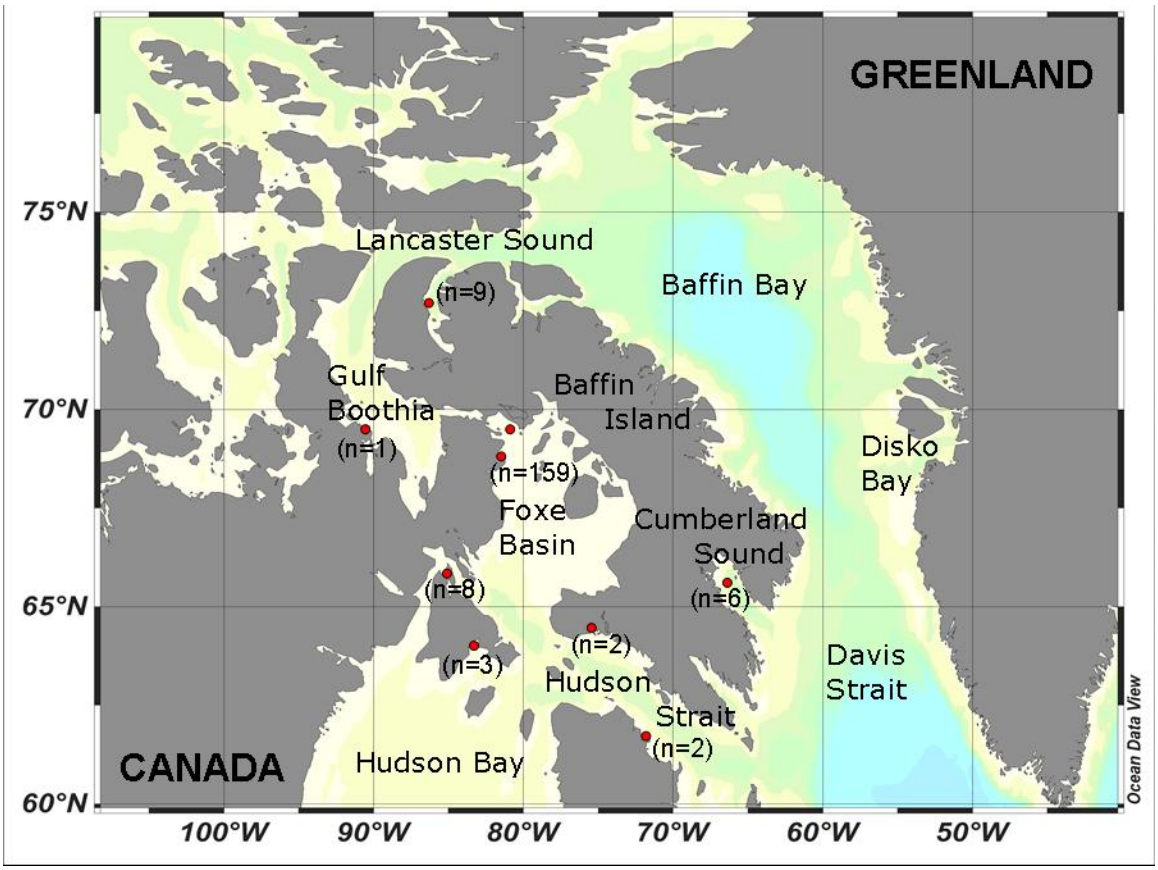

Fig 1. Sampling locations for bowhead whale skin samples without outliers (total n=190) in the Eastern Canadian Arctic.

AN ALASKAN CORDILLERAN ICE SHEET REFUGIUM IN SITKA SOUND DURING THE LAST GLACIAL MAXIMUM

Powell, Ross D. [1]; **Dzuryak**, John-Franklin [2]

[1] Northern Illinois University; ross@geol.niu.edu
[2] Northern Illinois University; jfdzuryak@niu.edu

History of the Alaskan Cordilleran Ice Sheet (ACIS) is poorly constrained even at the last glacial maximum (LGM) and younger. Last year we reported on the LGM history of the Glacier Bay Ice Stream as a component of ACIS and its retreat from the LGM on the outer continental shelf. Further work on the southern Alaskan coast reconfirms the notion of ice-free refugia spaced along the coast at the LGM, separated by tongues of ice streams covering the continental shelf and being fed from large valley/fjord glacial systems as components of the ACIS.

Here we outline a combination of marine morphological evidence and terrestrial volcanics that indicate the Sitka Sound area of southeastern Alaska was ice free at the LGM, although there is evidence for earlier occupation and erosion of the Sound by glaciers. In the area, Mt. Edgecumbe Volcanic Field (MEVF) as part of Kruzof Island on the northern side of Sitka Sound, has been actively producing lava flows, pyroclastic flows and ash falls through the Quaternary.

Evidence from multi-beam bathymetric surveys through Sitka Sound show deeply eroded troughs of similar morphology to others along the coast as having been glacially eroded. In outer Sitka Sound there is a broad, plateau-shaped, shallow sill extending out from Kruzof Island that can be traced back to terrestrial lava and pyroclastic flows dated in the range of 137 to 611ka using K-Ar (Riehle et al., 1989). This sill and associated bathymetric forms show no evidence of glaciation; in fact morphology characteristic of the relief on the tops of pyroclastic flows and hemipelagic material shows evidence of subaerial modification and erosion. We attribute such bathymetry to subaerial exposure of the sill during the eustatic sea level lowstand at the LGM.

Cores taken from basins inside the sill date to post-LGM using 14C and tephrochronolgy (Addison et al., 2010). They contain freshwater lacustrine diatoms within laminated siliceous muds intercalated between tephras, indicating inner Sitka Sound was isolated from the open Gulf of Alaska during deglaciation from the LGM (Addison et al., 2010). Although the cores were too short to recover LGM-age sediment, the presence of lakes dammed in inner Sitka Sound lends strong support for a lack of glaciation within Sitka Sound proper during and post-LGM.

Glaciers were present on land around Sitka Sound (cf. Riehle et al., 1989) and based on marine morphology, most likely existed to the north in Katlian Bay and Nakwasina Sound. Previous work by Mann (1986) indicates glaciers were present south of Sitka Sound on Baranof Island. Pebbly muds in the inner Sitka Sound cores show that glaciers on land may have ended in shallow water around the edges of the lake and/or as sea level rose through the Holocene.

Combined evidence suggests that Sitka Sound was rimmed by glaciers during the LGM-Holocene but remained non-glaciated within the Sound proper. Lakes were present in the inner Sound during early post-LGM (and probably during the LGM) and then became increasing estuarine as sea level rose.

Addison, J.A., Begét, J.E., Ager, T.A. and Finney, B.P., 2010, Marine tephrochronology of the Mt. Edgecumbe Volcanic Field Southeast Alaska, USA: Quaternary Research, v. 73, p. 277-292.

Mann, D.H., 1986, Wisconsin and Holocene glaciation of southeast Alaska. In Hamilton, T.D., Reed, K.M., Thorson, R.M., eds., Glaciation in Alaska— The Geologic Record. Alaska Geologic Society, p. 237-265.

Riehle, J.R., Brew, D.A. and Lanphere, M.A., 1989, Geologic Map of the Mount Edgecumbe Volcanic Field, Kruzof Island, Southeastern Alaska: U.S. Geological Survery, scale 63,360, 1 sheet.

NORTH ATLANTIC SUBPOLAR GYRE DYNAMICS IN THE ABSENCE OF MAJOR FRESHWATER FORCING

Quillmann, Ursula [1]; **Jennings**, Anne E [2]; **Marchitto Jr.**, Thomas M [3]; **Andrews**, John T [4]; **Haflidason**, Haflidi [5]; **Hall**, Ian R [6]

[1] INSTAAR; Ursula.Quillmann@Colorado.EDU
[2] INSTAAR; Anne.Jennings@Colorado.EDU
[3] INSTAAR; Thomas.Marchitto@Colorado.EDU
[4] INSTAAR; andrewsj@Colorado.EDU
[5] Univeristy of Bergen; Haflidi.Haflidason@geo.uib.no
[6] Cardiff University; Hall@cardiff.ac.uk

Pronounced changes in the water mass properties of the high-latitude North Atlantic have taken place over the last decade. Substantial evidence has been provided that these changes are associated with subpolar gyre (SPG) dynamics. Presently the SPG oscillates between an extended mode and a contracted mode (Fig 1). Preliminary results of records are presented starting at ~8000 cal yr BP, after the freshwater forcing from the decaying Laurentide ice sheet had waned. The marine sediments are expected to record SPG dynamics (Fig 2). NEAP4K lies within the SPG during its extended mode but lies to the east of the SPG during its contracted mode. Core JM96-1216 in the Denmark Strait should be sensitive to varying amounts of Atlantic Water carried northward by the Irminger Current (IC), which present-day observations show is enhanced during the contracted SPG mode. For comparison, cores MD99-2259 and MD99-2256 lie on the SW Iceland shelf and record the upstream water mass properties. HM119-04GC, in the main stream of North Atlantic Current entering the Nordic Seas is hypothesized have a stronger Atlantic water signal during the extended SPG mode, when more Atlantic water reaches the Norwegian Sea. $\delta^{18}O_{seawater}$ and temperature were reconstructed by paired measurements of $\delta^{18}O_{calcite}$ and Mg/Ca ratio of planktonic foraminifera. Faunal assemblages and mineralogy are available for some of the cores. These preliminary results are part of an overarching project to reconstruct the evolution of the SPG during the Holocene and map the northern and eastern boundaries of the gyre at different time slices.

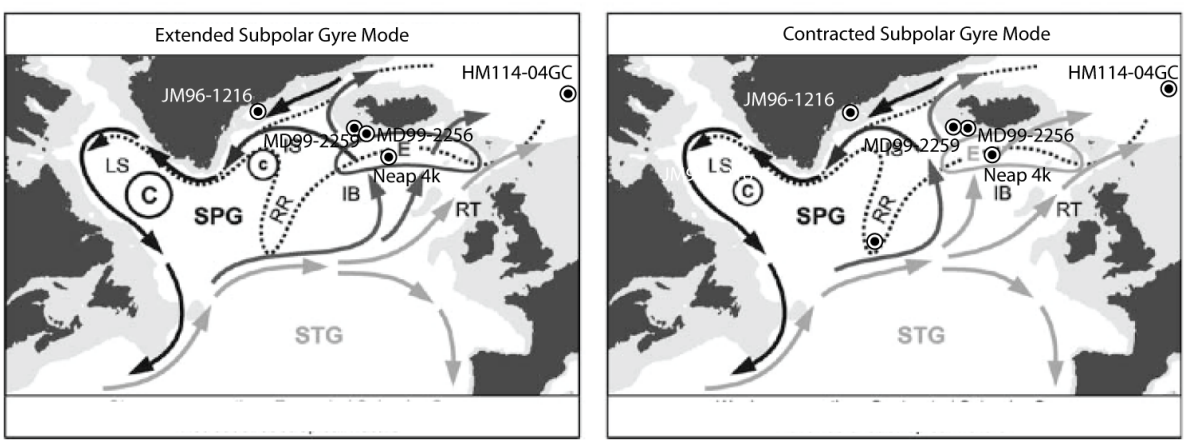

Fig 1. The two end members of the subpolar gyre modes as recognized over the past 50 years and their relationship with the North Atlantic Oscillation (Sarafanov et al., 2009, their fig 3). Darker (lighter) arrows indicate surface currents transporting colder, subpolar (warmer, more saline subtropical) water with the area "E" marking the location where the Atlantic waters are entrained into the Iceland Scotland Overflow Water. Dashed lines indicate pathways of Nordic Seas overflow waters. Other abbreviations: SPG - Subpolar Gyre, STG - Subtropical Gyre, c - convection (size of circles represent intensity of convection), IB - Iceland Basin, LS - Labrador Sea, RT- Rockall Trough, RR - Reykjanes Ridge. Shaded areas: <500 m water depths. RR). Figure: after Sarafanov, Falina, Mercier, Lherminier, and Soko. 2009. "Recent changes in the Greenland–Scotland overflow-derived water transport inferred from hydrographic observations in the southern Irminger Sea"

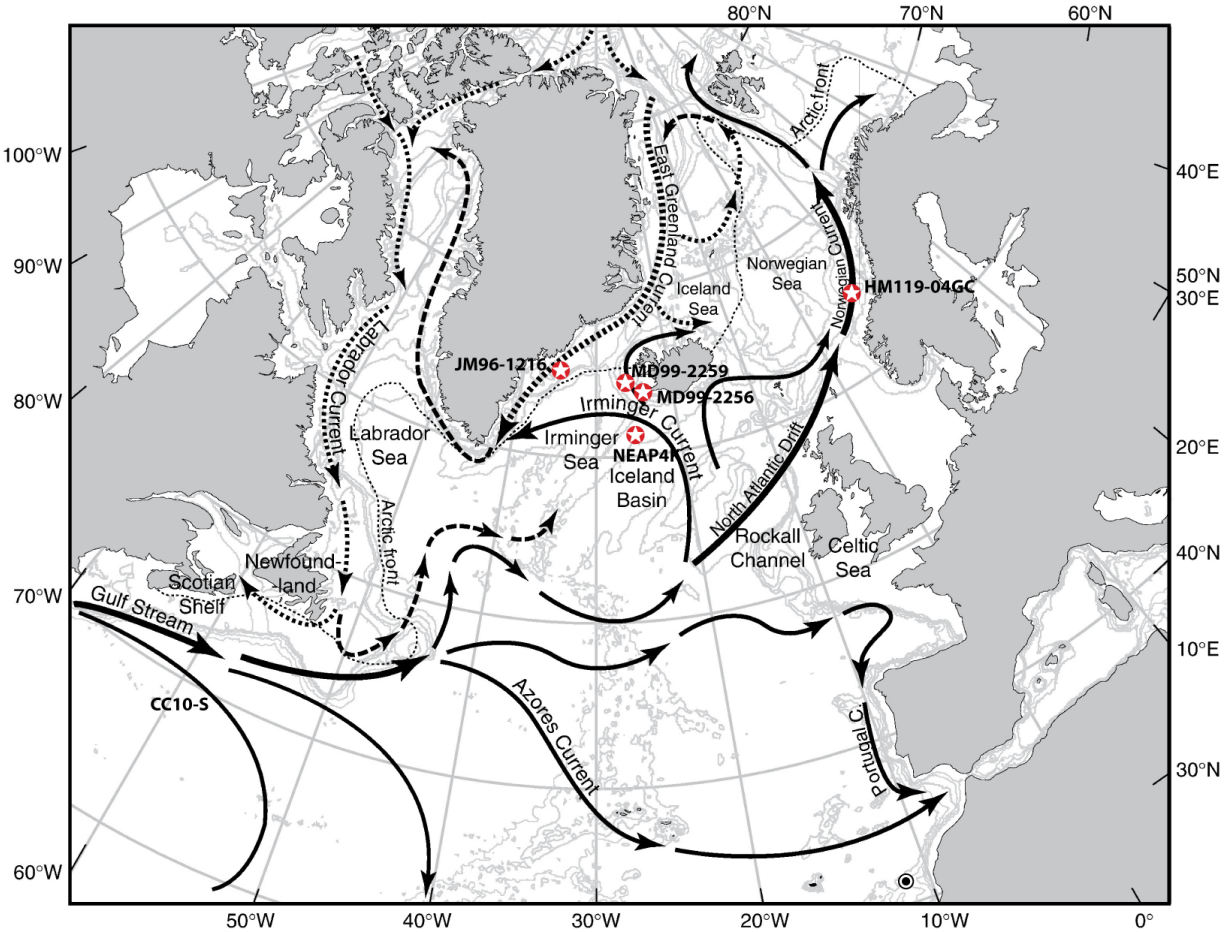

Fig 2. Map of study sites with surface currents. The study sites were chosen to capture the SPG in its extreme extended and contracted modes. Solid lines with arrows indicate warm currents and dashed lines cold currents

CHARACTERIZING FJORD OCEANOGRAPHY NEAR THE TIDEWATER GLACIER FACES IN KONGSFJORDEN, SVALBARD

Rajagopalan, Daksha M [1]; **Brigham-Grette**, Julie [2]; **Powell**, Ross D [3]; **Timmermans**, Mary-Louise [4]

[1] Yale University; daksha.rajagopalan@yale.edu
[2] University of Massachusetts Amherst; juliebg@geo.umass.edu
[3] Northern Illinois University; rpowell@niu.edu
[4] Yale University; mary-louise.timmermans@yale.edu

In recent years, warmer Atlantic-origin waters have appeared in Spitsbergen's west-coast fjords, significantly affecting both winter ice cover and biotic communities. In 2006, for example, relatively warm Transformed North Atlantic Water (TAW), a mixture of Arctic-type and Atlantic-type water, intruded farther than usual into Kongsfjorden, Svalbard. Kongsfjorden's oceanography is also significantly affected by meltwater from four tidewater glaciers, two of which (Kronebreen and Kongsvegen) lie at the head of the fjord. While the general fjord circulation of Kongsfjorden is well-understood, water masses closest to the ice margin -- and directly responsible for submarine glacial melt -- are more difficult to study. In addition to seasonality and winds, tidal cycles are also expected to play an important role.

The goal of this project is to characterize the water masses and interpret fjord circulation at the calving-fronts of Kronebreen and Kongsvegen, Svalbard. The CTD and relative turbidity data range from 200 m to 1.5 km from the ice face and were collected between 22 Jul and 6 Aug 2011. The oceanographic fieldwork was conducted along five primary transects, with the view to account for tidal influences as well. We also measured current velocities using drogues we constructed while in Svalbard.

We find two primary glacial discharges (the gravity current from the upwelling plume from Kronebreen, and the surface discharge from the Kongsvegen delta). We find a relatively turbid layer at about 30m depth coming from the delta discharge. We also find the Intermediate Water (IW) at depth to be warmer than was observed in the same region at comparable depths in 2005, by Trusel et al., who found a 0° local water (LC). These two layers lie above the TAW and may be warmer as a result of convection with increased TAW waters. Further research on current velocities would also shed more light on submarine glacial melt-rates.

The fieldwork was conducted with a team of six students and two faculty, as part of an NSF-funded REU program.

Trusel L., Powell R., Cumpston R., Brigham-Grette J., 2010, Modern glacimarine processes and potential future behaviour of Kronebreen and Kongsvegen polythermal tidewater glaciers, Kongsfjorden, Svalbard. Geological Society, London, Special Publications, v. 344, p. 89-102.

Svendsen, H., Beszczynska-Moller, A., et al., 2002, The physical environment of Kongsfjorden-Krossfjorden, an Arctic fjord system in Svalbard. Polar Research, v. 21, p. 133-166.

Willis K., Cottier F., Kwasniewski S., 2008, Impact of warm water advection on the winter zooplankton community in an Arctic fjord. Polar Biology, v. 31, p. 475-481.

Fig 1. A photo of the field site, taken from the south coast of Kongsfjorden. On the far right, at the head of Kongsfjorden, are the two glaciers whose processes we studied: Kronebreen and Kongsvegen.

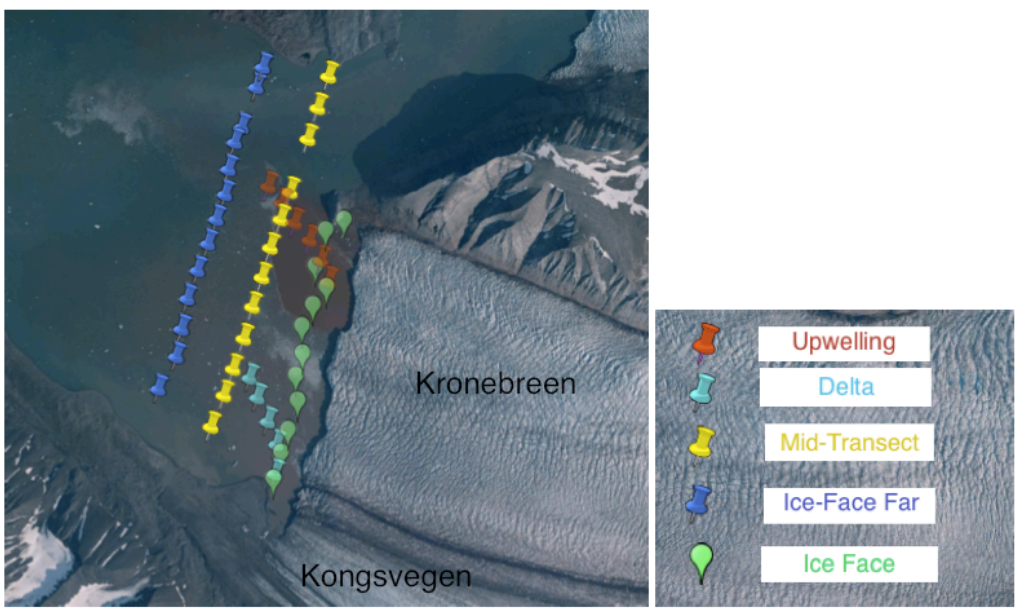

Fig 2. An aerial view of the field site. We took CTD casts along five key transects. Along the Upwelling and Delta (coming out from Kronebreen and Kongsvegen), we repeated the transects at least thrice at low tide and at high tide. Parallel to the glacier face (Mid-Transect, Ice-Face Far, and Ice Face), we sampled in order to tie-in the temporal resolution of Upwelling and Delta into a larger spatial region. (Photograph credit: Norsk Polar Institute, 2009)

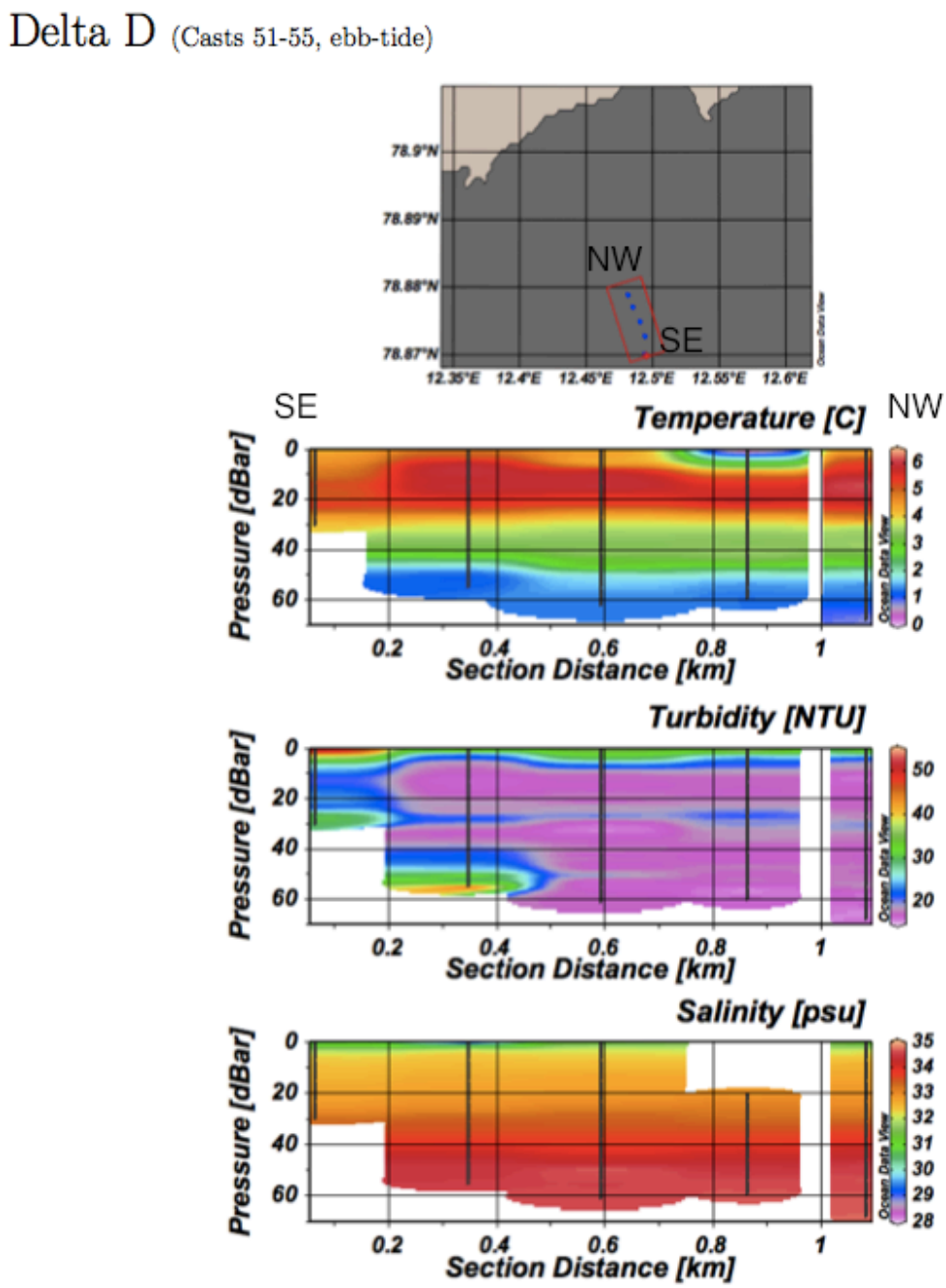

Fig 3. A sample transect, taken on 30 Jul 2011. The leftmost cast is closest to the delta, and the direction of the transect follows the delta discharge for that day. Note the turbid, fresh surface overflow (SO), and the relative turbidity max at about 30 m depth.

SUBMARINE LANDFORMS IN A SURGE-TYPE TIDEWATER GLACIER REGIME, ENGELSKBUKTA, SVALBARD

Roth, George E [1]; **Noormets**, Riko [2]; **Powell**, Ross D [3]; **Brigham-Grette**, Julie [4]

[1] University of Washington; georoth@u.washington.edu
[2] University Centre in Svalbard (UNIS); rikon@unis.no
[3] Northern Illinois University; ross@geol.niu.edu
[4] University of Massachusetts, Amherst; juliebg@geo.umass.edu

This project is an interpretation of bathymetric data taken at Engelskbukta, a bay located in West Spitsbergen in the Norwegian high arctic archipelago of Svalbard. Engelskbukta is bordered on the southeast by Comfortlessbreen, a large tidewater glacier, and on the northeast by Uversøyra, a delta formed by the melting and outwash of the land-anchored Uversbreen glacier (Fig. 1).

The Norwegian Mapping Authority (Statens Kartverk) conducts high-resolution multibeam bathymetric surveys around Norway and Svalbard. The Engelskbukta dataset (Fig. 2) was acquired between 2004 and 2008 at 5-meter resolution, and has already been post-processed and corrected for tides, ship parameters, and noise artifacts.

Comfortlessbreen is a surge-type glacier, and detailed observations of terminus positions and crevasse propagation beginning in 2001 confirmed that by 2006, it had entered active surging with an average velocity of 2 m d^{-1}, compared to a quiescent-phase velocity at nearby glaciers on the order of 5 m yr^{-1}. (Sund, 2010)

Initial interpretations of the seafloor morphology indicate a retreat moraine series (Fig. 3), representative of long-term warming and recession of the glacier terminus, and larger thrust moraines indicative of active surging phases. (Ottesen, et. al., 2008) Fluvial features, such as glacier-proximal grounding line fans and channels, indicate zones of past and present subglacial sediment flux from Comfortlessbreen and deltaic flux from Uversøyra, formed from the melting and outwash of the land-anchored Uversbreen glacier.

Though previous surging events at Comfortlessbreen have not been directly observed, satellite and aerial imagery, descriptive models of surge-type glaciers, and in-situ sediment dating from the adjacent Kongsfjorden offer further opportunities to constrain both retreat rate and surge frequency and predict future dynamic responses to climate forcing.

Ottesen, D., Dowdeswell, J. A., Benn, D. I., Kristensen, L., Christiansen, H. H., Christensen, O., Hansen, L., et al., 2008, Submarine landforms characteristic of glacier surges in two Spitsbergen fjords: Quaternary Science Reviews, v. 27, p. 1583-1599.

Sund, M., & Eiken, T., 2010, Recent surges on Blomstrandbreen, Comfortlessbreen and Nathorstbreen, Svalbard: Journal of Glaciology, v. 56, p. 182–184.

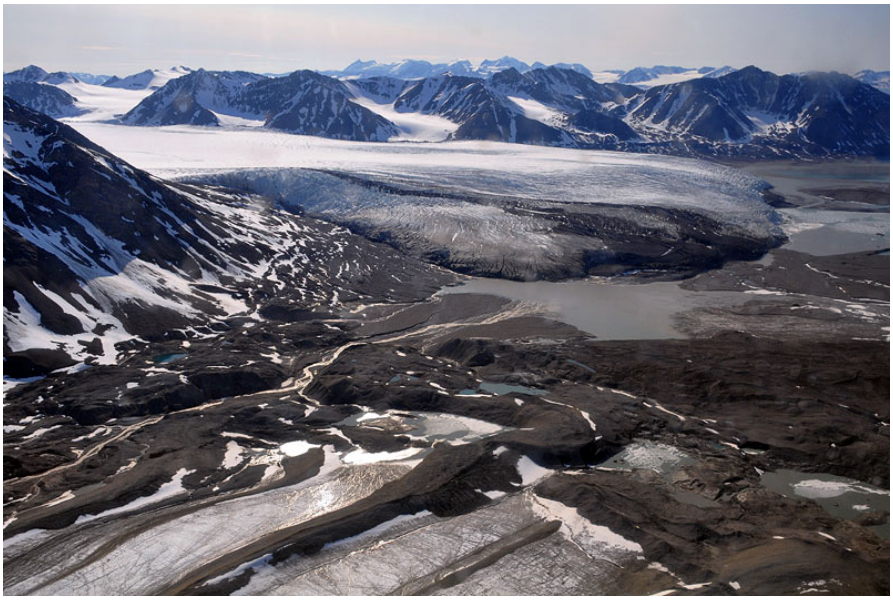

Fig 1. Uversbreen and Uversøyra (bottom) and Comfortlessbreen (top) Photo credit: Michael Hambrey, Centre for Glaciology, Aberystwyth University

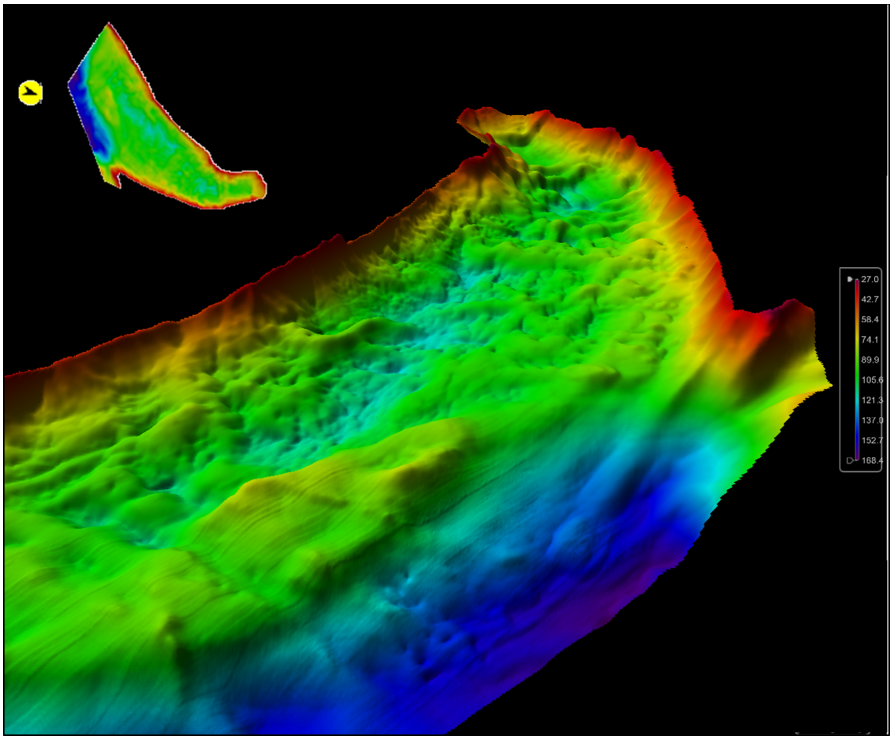

Fig 2. A three-dimensional view of the Engelskbukta bathymetric dataset, looking towards the Comfortlessbreen terminus. Relief has been exaggerated.

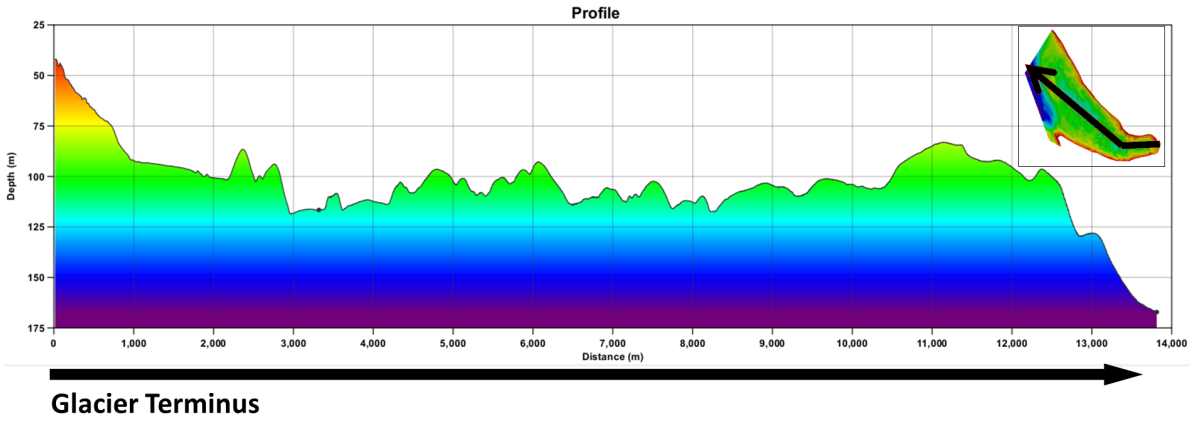

Fig 3. Bathymetric profile from the Comfortlessbreen terminus to the mouth of Engelskbukta, revealing a significant moraine series.

IDENTIFICATION OF PERMAFROST SLOPE DISTURBANCES USING MULTI-TEMPORAL IMAGERY AND CHANGE DETECTION TECHNIQUES, CAPE BOUNTY, MELVILLE ISLAND, NUNAVUT

Rudy, Ashley [1]; **Lamoureux**, Scott F [2]; **Treitz**, Paul [3]

[1] Queen's University; ashley.rudy@gmail.com
[2] Queen's University; scott.lamoureux@queensu.ca
[3] Queen's University; paul.treitz@queensu.ca

Active layer detachments (ALDs) are a common form of permafrost disturbance that represent translational landslides of soil, vegetation and other surface material in the thawed or thawing active layer. Factors attributed to the increasing accounts of permafrost degradation seen across the Arctic include changes to thermal, hydrological and geotechnical conditions, all of which can lead to slope detachment. Extensive slope failures were observed at the Cape Bounty Arctic Watershed Observatory (CBAWO), Melville Island, Nunavut, during the summers of 2007/8. Higher than normal air temperatures thickened the active layer and the resultant ground ice melt along with summer rainfall events destabilized slopes resulting in ALDs. The primary objective of this study was to utilize IKONOS satellite data acquired pre- and post-disturbance (2004, 2010) in combination with vegetation index differencing, in order to identify landscape change associated with ALDs. In addition to identifying the presence of ALDs, further research objectives included: 1) determining the degree of disturbance identified within a known ALD mapped by GPS; and 2) examining the influence that disturbance size and morphology have on the accuracy of automatic change detection analysis in this context.

Geometric rectification, image registration and radiometric corrections were applied to the IKONOS data through a series of preprocessing steps prior to image analysis. Near infrared and red spectral bands were used to compute the Normalized Difference Vegetation Index (NDVI) for each of the two dates and were then subtracted to generate a NDVI difference map to indicate areas in which vegetation was removed in the 2010 image. Using areas devoid of vegetation as a proxy for the presence of ALDs, a multiresolution segmentation algorithm in Trimble's Ecognition software was used to threshold the NDVI difference map. The thresholded image depicts areas where vegetation was fully or partially removed between 2004 and 2010, signifying the presence of an ALD. The thresholded image was validated using a disturbance inventory that was mapped with GPS during the 2009 field season.

In total, 29 disturbances were detected automatically throughout the study area. This compares with 69 disturbances that were mapped in the field, suggesting an overall recognition accuracy of 42% when no thresholds were applied. However, the accuracy of this automated approach can be addressed with respect to minimum ALD size and morphology. The minimum area accurately detected within a single ALD was 160 m^2, much less than the corresponding mapped area of 290 m^2. Using 290 m^2 as the minimum size an ALD must be to for detection, a threshold was set where mapped disturbances less than 290 m^2 were removed from the disturbance inventory. In all cases the areas of change that were detected are zones of bare soil found just below the scarp or in the scar track. Morphologically, these areas of bare soil are more commonly developed in elongate ALDs. Elongated forms are characterized by a larger scar zone where the extent of the disturbance can span the length of the slope and results in a highly deformed toe. Of the ALDs observed in the field, those with elongate morphometry typically were constrained by length to width ratios ≥ 2. ALDs classified as compact disturbances had length to width ratios <2, tended to be smaller, and displayed curved headwalls with sliding distances generally only a few metres. This morphometry accounts for their minimal internal deformation and surface displacement. As a result, the compact failures appear nearly indistinguishable from surrounding vegetated areas resulting in their low detection accuracies. By contrast, elongate forms, with their larger scar zones, are identified more readily. With this additional consideration of size and morphology, the classification accuracy of the elongate ALDs increases to 70%.

Quantifying areas of disturbance is the first step towards creating disturbance maps and investigating the spatial controls over ALD susceptibility. With projected climate change and accelerating industrial development within the Arctic, these methods, in combination with subsequent landscape disturbance modeling, will provide insight for explaining the extent of permafrost degradation across the region and identifying areas of potential disturbance.

GEOMORPHOLOGICAL MAPPING OF QUATERNARY LANDFORMS AND SEDIMENTS FOR GEOHAZARD ASSESSMENT IN SELECTED CULTURAL HERITAGE SITES ON SVALBARD

Sessford, Evangeline G [1]; **Hormes**, Anne [2]; **Etzelmüller**, Bernd [3]

[1] University of Oslo and University Centre in Svalbard; EvangelineS@unis.no
[2] University Centre in Svalbard; Anne.Hormes@unis.no
[3] University of Oslo; bernd.etzelmuller@geo.uio.no

High Arctic geohazards are a phenomenon that has recently become a scientific focus and Svalbard, unlike most other high arctic islands and archipelagos, has a thriving city and numerous cultural heritage sites which are frequented by residents and tourists alike. Such a situation provides the ultimate circumstances for this M. Sc. which aims to develop a risk analysis model for High Arctic cultural heritage sites that is founded upon spatial and chronological terrestrial assessment of geological hazards. Two field sites have been chosen due to their presence of cultural heritage (all structures and sites containing traces of human activity dating from 1945 and earlier) and geohazard landforms. Fredheim, an old trapper's station is threatened by coastal erosion where sediment loss is approximately 25cm/year (this study). This is considered a high risk and, assuming degradation rates remain fairly constant, in 14.5 years the buildings will begin to gradually be washed into the fjord and be gone by 2121. At Skansebukta, an unproductive gypsum mining site, geohazards are less pressing, though debris flow, rock fall and gelifluction activity needs a thorough investigation.

We present detailed Quaternary geological maps of geohazards at the two field sites including specific geohazards that are not included in inventories of the Norwegian mainland. These maps will serve as basis to develop dating strategies in order to analyze geohazard frequency during past Holocene climate and consequentially produce vulnerability and risk assessment maps. The past frequency is critical for future risk assessment and if climate variability or other factors contributed to past frequency patterns.

This presentation will highlight the methods of producing a Quaternary geological map and risk analysis model while revealing some significant initial results from the geohazard assessment.

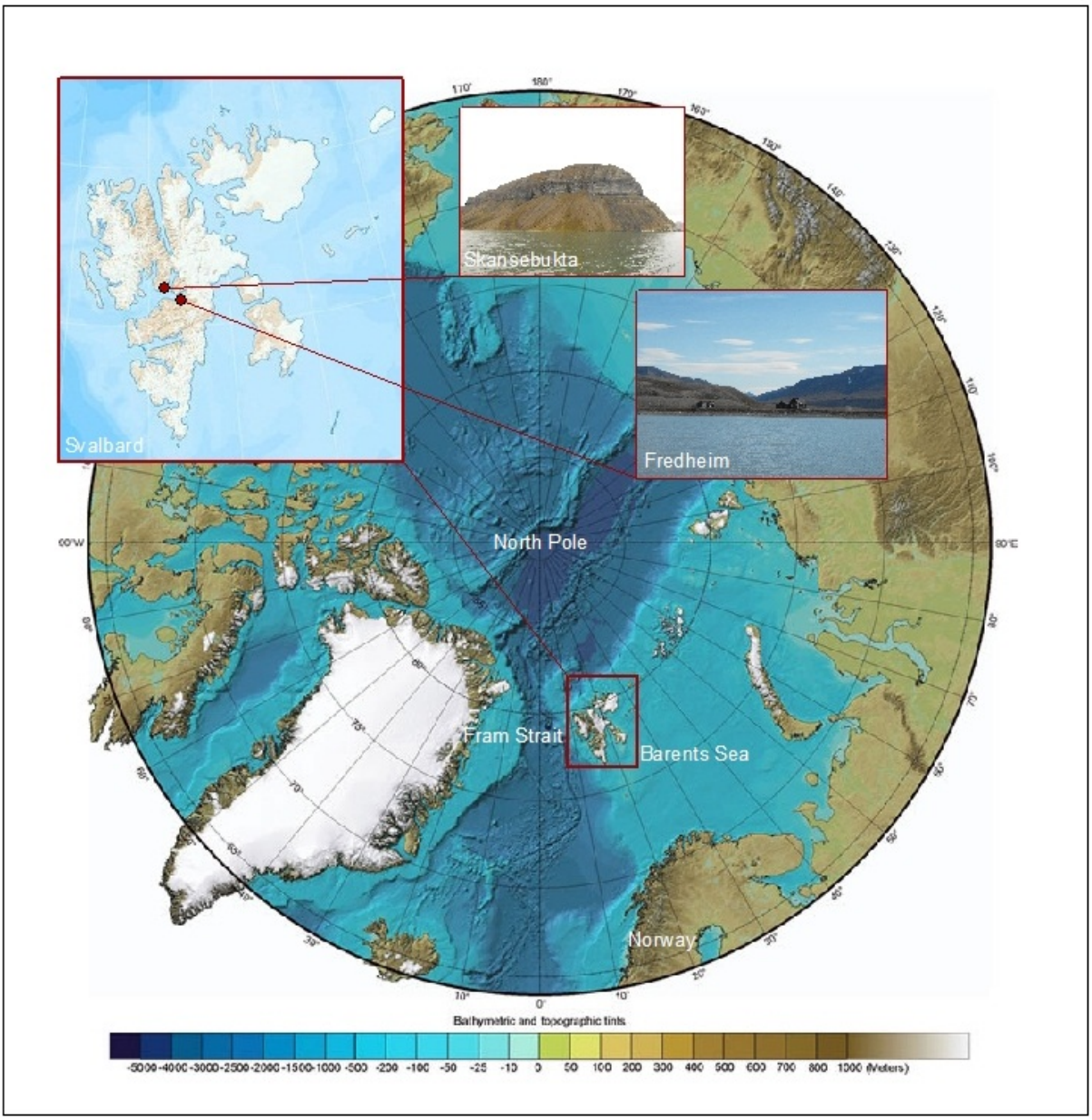

Fig 1. Location of Svalbard and field sites, Skansebukta and Fredheim. Image adapted from http://geology.com/world/arctic-physical-map.jpg

INFLUENCE OF MARINE AND CLIMATIC DYNAMICS ON SHORT TERM CALVING PROCESSES AT THE KRONEBREEN-KONGSVEGEN GLACIER SYSTEM, SVALBARD

Siegel, Rebecca [1]; **Brigham-Grette**, Julie [2]; **Powell**, Ross [3]; **Roof**, Steve [4]

[1] Hampshire College; rss07@hampshire.edu
[2] University of Massachusetts, Amherst;
[3] Northern Illinois University;
[4] Hampshire College; sroof@hampshire.edu

Calving is a key part of tidewater glacier mass balance. However, while models and other methods have been used to investigate long term calving processes, factors that immediately affect calving are poorly understood. Short term calving processes were studied at the retreating Kronebreen and Kongsvegen glaciers in Kongsfjorden, Svalbard 12°34'E, 78° 50'N) during July and August, 2011. Water depth dataloggers recorded the larger than normal waves caused by calving events, providing a record of the timing of iceberg calving. I examined the effect of temperature, precipitation, tide stage, tide amplitude, and water level. I found no correlation between water level at the time of calving and the frequency of calving events nor between tide stage and calving event frequency. I did not have enough data to examine precipitation. Both daily temperature and tidal amplitude had weak relationships with calving event frequency. Based on these results, the Kronebreen-Kongsvegen glacier system does not appear to follow the relationships with environmental factors that have been described in the literature about Alaskan tidewater glaciers.

HOLOCENE DYNAMICS OF RIPARIAN ECOSYSTEMS ALONG A SUBARCTIC RIVER (BONIFACE RIVER, QUÉBEC)

St-Amour, Francis [1]; **Payette**, Serge [2]

[1] Laval University, Centre for Northern Studies, Northern Research Chair on Disturbance Ecology; francis.st-a.1@ulaval.ca
[2] Laval University, Centre for Northern Studies, Northern Research Chair on Disturbance Ecology; serge.payette@bio.ulaval.ca

Most studies on the dynamics of riparian ecosystems have documented the relationships between morpho-sedimentary landforms and hydrological regime. However, few studies have focused on soil analysis to document the dynamics and development of riparian ecosystems. In this study, a geopedological approach, including tree-ring analysis and ^{14}C dating, was used to reconstruct the dynamics of riparian ecosystems of a subarctic river (Boniface River: 57° 45' N, 76° 20' W), in particular the influence of water-level fluctuations, during the Holocene, on the construction and development of ice-push boulder ridges, sand beaches and vegetated platforms.

Boniface River is located in the northern part of the forest-tundra (about 133 km long, watershed surface of 3630 km^2) flows westward to Hudson Bay. The water supply of the river depends on regional precipitations, mainly snowfalls. Consequently, the river level varies considerably on a year basis depending on the amount of snow accumulated. Physical and chemical components of riparian soils and paleosols were used to document periods of changing water levels. Low water levels are generally associated with stabilization stages, facilitating vegetation encroachment and expansion and soil development. By contrast, high water levels correspond to aggradation stages with consecutive vegetation decline and soil burial.

Three different ecosystems distributed in 8 different sampling sites were analyzed, i.e., 1 ice-push boulder ridge, 5 beaches, and 2 vegetated platforms, focusing on soil development and paleosols. Twelve trenches were dug perpendicular to the shoreline. Along the trenches, morphology and chemical content of the soil horizons were documented, based on the National Soil Survey Committee of Canada (NSSC) procedure. Soil profiles containing buried organic horizons were collected for radiocarbon dating (n = 65 based on AMS dating). Buried black spruce (*Picea mariana* [Mill] B.S.P) but still rooted in the shore zone were sampled to determine establishment and mortality dates over the last 300 years.

At one particular beach site, low water level around 675 cal. years BP (1275 AD) facilitated vegetation expansion, pedogenetic development and black spruce establishment until the early 19th century. High water level prevailed thereafter, particularly after the late 19th century, damaging riparian vegetation and causing the burial of the orthic gleysol. Mass mortality of black spruce culminated during the 1940s when the water level of the river was at its maximum. The inception of a cumulic regosol developed since the burial of the orthic gleysol suggests that present hydrodynamic system contributed to the maintenance of the beach.

Lower water levels of the rivière Boniface prevailed between 4000 and 2000 cal. years BP, which allowed vegetation and soil development in the shore zone. The hydrological regime probably changed around 2000 years cal. BP. Likewise, high water levels (or major floods) were responsible for the burial of most well-developed humo-ferric podzols and dystric brunisols between 520 and 285 years cal. BP. Then, major lowering of the water level occurred during the Little Ice Age, which facilitated the establishment and growth of black spruce in the upper part of the river shore. However, mass mortality of black spruce combined with the presence of regosols provide direct evidence for the influence of high water levels during the 20th century on the formation and development of present riparian ecosystems.

BLACK SPRUCE COLONIZATION OF FOREST-TUNDRA SNOW PATCHES OF EASTERN CANADA

Truchon-Savard, Alexandre [1]; **Payette**, Serge [2]

[1] Université Laval - Center for Northern Studies - Northern research chair on disturbance ecology; alexandre.truchon-savard.1@ulaval.ca
[2] Université Laval - Center for Northern Studies - Northern research chair on disturbance ecology; serge.payette@bio.ulaval.ca

Snow patches are snow-rich treeless ecosystems distributed in depressions of the forest tundra and arctic tundra. Most snow patches of the forest tundra are located on lee slopes exposed to the North and the Northeast where a thick snow cover accumulates in winter. Due to thick snow pack and aspect, snow melt is delayed until early- and mid-summer, a situation causing a shorter growing season. Several chionophilous shrub and herb species tolerate these conditions, and occupy the center of snow patches (Björk and Molau 2007, Kudo 1991) whereas the margins are occupied by deciduous shrubs (Shrub birch, *Betula glandulosa* Michx.) and small trees (black spruce, *Picea mariana* [Mill.] B.S.P.). Snow patches are sporadically occupied by tree species during periods of relatively dry winters and warm summers, like in the 1960s when snow accumulation was reduced (Mathieu et al.1987). Black spruce colonization also occurred recently in snow patches of the Boniface River area (57° 45' N, 76° 20' W), 10 km south of the treeline.

The aim of this study is to evaluate the impact of climate (temperature and snow accumulation) and site conditions (seed bed, slope, and proximity of mature trees) on the success of spruce colonization in the snow environment. Three types of snow patches (tundra-like, semi-forested and forested) are widespread in the Boniface area. Eight snow patches of each type were randomly selected. Size, presence of chionophilous species, slope, shrub height and area occupied by *B. glandulosa* were recorded in each snow patch. Cones were harvested on two mature trees around each snow patch to evaluate their reproductive potential. Living or dead spruce seedlings and saplings growing in snow patches were mapped, described in terms of seedbed conditions and tree-ring dated using stem analysis. Annual growth and year of spruce establishment were analyzed according to climatic data.

Since the 1990s, faster growth and increased seedling establishment occurred in all forested and semi-forested snow patches. Spruce establishment was more frequent near the forest margin and in the lower and wetter parts of snow patches, particularly on moss carpets and bare ground. Dense birch shrub cover generally inhibited seedling establishment. In the 1960s, snow precipitation was less abundant, allowing spruce colonization of snow patches. This cohort was detected in the establishment data. Since then, almost no colonization was recorded until the beginning of the 1990s. Both growth and establishment were correlated with temperatures. Tree colonization of snow patches is associated with reduced snow precipitation and warmer conditions allowing earlier snow melt. Forested and semi-forested snow patches are most sensitive to climate change. In the current context of global warming, chionophilous species may suffer a greater competitive pressure, causing a change in plant community composition.

Björk, R. G. and Molau, U., 2007, Ecology of Alpine Snowbeds and the Impact of Global Change: Arctic, Antarctic and Alpine Research v. 39 (1), p. 34-43.

Kudo, G., 1991, Effects of Snow-Free Period on the Phenology of Alpine Plants Inhabiting Snow Patches: Arctic and Alpine Research, v. 23 (4), p. 436-443.

Mathieu, C., Payette, S. and Morin, H., 1987, Chronologie 14C et développement des combes à neige du lac à l'Eau Claire, Québec nordique: Géographie Physique et Quaternaire, v. 41 (1), p. 97-108.

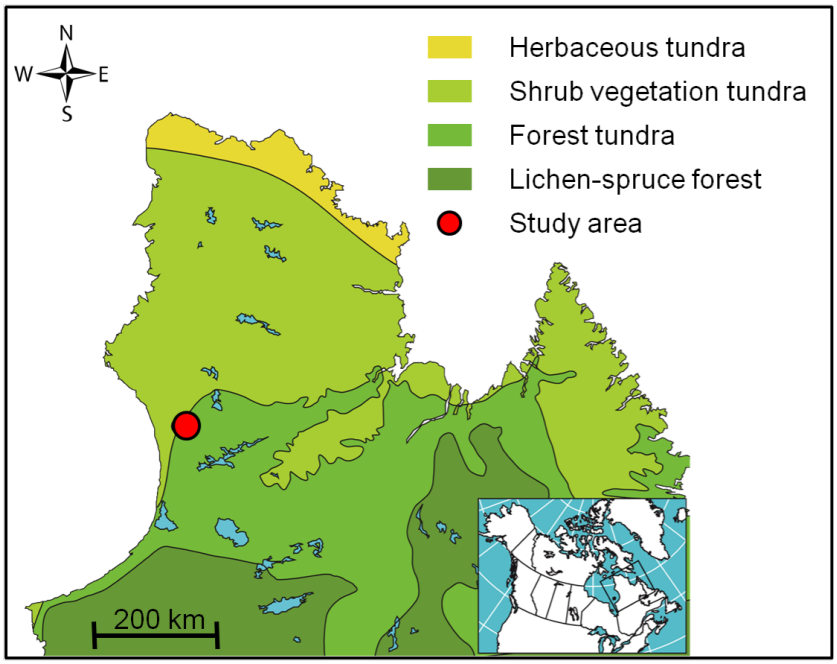

Fig 1. Study area (57˚ 45' N, 76˚ 20' W) 10 km south of the northern treeline in Quebec.

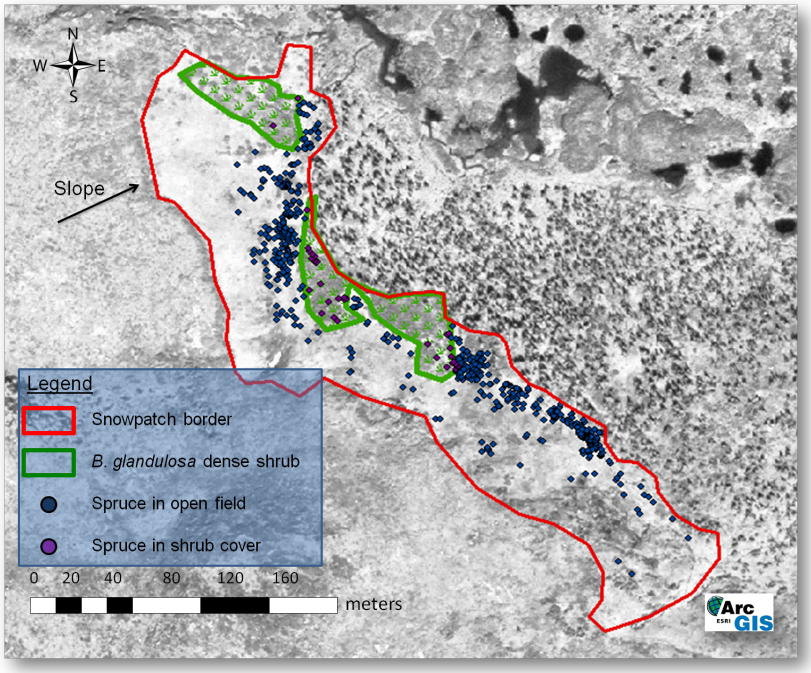

Fig 2. Semi-forested snow patch. Most of the colonization takes place downslope in open field area. Dense shrub limits the establishment.

HYDROGEN ISOTOPES OF N-ALKANOIC ACIDS FROM LAKE SEDIMENTS REFLECT CHANGES IN ANNUAL PRECIPITATION OVER THE 20TH CENTURY, ADAK ISLAND, ALASKA.

Vaillencourt, David A [1]; **Kaufman**, Darrell S [2]; **D'Andrea**, William J [3]; **Anderson**, Scott [4]

[1] Northern Arizona University; davev@nau.edu
[2] Northern Arizona University; darrell.kaufman@nau.edu
[3] Columbia University; dandrea@ldeo.columbia.edu
[4] Northern Arizona University; scott.anderson@nau.edu

This study focuses on hydrogen isotopes of organic compounds from sediments of Andrew Lake, Adak Island located in the central Aleutian Islands (51.93° N 176.63° W, 5 m a.s.l., Fig. 1). Hydrogen isotopes of n-alkanoic acids, fatty acids (FAs) synthesized by terrestrial and aquatic organisms, can provide evidence for shifts in past climate regimes. Here, we demonstrate that the δD from C26 n-alkanoic acids correlate with changes in annual precipitation and number of intense storm events at Adak Island over the instrumental record. This relationship will allow us to use δD downcore to reconstruct changes in annual precipitation, filling in a large spatial gap of paleoclimate data from the North Pacific.

The mean δD value for C26-FAs at our site over the past 100 years is -193 ± 12‰. According to isotope modeling, average annual precipitation δD at Adak Island is -66‰ (Bowen and Revenaugh 2003). Consistent with our findings, previous studies have shown leaf wax δD to be isotopically depleted by approximately 100-130‰ relative to δD of the source water (Hou et al. 2008, Polissar and Freeman 2010).

We compared our δD measurements with monthly instrumental data from the National Climate Data Center (NCDC), which are available between 1942-1994. The results show a significant inverse correlation between δD of C26-FAs and total annual precipitation on Adak Island (r2=0.40, p=0.02 (adjusted for autocorrelation), n=16, Fig 3). Notably, periods of increased annual precipitation (e.g. between 1950 and 1960, average >2000 mm) correspond to low C26-FA δD values (-211‰), and an interval of decreased annual precipitation around 1990 (average 1300 mm) relates to relatively positive δD values (-186‰).

The instrumental record also shows that years with higher amounts of precipitation correspond with an increase in the number of high-intensity storms, defined here as the number of days with >19 mm (0.75 in) of precipitation (r2=0.81, p<.001, n=49). Conversely, there is negligible correlation (r2<0.10) between the total number of days per year with precipitation and the annual amount of precipitation. This indicates that, at least over the instrumental period, annual precipitation amount at Adak Island is controlled by the number of large storms received, rather than the number of low-precipitation events.

The correlation between annual precipitation and δD is consistent with the amount effect (Dansgaard 1964), whereby intense storms produce precipitation with lower δD values primarily due to evaporative processes within storm systems. The amount effect was originally described from the monthly precipitation records at sub-tropical to tropical sites, where the majority of precipitation is delivered by large convective storms (Rozanski et al. 1993). Generally, isotopes in precipitation at mid- to high-latitudes are controlled by precipitation temperature more than precipitation amount (Dansgaard 1964). Adak Island, in the north-central Pacific, receives high annual precipitation (average 1370 mm) with little annual temperature variability (10 °C) compared to locations of similar latitude. Thus, we argue that the isotopic composition of Adak Island precipitation is strongly influenced by the amount effect, and that this signal is captured in the C26-FA δD from Andrew Lake sediments.

Enrichment of δD between environmental water and plant leaf waxes has been shown to vary, with grasses as much as 50‰ more depleted in δD than trees (Liu and Huang 2005, Hou et al. 2007). A palynological study on Adak Island constrains the proportions of vegetation types (shrubs, grasses, and herbs) over the last 10 ka, confirming that trees were never present (Heusser 1978). Preliminary results from a higher-resolution study of pollen in lake sediments from nearby Heart Lake confirm the findings of Heusser (1978). This minimizes the likelihood of extraneous factors (such as significant flora changes) affecting the variation in δD from the C26-FAs other than shifts in annual precipitation.

This is the first study that we know of documenting a downcore correlation between δD of organic material (specifically n-alkanoic acids derived from terrestrial sources) and annual precipitation amount. Ongoing work includes further downcore δD analysis to extend this record to 7 ka, which will be coupled with several other paleoenvironmental proxies (including biogenic silica, loss-on-ignition and δ18O of diatoms) from Andrew Lake and nearby Heart Lake to allow multi-proxy interpretation of Adak Island's climate history beyond the instrumental record. Thus far, our study has demonstrated the novel applicability of δD in fatty acids as a proxy for precipitation amount on a remote island, which will help fill in a large spatial gap of paleoclimate data.

Methods:

The sediment core used for this study was dated with lead and plutonium activities (Fig 2). Samples for δD analysis were taken in 0.5 cm increments for the 20th century, providing average sample resolution of 3 years. Samples were freeze-dried, and free lipids extracted with CH2Cl2/CH3OH (9:1 v/v) by Accelerated Solvent Extraction (Dionex 200 ASE). To isolate the n-alkanoic acids and prepare for gas chromatograph (GC) analysis, compounds were converted to fatty acid methyl esters (FAMEs) following the procedures of Hou et al. (2008). Compounds were identified using GC- mass spectrometry (MS) and quantified using a GC- flame ionization detector (FID) at the University of Massachusetts Amherst Biogeochemistry Lab. Samples were then analyzed for hydrogen isotope values using GC-isotope ratio mass spectrometry (irMS) at the Lamont-Doherty Earth Observatory Organic Geochemistry and Stable Isotope Laboratory.

Bowen, G.J and Revenaugh, J., 2003, Interpolating the isotopic composition of modern meteoric precipitation: Water Resources Research, v. 39, p. 1-13.

Dansgaard, W., 1964, Stable isotopes in precipitation: Tellus, v. 16, p. 436-468.

Heusser, C.J., 1978, Postglacial vegetation on Adak Island, Aleutian Islands, Alaska: Bulletin of the Torrey Botanical Club, v. 105, p. 18-23.

Hou, J., et. al., 2007, Hydrogen isotopic variability in leaf waxes among terrestrial and aquatic plants around Blood Pond, Massachusetts (USA): Organic Geochemistry, v. 38, p. 977-984.

Hou, J., D'Andrea, W.J., Huang, Y., 2008, Can sedimentary leaf waxes record D/H ratios of continental precipitation? Field, model, and experimental assessments: Geochimica et Cosmochimica Acta, v. 72, p. 3503-3517.

Liu, W. and Huang, Y., 2005, Compound specific D/H ratios and molecular distributions of higher plant leaf waxes as novel paleoenvironmental indicators in the Chinese Loess Plateau: Organic Geochemistry, v. 36, p. 851-860.

Paillard, D., Labeyrie, L., Yiou, P., 1996, Macintosh program performs time-series analysis: Eos Transactions AGU, v. 77, p. 379.

Polissar, P.J. and Freeman, K.H., 2010, Effects of aridity and vegetation on plant-wax δD in modern lake sediments: Geochimica et Cosmochimica Acta, v. 74, p. 5785-5797.

Rozanski, K., et. al., 1993, Isotopic Patterns in Modern Global Precipitation: Climate Change in Continental Isotopic Records, v. 78, p. 1-36.

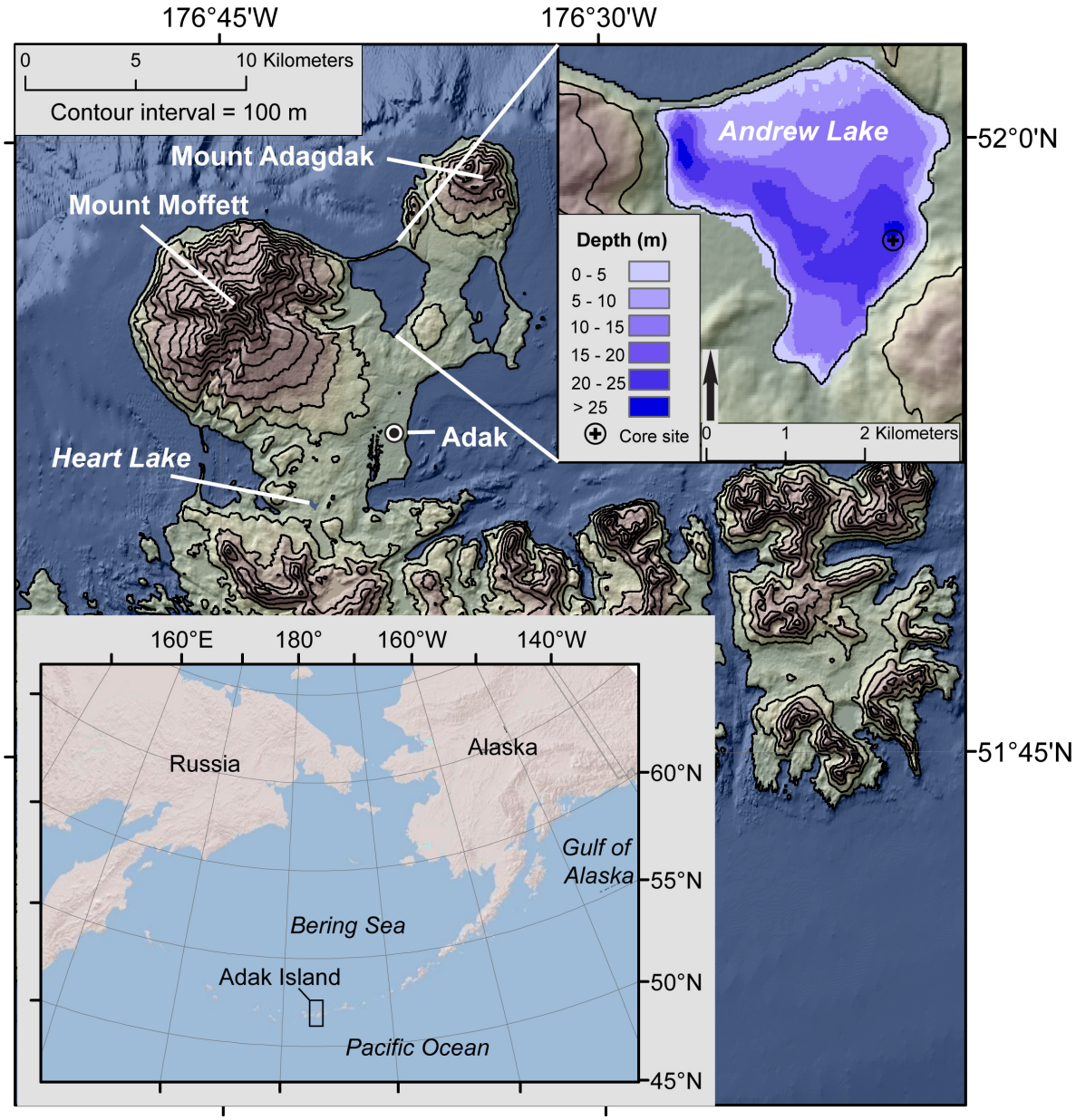

Fig 1. Location of major features on Adak Island, bathymetric map of Andrew Lake with coring location (top right) and Adak Island location in the north Pacific (bottom left).

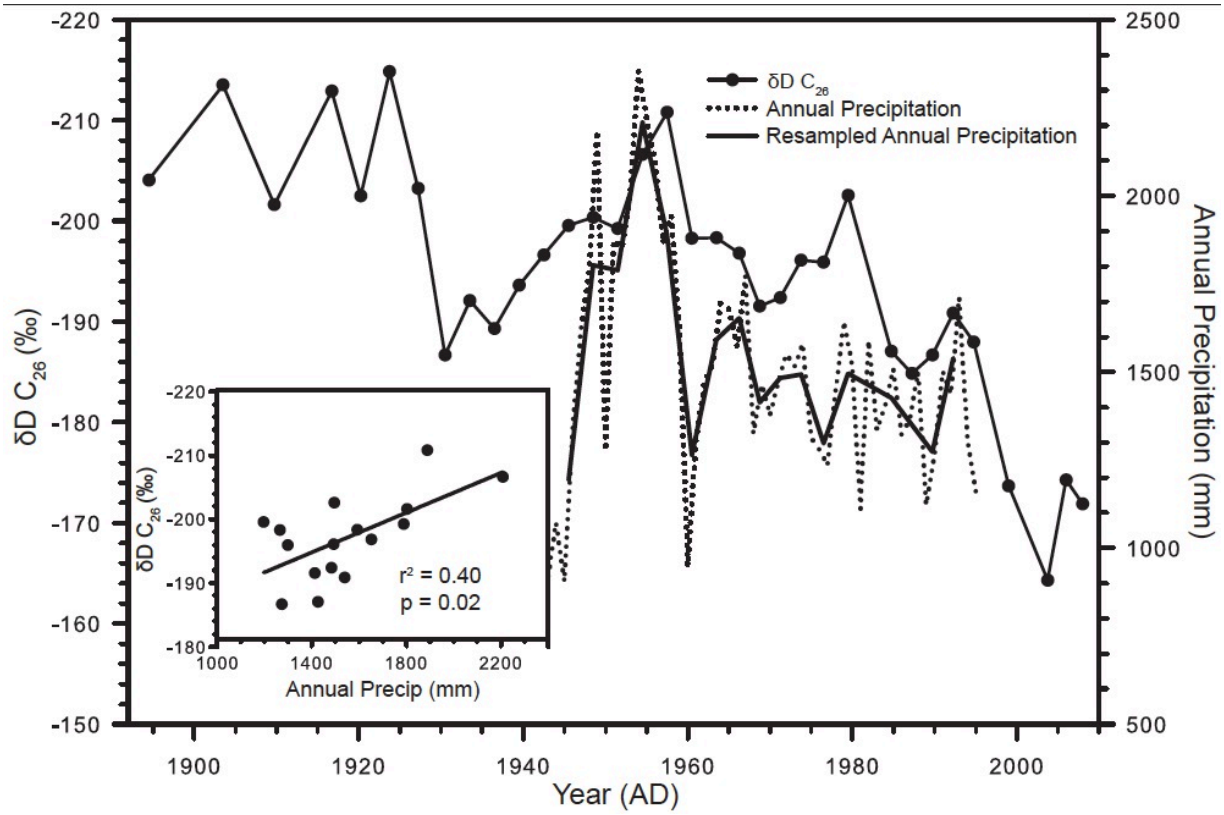

Fig 2. Annual precipitation was resampled with a linear interpolation to match the resolution of the FAME samples using Analyseries v. 2.0.4.2 (Paillard et al. 1996). Linear regression (inset) shows relationship of δD to annual precipitation with p-value adjusted for auto-correlation.

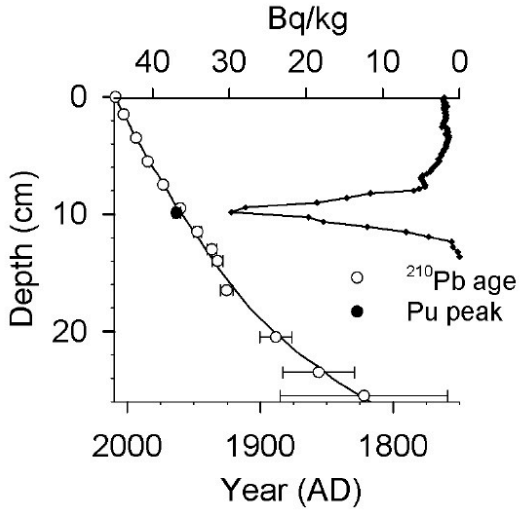

Fig 3. Plutonium activity in Bq/kg (top axis, right line) and age model with depth (bottom axis, left line) based on twelve ^{210}Pb dates and Pu peak.

MONITORING FJORD FLOOR SEDIMENTOLOGY AND GEOCHEMISTRY IN AN ICE-PROXIMAL REGION: A CASE STUDY FROM THE KRONEBREEN-KONGSVEGEN CONFLUENT TIDEWATER GLACIAL SYSTEM

Valletta, Rachel D. [1]; **Brigham-Grette**, Julie [2]; **Powell**, Ross [3]; **Scholz**, Christopher A. [4]

[1] Syracuse University; rdvallet@syr.edu
[2] UMass Amherst; juliebg@geo.umass.edu]
[3] Northern Illinois University; rpowell@niu.edu
[4] Syracuse University; cascholz@syr.edu

The primary objective of this study is to characterize ice-proximal sedimentation at the face of the Kronebreen/Kongsvegen glacial system in Svalbard, Norway. Voluminous sediment originates from two sources at this site: a subglacial river at mid-ice face and an ice marginal stream at its southern terminus (Fig. 1). Of particular interest is a Gilbert-type delta prograding ahead of the Kongsvegen terminus, where sedimentation rates are ten times higher than the area ahead of the subglacial stream.

During the 2011 summer Research Experience for Undergraduates (REU) six students traveled to Kongsfjorden, a fjord on the island of Spitsbergen, Svalbard. Data collection methods included CTD casts, HOBO data, box coring and gravity coring. This project utilizes six <1 m long sediment cores collected in a transect across the ice face. Initial core descriptions reveal textural and mineralogical differences between the two sediment sources. In addition to manual descriptions, core analyses include smear slides, granulometry, and comparison of GRAPE measurements, magnetic susceptibility profiles and x-rays.

Additionally, x-ray fluorescence (XRF) scans from an Itrax core scanner provide high-resolution geochemical data otherwise unobtainable by these core analysis methods. This poster will focus heavily on XRF-obtained chemical profiles, especially element ratios that help to constrain each sediment source's signature (Fig. 2). The project will attempt to reveal whether or not sediment deposition occurs immediately ahead of the delta or progrades cross ice-face and if this can affect future ice terminus behavior.

The Kongsvegen system may be building up towards a new surging event following a long-standing quiescent stage (Melvold and Hagen, 1998). Continued sediment deposition at the delta could help stabilize Kongsvegen during a surge. Sediment core analysis will allow us to assess patterns of sedimentation from the ice-marginal stream to the subglacial river. If sedimentation from the ice-marginal stream is found to deposit immediately ahead of the delta it will increase the likelihood of the delta as a support mechanism for a future Kongsvegen surge.

Melvold, K. and Hagen J.O., 1998, Evolution of a surge-type glacier in its quiescent phase: Kongsvegen, Spitsbergen, 1964-95: Journal of Glaciology, v. 44, n. 147, p. 394-404.

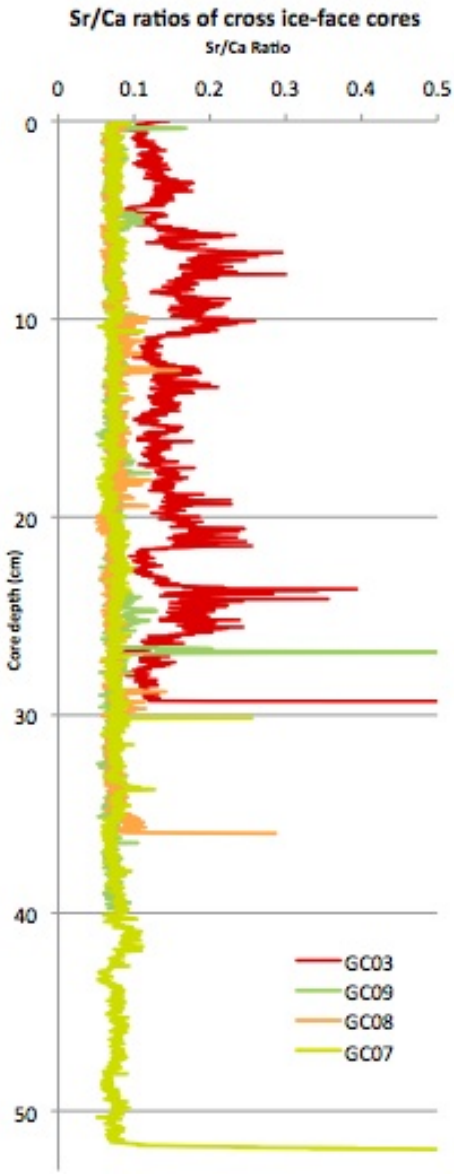

Fig 1. The terminus of the Kronebreen-Kongsvegen confluent glacier system. Core locations and names are marked as blue dots. Sediment sources include: A) ice-marginal stream and B) subglacial river.

Fig 2. Figure 2: Example XRF curves of element ratios across the ice face. The Sr/Ca curve is particularly useful for determining sediment provenance, and shows here that delta-originated sediments have a near double Sr/Ca ratio than the subglacial river sediments.

PHYTOLITHS FROM SANAK ISLAND, WESTERN GULF OF ALASKA

Wilbur, Cricket C [1]; **Jordan**, James J [2]; **Pearsall**, Deborah M [3]

[1] Antioch University New England; cwilbur@antioch.edu
[2] Antioch University New England; jjordan@antioch.edu
[3] University of MIssouri, Columbia; PearsallD@missouri.edu

Phytoliths provide a tool to explore environmental change in general and a new approach for interpreting Holocene climate variability in Alaska in particular. Our understanding of late Quaternary environmental change in Alaska has been mainly based on pollen records; while this research has been essential to reconstructing the environmental history of this landscape, it is regionally incomplete and locally discontinuous. This is not surprising, however, considering the latitudinal and longitudinal extent of Alaska and the differential influences of maritime climate. Phytolith analysis in southern Alaska complements the existing pollen record by providing an independent botanic profile as taxa that are often weakly represented with respect to pollen are robust with respect to phytoliths.

Phytoliths were recovered from a sediment core on Sanak Island, an island group in the eastern Aleutian archipelago, that spans the entire Holocene. The grass phytolith forms are dominated by long cells though non-grass forms are also present. However assigning phytolith forms to a taxonomic classification even with the described regional flora of the Aleutian Islands is challenging with the limited published information available. A modern analog collection of maritime tundra in southwest Alaska may improve the taxonomic association of phytoliths. Although if some of the grass phytoliths are consistent with Festucoid grasses, it suggests the influence on vegetation by the region's maritime setting, which is largely controlled by the location and intensity of the Aleutian low pressure center.

COMPARATIVE OSTEOHISTOLOGY OF *PYGOSCELIS* PENGUINS: IMPLICATIONS FOR BEHAVIORAL AND ENVIRONMENTAL INFLUENCES ON BONE GROWTH

Wilson, Laura E [1]

[1] University of Colorado, Boulder; Laura.Wilson@colorado.edu

Penguins are well known for their unique structural and physiological adaptations to extreme lifestyle (flightlessness) and environments (high latitudes). While many aspects of their biology and ecology garner much scientific and public attention, to date, only a few studies have focused on exploring the dynamics of their bone growth (Meister, 1962; Margerie et al., 2004). Three closely related penguin species – *Pygoscelis adeliae* (Adélie), *P. antarctica* (Chinstrap), *P. papua* (Gentoo) – are found along a latitudinal range of Antarctic and sub-Antarctic environments (46-77ºS), and breed sympatrically in some regions. Breeding behavior and chick growth dynamics have been relatively well studied in these species, especially where they are sympatric. Though differences have been identified in pygoscelid breeding behavior, chick growth, foraging behavior, and migration patterns (Table 1), how these differences affect their skeletal development are poorly understood.

Osteohistology (the study of bone tissue) is an effective tool for analyzing growth strategies in vertebrates, with four primary factors affecting bone microstructure: phylogeny, ontogeny, functional morphology, and environment (e.g. Ricqles et al., 1991; Horner et al., 2000). Amprino (1947) was the first to identify the relationship between growth rates and bone microstructure, a concept now known as "Amprino's rule". Amprino's Rule states that organisms with different growth rates record distinctive suites of characters in their bone microstructure. Vascular canal orientation, primary osteon size, vascular canal density (vascularity), presence or absence of growth lines, and secondary bone reconstruction (Figure 1) are used to make inferences concerning relative growth rates and functional mechanics. Here, pygoscelid penguin bones are analyzed to better understand how differences in growth rates due to breeding strategies and biogeography affect bone tissue development. Given that all species are closely related, share the same functional adaptations to flightlessness and wing-propelled pursuit-diving, and were skeletally mature at the time of death, differences in bone microstructure likely correlate in part with environment and behavior. As a result, *Pygoscelis* penguins are an ideal group for analyzing behavioral, biological, and ecological effects on avian bone development.

Femora from adult *P. adeliae* (Adélie), *P. antarctica* (Chinstrap), and *P. papua* (Gentoo) specimens were histologically analyzed, and results reveal differences in bone tissue development among species. Most notable differences are found in cortical bone thickness, vascular canal density, and vascular canal orientation. Overall, Adélie and Chinstrap penguin femora are more similar to each other than either is to Gentoo bones. Adélie and Chinstrap cortical bone is dominated by longitudinally-oriented vascular canals, with a few reticular canals in the outer cortex. Gentoo penguins, on the other hand, have more radially-oriented canals throughout the cortex and a higher overall vascular canal density. Vascular canal orientation is correlated with bone growth rates, and radial canal orientation is common in faster-growing bone tissue in at least some penguin species (King penguins; Margerie et al., 2004). Likewise, high vascularity has also been associated with higher growth rates in tetrapods. Interestingly, although Adélie penguins have the highest documented growth rates of the three *Pygoscelis* species (Volkman & Trivelpiece, 1980; Table 1), they do not have femoral bone tissue that reflects this. Rather, Gentoo penguin bones have microstructural patterns associated with higher rates of bone tissue deposition than either Adélie or Chinstrap penguins.

Variations in chick growth dynamics are hypothesized to relate to breeding behavior, body size, and climate, and may help explain differences in pygoscelid bone microstructure. Despite Gentoos having the slowest documented growth rates in terms of absolute weight gain (g/day; Trivelpiece et al. 1987) and lengthening of specific anatomical features (feet, flipper, culmen; Volkman & Trivelpiece 1980), they have histologic patterns associated with faster bone growth than their congeners. Though overall growth rates may be lower, the period of rapid growth lasts longer in Gentoos than Adélies and Chinstraps (Volkman & Trivelpiece 1980), as Gentoos reach 104% of adult mass before fledging at 79 days, while Adélies reach 79% and Chinstraps reach 89% of adult body mass before fledging at 52 days (Trivelpiece et al. 1987). In addition to a prolonged rapid growth phase, Gentoo penguins also have a larger average body size compared to their congeners. Body size is strongly correlated with bone microstructure patterns (e.g. Cubo et al., 2005), as larger bones generally show patterns associated with faster bone development. Lastly, Gentoo penguins are known to grow faster in the southern portions of their geographic range (e.g. Williams, 1995), where specimens used in this study were collected (South Shetland Islands, ~62ºS). Trivelpiece et al. (1987) suggest that these Gentoo growth trends may result from higher energy requirements to maintain homeostasis for individuals breeding farther south. Consequently, chick growth periods, body size, and biogeographic ranges all likely contribute to differences in pygoscelid penguin bone development and account for discrepancies between measured growth rates in chicks and inferred growth rates from bone microstructure. These results also indicate that penguin growth is more dynamic than can be understood by simple growth parameters.

Amprino, R., 1947, La structure du tissu osseux envisagee comme expression de differences dans la vitesse de l'accroissement: Archivos de Biologia, v. 58, p. 315-330.
Cubo, J., Ponton, F., Laurin, M., de Margerie, E., Castanet, J., 2005, Phylogenetic signals in bone microstructure of sauropsids: Systematic Biology, v. 54, p. 562-574.
Horner, J. R., de Ricqles, A., Padian, K., 2000, Long Bone Histology of the Hadrosaurid Dinosaur Maiasaura peeblesorum: Growth Dynamics and Physiology Based on an Ontogenetic Series of Skeletal Elements: Journal of Vertebrate Paleontology, v. 20, p. 115-129.
de Margerie, E., Robin, J.-P., Verrier, D., Cubo, J., Groscolas, R., Castanet, J., 2004, Assessing a relationship between bone microstructure and growth rate: a fluorescent labelling study in the king penguin chick: Journal of Experimental Biology, v. 207, p. 869-879.
Meister, W., 1962, Histological Structure of the Long Bones of Penguins: The Anatomical Record, v. 143, p. 377-387.
de Ricqles, A., Meunier, F. J., Castanet, J., Francillon-Viellot, H., 1991, Comparative microstructure of bone, p. 1-78 in B. K. Hall (ed.), Bone. CRC Press, Boca Raton.
Williams, T. D., 1995, The penguins: Spheniscidae. Oxford University Press, 295 pp.

Common Name	Species Name	Specimen Provenance	Average Mass (kg)	Diet	Migratory Behavior	Breeding Behavior	Growth Constant[1]
Adélie Penguin	*Pygoscelis adeliae*	Cape Royds, Ross Island: 77ºS Penguin Point, Seymour Island: 64ºS	Male: 5.4 Female: 4.8	Krill, + some fish, amphipods	Migratory	Timing: Oct/Nov Incubation: 23-35 days Fledging: 48-64 days Sexual maturity: F: 4.7-5 years, M: 6.2-6.8 years	0.146 (fastest)
Chinstrap Penguin	*Pygoscelis antarctica*	Meade Island, South Shetland Islands: 64ºS	Male: 5.0 Female: 4.8	Krill	Migratory	Timing: Nov/Dec Incubation: 33-36 days Fledging: 52-60 days Sexual maturity: 2+ years	0.127 (intermediate)
Gentoo Penguin	*Pygoscelis papua*	Aitcho Island, South Shetland Islands: 64ºS	Male: 5.6 Female: 5.1	Krill	Non-Migratory	Timing: Oct/Nov Incubation: 34-37 days Fledging: 80-105 days Sexual maturity: 2-4 years	0.113 (slowest)

Fig 1. Comparison of the general biology, behavior, and physiology of *Pygoscelis* penguins. Data compiled from Davis & Reener (2003) and Williams (1995), unless otherwise noted. [1] Growth constant of sympatric pygoscelid penguins from King George Island (South Shetland Islands) recorded by Volkman & Trivelpiece (1980).

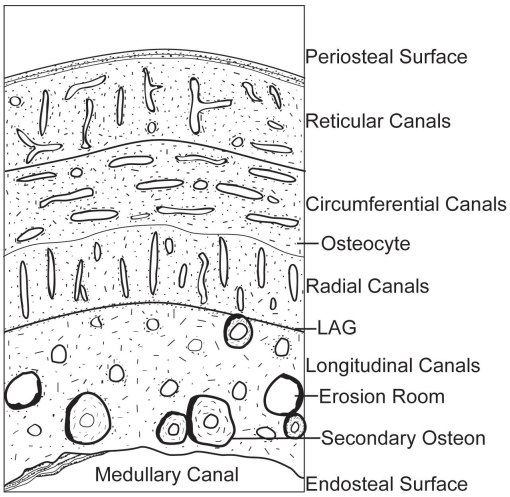

Fig 2. Cartoon illustrating the major microstructure features of fibro-lamellar bone tissue. Many of these features are directly correlated with growth rates and are observed in *Pygoscelis* penguin bones.

ASSESSING TREND AND VARIATION OF ARCTIC ICE EXTENT DURING 1979-2010 FROM AN ICE EDGE LATITUDE PERSPECTIVE

Xia, Wentao [1]; **Xie**, Hongjie [2]; **Ackley**, Stephen Fred [3]

[1] Laboratory for Remote Sensing and Geoinformatics, University of Texas at San Antonio; kv85kv@hotmail.com
[2] Laboratory for Remote Sensing and Geoinformatics, University of Texas at San Antonio; Hongjie.Xie@utsa.edu
[3] Laboratory for Remote Sensing and Geoinformatics, University of Texas at San Antonio; Stephen.ackley@utsa.edu

Abstract: Effective and feasible large scale sea ice records from satellites can provide fundamental information about ice concentration, extent, thickness and other characteristics. Monthly vector datasets of Arctic ice extent of the last 32 years (1979-2010) from the ice index maintained by National Snow and Ice Data Center (NSIDC) are analyzed, by retrieving the latitudinal ice edge of Arctic pack ice reached along each longitude, to assess inter-annual and seasonal spatial variation of sea ice extent. Comparison of seasonal circle of sea ice melting/formation indicates after the year 2000 a more rapid melting from April to September, and a slightly slower ice formation (or edge advance) from November to January. Statistical Analysis of long-term trend suggest that: (1) for summer months from July to September, there is a long-term declining trend in ice extent in most longitudes, the retreat rate 0.0528 -0.0783 latitude degree/year to the north; (2) for pack ice not reaching continental coastline in winter season, there is a slightly lower decline rate, 0.0217-0.0563 latitude degree/year to the north; and (3) for pack ice reaching continent coastline in winter season, there is less variability in winter month from January to April; Interpretation of spatial variability shows that the most significant sea ice decline occurs in: (1) Chukchi Sea from August to October; (2) Hudson Bay in June; (3) southern part of Greenland from January to May, as sea ice can no longer surround entire southern Greenland in winter; (4) Barents Sea in almost all months; (5) Kara Sea from July to August; (6) Laptev Sea and Eastern Siberian Sea in August and September. Differing from previous result of mean ice edge decline in the last 30 years, this study provides the first perspective of ice retreat and advance along each longitudinal degree and in different regions. This study reveals a more complex spatial and temporal variability of ice retreat and advance than that suggested by the mean ice edge decline typically shown for the Arctic region. Prediction of future decline may have to account for these regional differences.

THE YOUNGER DRYAS COLD INTERVAL WAS NOT THAT COLD: INSIGHTS FROM BAFFIN ISLAND, ARCTIC CANADA

Young, Nicolas E [1]; **Briner**, Jason P [2]

[1] University at Buffalo; nyoung2@buffalo.edu
[2] University at Buffalo; jbriner@buffalo.edu

An extensive moraine system deposited parallel to eastern Baffin Island fiord heads was originally believed to demarcate the late Wisconsin maximum extent of the Laurentide Ice Sheet (LIS; Falconer et al., 1965; Miller and Dyke, 1974). Recent work, however, has demonstrated that during the late Wisconsin the LIS extended to at least fiord mouths and likely out onto the Baffin Bay continental shelf with regional deglaciation commencing ca. 15 - 16 ka (Briner et al., 2006; Davis et al., 2006). Thus, fiord head moraines deposited during the Cockburn substage (~8 – 9.5 cal ka BP; Andrews and Ives, 1978) represent an advance of the LIS superimposed on deglaciation. Considered correlative with these "Cockburn moraines" are moraines that were deposited by local mountain glaciers that became independent of the LIS during deglaciation. Fiord head moraines are currently dated by conventional radiocarbon ages from marine fauna that broadly constrain moraine deposition to ~8 – 9.5 cal ka BP; this chronology has remained relatively unchanged for three decades (Andrews and Ives, 1978).

Here, we present new ^{10}Be surface exposure ages from moraines deposited by two local glaciers in northeastern Baffin Island, and review preexisting ^{10}Be and ^{14}C ages from the area, which reveal that both LIS outlet glaciers and independent mountain glaciers advanced in unison in response to the ~150-yr long 8.2 ka event. In addition, our data suggest that mountain glaciers during the 8.2 ka event were larger than their Younger Dryas (12.9 – 11.7 kyr ago) predecessors. This finding implies that summer temperature depression was greater during the 8.2 ka event than during the Younger Dryas; a nearby chironomid-inferred reconstruction of summer temperatures indicates that regional cooling during the 8.2 ka event was ~3.5 °C (Axford et al., 2009). Despite central Greenland ice cores indicating that mean annual temperatures during the Younger Dryas and the 8.2 ka event were 15 ± 3 and 3.3 ± 1.1 °C colder-than-today, respectively, our data suggest that 8.2 ka event summertime cooling was of greater magnitude than summertime cooling during the Younger Dryas. The lack of significant summertime cooling during the Younger Dryas has been documented elsewhere in the Arctic (e.g. Bjork et al., 2002; Mangerud and Landvik, 2007) and with these new data from Baffin Island, we agree with recent works (e.g. Broecker et al., 2010) that there remains much to be learned about this unusual event.

Andrews, J.T., and Ives, J.D., 1978, "Cockburn" nomenclature and the late Quaternary history of the eastern Canadian Arctic: Arctic and Alpine Research, v. 10, p. 617 – 633.

Axford, Y. et al., 2009, Paleoecological evidence for abrupt cold reversals during peak Holocene warmth on Baffin Island, Arctic Canada: Quaternary Research, v. 71, p. 142-149.

Björk, S. et al., 2002, Anomalously mild Younger Dryas summer conditions in southern Greenland: Geology, v. 30, 427 - 430.

Briner, J.P. et al., 2006, Cosmogenic radionuclides from fiord landscapes support differential erosion by overriding ice sheets: GSA Bulletin, v. 118, p. 406 – 420.

Broecker, W.S. et al., 2010, Putting the Younger Dryas cold event into context: Quaternary Science Reviews, v. 29, p. 1078-1081.

Davis, P.T. et al., 2006, Preservation of Arctic landscapes overridden by cold-based ice sheets: Quaternary Research, v. 65, p. 156-163.

Falconer, G., Andrews, J.T., and Ives, J.D., 1965, Late-Wisconsin end moraines in Northern Canada: Science, v. 147, p. 608 - 610.

Mangerud, J., and Landvik, J., 2007, Younger Dryas cirque glaciers in western Spitsbergen: smaller than during the Little Ice Age: Boreas, v. 36, 278-285.

Miller, G.H., and Dyke, A.S., 1974, Proposed extent of late Wisconsin Laurentide Ice on eastern Baffin Island: Geology, v. 2, p. 125 - 130.

HOLOCENE CLIMATIC VARIABILITY AND EXTENT OF THE SHERIDAN GLACIER INFERRED FROM THE SEDIMENT OF CABIN LAKE, ALASKA

Zander, Paul D [1]; **Kaufman**, Darrell S [2]; **Anderson**, R Scott [3]

[1] Northern Arizona Univeristy; pdz2@nau.edu
[2] Northern Arizona University; Darrell.Kaufman@nau.edu
[3] Northern Arizona University; Scott.Anderson@nau.edu

Cabin Lake (0.1 km2; 4.8 m deep) is located 16 km east of Cordova on the east side of Prince William Sound and about 5 km from the terminus of the Sheridan Glacier, Alaska. The lake is currently separated from the glacier outflow by a low topographic divide, but meltwater entered the lake when the Sheridan Glacier was advanced farther down-valley of its current terminal position. A 3.5-m-long sediment core was recovered from Cabin Lake and was dated using a plutonium-activity profile and seven radiocarbon ages. The full length of the core was analyzed for magnetic susceptibility, dry bulk density, and organic-matter content, and the most recent 250 years of sediment was analyzed for biogenic-silica content. This study uses variations in characteristics of the sediment deposited at Cabin Lake, such as intervals of glacial rockflour or peat accumulation, to infer past changes in lake level and the extent of the nearby Sheridan Glacier. This information allows conclusions to be made about variations in the North Pacific climate.

The sediment core extends to 7.3 cal ka. The stratigraphy includes intervals of inorganic clayey silt, organic-rich mud, and peat (Fig. 1). The oldest unit is inorganic clayey silt interpreted as rockflour deposited by glacial meltwater entering the lake from 7.2 to 6.9 cal ka, when the Sheridan Glacier likely expanded. The rockflour is overlain by increasingly organic-rich and coarser-grained sediment, which accumulated between 6.9 and 5.9 cal ka, and indicates the cessation of meltwater input to the lake, and a shift towards a more productive lake, as the glacier retreated. The lacustrine mud is overlain by a transitional unit of muddy peat with variable, but generally increasing organic content and coarseness that spans from 5.9 to 4.7 cal ka, indicating a lowering of lake level. Coarse organic material was consistently deposited from 4.7 to 0.9 cal ka, when the site was occupied by a peat bog or fen. Beginning around 1090 AD glacial meltwater entered the lake again, depositing another unit of inorganic clayey silt and dramatically increasing the sedimentation rate. Two layers with higher organic-matter content interrupt this inorganic unit, indicating that glacial meltwater briefly stopped entering the lake from about 1150 to 1230 AD and 1510 to 1560 AD. Since approximately 1770 AD, no glacier meltwater has entered the lake and the sediment has become increasingly organic rich.

A high-resolution 250-year-long record of biogenic silica (BSi) was produced for the uppermost unit of organic-rich mud by sampling every 2 mm (about 3.1 year per sample). BSi measures the abundance of diatoms preserved in lake sediment, and is used as a proxy for productivity in the lake. BSi in the sediment of Cabin Lake peaked around 1920 AD and then decreased during the past 90 years. The average regional temperatures from coastal Alaska (Kodiak, Seward, Juneau, Sitka, and Cordova) have a weak positive correlation with BSi flux from Cabin Lake ($r2 = 0.18$, $p = 0.11$ adjusted for autocorrelation). The Cabin Lake BSi record also correlates significantly ($r2 = 0.18$, $p = 0.012$ adjusted for autocorrelation) with temperatures reconstructed from tree rings from around the Gulf of Alaska region (D'Arrigo et al., 2006). This provides confidence that BSi in Cabin Lake responds to climatic variables affecting the entire Gulf of Alaska region and can be used as a proxy for annual regional temperature. The BSi record over the past 250 years indicates a general increasing trend in regional temperatures from 1760 until 1915 AD, and a significant cooling from 1915 until present.

Preliminary conclusions can be made about regional climatic variations over the past 7.3 cal ka based on the sediment of Cabin Lake. Peat accumulation at Cabin Lake between 4.7 and 0.9 cal ka might indicate that the groundwater table was significantly lower and the regional climate was likely dryer than present. The peat accumulation could also be the result of a change in the hydrology of the catchment of Cabin Lake that resulted in less inflow to the basin. Some climate models indicate that

precipitation in Alaska decreased steadily throughout the Holocene (Renssen et al., 2004), though the more prevalent view is that precipitation along the Gulf of Alaska began to increase around 6 ka with the onset of Neoglaciation (Barclay et al., 2009; Mann et al., 1998). Several intervals of glacial advance were identified by the presence of glacial rockflour in the sediment. The earliest period of advanced glacier ice lasted from 7.2 to 6.9 cal ka, a time few other glacial-geological records in Alaska indicate an advance. In fact, this interval corresponds with relatively high summer temperatures associated with the end of the Holocene thermal maximum and prior to cooling associated with the onset of Neoglaciation (Mann et al., 1998). This suggests that the advance was driven by increased snowfall rather than decreased ablation. In the Canadian Cordillera, wood from glacial forefields indicate an advance from 7.45-6.45 cal ka (Menounos et al., 2009), correlative with the advance of the Sheridan Glacier. The dates of glacial advance inferred from Cabin Lake sediment also agree well with Tuthill et al.'s (1968) reconstruction of the terminus positions of the Sheridan Glacier, which indicates that the glacier advanced between 1300 and 1500 AD, retreated to about 700 m down-valley of its 1965 terminus between 1500-1600, and advanced to its Holocene maximum at 1700 AD. The Cabin Lake record further clarifies the history of glacier fluctuations. Based on the reconstructed terminus position and on our ages for rockflour deposition in Cabin Lake, it appears that meltwater reached the lake when the Sheridan Glacier was more than 800 m down-valley of its 1963 terminus.

Most glacier reconstructions from southern Alaska show evidence for a first millennium advance of glacial ice that occurred between 500 and 700 AD, and that the Little Ice Age included three phases of glacier expansion: 1180-1300, 1600-1715, and 1810-1880 AD (Barclay et al., 2009). The periods of rockflour input to Cabin Lake (1090-1150, 1230-1510, and 1560-1770 AD) align somewhat with glacier reconstructions from the region, but there are important differences. First, the late phase of the Little Ice Age (LIA) does not appear in the Cabin Lake record. Tuthill et al. (1968) dated a moraine from 1890 AD indicating that the Sheridan Glacier did experience a late LIA maximum during this time, but the meltwater did not reach Cabin Lake probably due to a larger 1700 AD moraine blocking its path. Second, the Sheridan Glacier was larger during the late Medieval Warm Period and early LIA than during the first millennium AD, when many other glaciers in the region were advancing. Buried stumps indicate that the Sheridan Glacier advanced in the late first millennium and then retracted enough during the Medieval period for trees to grow on the forefield around 950 AD (Barclay et al., 2009). The Cabin Lake record does not contradict this information, but it does suggest that the first millennium advance was smaller than the more recent advances, and that the Sheridan Glacier was likely advanced more than 800 m beyond its 1965 terminus in the second half of the Medieval period starting around 1090 AD. The Medieval Warm Period is thought to have been associated with enhanced La Nina conditions (Mann et al., 2009), which may have increased precipitation enough to cause the Sheridan Glacier advance despite warmer temperatures (D'Arrigo et al., 2006). This is suggested for other glaciers in southern Alaska and in western Canada (Koch & Clauge, 2011). We suggest that glaciers in southern Alaska and western Canada advanced during the Medieval Warm Period in response to a northward shift in the dominant storm track during this time, which was associated with a long-term drought across the southwest United States (Stine, 1994).

Barclay, D., Wiles, G., Calkin, P., 2009, Holocene glacier fluctuations in Alaska: Quaternary Science Reviews 28, p. 2034-2048.

D' Arrigo, R., Wilson, R., Jacoby, G., 2006, On the long-term context for late twentieth century warming: Journal of Geophysical Research 111, p. 1-12.

Koch, J., and Clauge, J., 2011, Extensive glaciers in northwest North America during Medieval time: Climatic Change 107, p. 593-613.

Mann, D., Crowell, A., Hamilton, T., Finney, B., 1998, Holocene climatic and geologic history around the Gulf of Alaska: Arctic Anthropology v. 35, 1, p. 112-131.

Mann, M., Zhang, Z., Rutherford, S., Bradley, R., et al., 2009, Global Signatures and Dynamical Origins of the Little Ice Age and Medieval Climate Anomaly: Science 326 (5957), p. 1256-269.

Menounos, B., Osborn, G., Clague, J., Luckman, B., 2009, Latest Pleistocene and Holocene glacier fluctuations in western Canada: Quaternary Science Reviews 28, p. 2049-2074.

Renssen, H., Goosse, H., Fichefet, T., Brovkin, V., et al., 2005, Simulating the Holocene climate evolution at northern high latitudes using a couple atmosphere-sea ice-ocean-vegetation model: Climate Dynamics 24, p. 23-43.

Stine, S., 1994, Extreme and persistent drought in California and Patagonia during medieval time: Nature 369, p. 546-549.

Tuthill, S., Field, W., Clayton, L., 1968, Postearthquake studies at Sherman and Sheridan glaciers, in the great Alaska earthquake of 1964 – Hydrology 1603, p. 318–328.

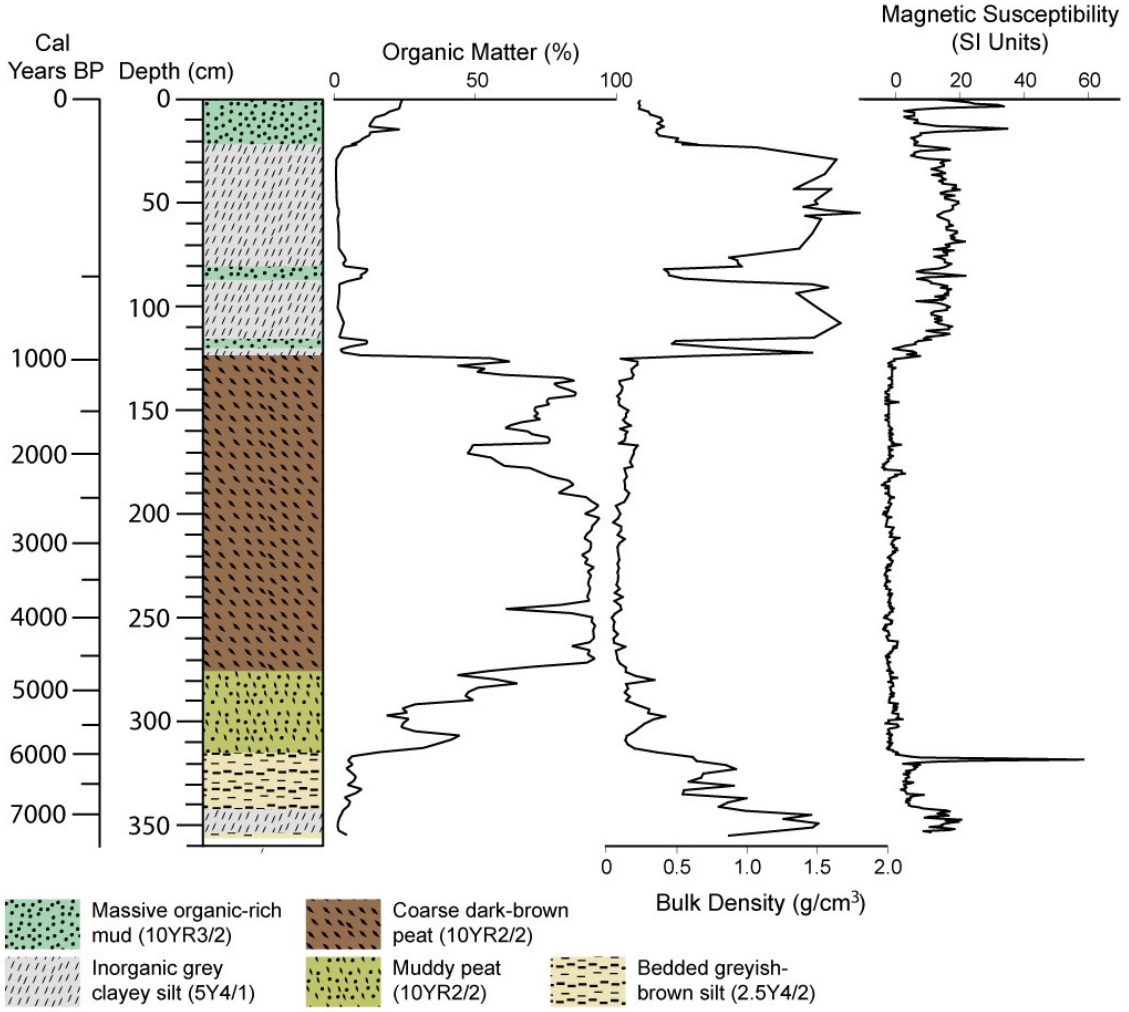

Fig 1. Stratigraphic units of the sediment core, along with sediment analyses (organic content, bulk density, magnetic susceptibility) plotted by depth and a preliminary age model.

SPECIAL 30 MIN TALK

WORKSHOPS POSITIONING YOUTH AS FILM PRODUCERS OF CRITICAL GLOBAL SYSTEMS: AUTHENTIC ARCTIC CONTENT FROM NORTHWEST GREENLAND

Vachon, Ryan[1]

[1] INSTAAR, University of Colorado; ryan.vachon@colorado.edu

Arctic systems sciences are replete with cross-disciplinary collaborations; feedbacks with worldwide ramifications, and utterly fascinating field, lab and computational methods. For a more sustainable future, it is paramount that global communities understand how these systems function and how applicable they are to lives so far removed from where their conditions first manifest. While beset with challenges, educating the public on such topics is an invaluable opportunity to meet advancing directives in education standards.

Science, Technology, Engineering and Math (STEM) are core educational subjects, fundamental for public, environmental, economic and health advances. Schools, government agencies and businesses recognize the training and engagement of the next generation of scientists as critical for staying ahead of the curve of highly competitive global markets and work forces. Methods for teaching and learning STEM are rapidly changing. New technologies demonstrate or illustrate processes or conditions in ways that were inaccessible to classrooms merely a decade ago. Think, Power Point, classroom web access, video and affordable animation software. No one method is the silver bullet for more effective education. However, if properly leveraged, well-assembled combinations of these tools present rousing opportunities for engaging youth with STEM content.

In this presentation a new, STEM formatted, enterprise undertaken by Earth Initiatives will be discussed. Earth Initiatives is a non-profit organization affiliated with the Institute of Arctic and Alpine Research devoted to streamlining the communication of crucial science to different sectors of the public.

Our program leverages the bounty of exciting and relevant ecosystem sciences taking place in Northwest Greenland to inspire middle and high school students to 1) appreciate science as an invaluable tool for prosperity, 2) think critically about the consequences of natural changes and human actions, 3) formulate cogent opinions, and 4) take action on their convictions. We accomplish these objectives by empowering students by becoming partners in the fabrication process of one of the most potent communication methods, film. Workshop 1 (1-2 hours): Armed with prefabricated, compelling videos about the science taking place in the Thule, Greenland region, students are asked to step into the shoes of being the individuals to doing something special – create a deliverable that aligns with their knowledge, interests and passions. What about the offered videos could be modified, added or omitted to give these products traction? Students are called upon to use their vision of successful teaching methods and hooking viewers to accomplish the overlying goal of effective youth education. Workshop 2 (full day): Over the course of an entire day, students are taken through a rigorous yet empowering exercise of collaborating with their "production team"(other students and Earth Initiative specialists) to direct filming, define overlying messages, refine storylines, establish voice, edit video content, refine their production and celebrate the process of taking a simple belief or concept, and giving it grip through video.

Our programs teach students about the fundamentals of Arctic sciences, with the understanding that it is their duty to help "us" (educators, scientists, parents, politicians and businesses) effectively convey these lynch-pin concepts to the public. Not only do they include video into the learning process, but they empower students to use alternative/popular media to be their voice. Outcomes: Concept retention. Learning technical skills. Cooperation. Responsibility. Empowerment to take action. Infusion of STEM thinking into the lives of many youth.

Workshop Participants

John Andrews
University of Colorado
INSTAAR, Box 450
Boulder, CO 80309 United States
andrewsj@colorado.edu

Sarah Appleton
The College of Wooster
1189 Beall Ave
C1050
Wooster, OH 44691 United States
Sappleton12@wooster.edu

Megan Arnold
NAU
2858 S. Highland Mesa
Flagstaff, AZ 86001 United States
msa69@nau.edu

Michael Badding
University at Buffalo
1380 Amherst St
Buffalo, NY 14216 United States
mbadding@buffalo.edu

Joscelyn Bailey
University of Waterloo
501 University Crescent
Winnipeg, MB R3T 2N6 Canada
Joscelyn.Bailey@Dfo-mpo.gc.ca

Adam Barker
University of Washington
University of Washington
Johnson Hall Rm-070, Box 351310
Seattle, WA 98195 United States
adbarker@uw.edu

Michael Becker
McGill University
4066 St. Denis (#204)
Montreal, QC H2W2M5 Canada
michael.becker@mail.mcgill.ca

Gerald Bigelow
Bates College
Department of History
Pettengill Hall, Bates College
Lewiston, ME 04240 United States
gbigelow@bates.edu

Brandon Boldt
Northern Arizona University
3320 South Moore Cir.
Flagstaff, AZ 86001 United States
brb257@nau.edu

Julie Brigham-Grette
UMass-Amherst
Dept of Geosciences
University of Massachusetts
Amherst, MA 01003 United States
juliebg@geo.umass.edu

Jason Briner
University at Buffalo
411 Cooke Hall
Buffalo, NY 14260 United States
jbriner@buffalo.edu

Seth Campbell
University of Maine
236 Sawyer Hall
Orono, ME 04469 United States
Seth_Campbell@umit.maine.edu

Elizabeth Ceperley
Beloit College
700 College St.
Beloit, WI 53511 United States
ceperlee@beloit.edu

Celene Christensen
University of Colorado Boulder, INSTAAR
465 s 43 rd st
Boulder, CO 80305-6007 United States
celene.christensen@colorado.edu

Stéphanie Coulombe
University of Montreal
520 chemin de la Côte-Ste-Catherine
Montreal, QC H2V 2B8 Canada
stephanie.coulombre@umontreal.ca

Maciej Dąbski
University of Warsaw
ul. Krakowskie Przedmiescie 26/28
Warszawa, Poland 00-927 Poland
mfdbski@uw.edu.pl

Karin Ebert
Stockholm university
Dept of Physical Geography and Quaternary Geology
Stockholm, Sweden 10691 Sweden
karin.ebert@natgeo.su.se

Jeremy Fyke
Los Alamos National Laboratory
2815 Arizona Avenue
Los Alamos, NM 87544 United States
fyke@lanl.gov

Aslaug Geirsdottir
Inst of Earth Sciences, University of Iceland
Askja, Sturlugata 7
Reykjavik, Iceland 101 Iceland
age@hi.is

Endre Gjermundsen
The University Centre in Svalbard
UNIS, P.O. Box 156
Longyearbyen, Svalbard 9171 Norway
Endre.For.Gjermundsen@unis.no

Valeriy Ivanov
University of Michigan
1351 Beal Avenue, 105 EWRE
Ann Arbor, MI 48109-2125 United States
ivanov@umich.edu

Anne Jennings
INSTAAR, University of Colorado
1560 30th St.
Boulder, CO 80309-0450 United States
anne.jennings@colorado.edu

Kasey Kathan
Queen's University
Department of Geography
D102 MacKintosh-Correy Hall
Kingston, ON K7L 3N6 Canada
kmkathan@gmail.com

Anne Krawiec
Northern Arizona University
1708 N. Main Street
Flagstaff, AZ 86004 United States
ack62@nau.edu

Karl Kreutz
University of Maine
236 Sawyer Hall
Orono, ME 04469 United States
karl.kreutz@maine.edu

Noah Kreutz
University of Maine
236 Sawyer Hall
Orono, ME 04469 United States
karl.kreutz@maine.edu

Darren Larsen
INSTAAR
University of Colorado Boulder
Campus box 450
Boulder, CO 80309 United States
darren.larsen@colorado.edu

Jessica Liptak
University of Utah Dept. Atmospheric Sciences
Atmospheric Sciences University of Utah
135 S 1460 East Rm 819
Salt Lake City, UT 84112-0110 United States
jessica.liptak@utah.edu

Brian Maclean
Natural resources canada
1 challenger drive
dartmouth, NS b2y 4a2 Canada
brimacle@nrcan.gc.ca

Daren McGregor
Colby College
8033 Mayflower Hill
Waterville, ME 04901 United States
damcgreg@colby.edu

Andreas Mikkelsen
University of Copenhagen
Øster Voldgade 10
Copenhagen, Non US/Canada 1350 Denmark
abm@geo.ku.dk

Martin Miles
Uni research - Bjerknes Centre
Allegaten 70
Bergen, Hordaland 5227 Norway
martin.miles@uni.no

Gifford Miller
INSTAAR
INSTAAR
University of Colorado
Boulder, CO 80309 United States
gmiller@colorado.edu

Astrid Ogilvie
INSTAAR
1560 30th Street
Campus
Boulder, CO 80309-0450 United States
Astrid.Ogilvie@colorado.edu

Tad Pfeffer
INSTAAR
1560 30th Street
Campus
Boulder, CO 80309-0450 United States
wtpfeffer@gmail.com

Corinne Pomerleau
UQAR and DFO
9860 West Saanich Road
Institute of Ocean Science
Sidney, BC V8L4B2 Canada
corinne.pomerleau@dfo-mpo.gc.ca

Ross Powell
Northern Illinois University
Department of Geology and Environmental Geoscience
DeKalb, IL 60115 United States
ross@geol.niu.edu

Ursula Quillman
University of Colorado
INSTAAR, Box 450
Boulder, CO 80309 United States
Ursula.Quillmann@Colorado.edu

Daksha Rajagopalan
Yale University
PO Box 202140
New Haven, CT 06520 United States
daksha.rajagopalan@yale.edu

George Roth
University of Washington
4341 8th Ave NE
Seattle, WA 98105 United States
georoth@u.washington.edu

Denis-Didier Rousseau
INSU-CNRS
ENS, LMD
24 rue Lhomond
Paris, Ile de France 75231 France
denis.rousseau@lmd.ens.fr

Ashley Rudy
Queen's University
228 Brock St.
Kingston, ON N2P 1Z2 Canada
ashley.rudy@gmail.com

Evangeline Sessford
University Centre In Svalbard (UNIS) and University of Oslo (UiO)
Pb. 1037
Longyearbyen, Svalbard 9171 Norway
EvangelineS@unis.no

Rebecca Siegel
Hampshire College
Box 1083 Hampshire College
893 West St
Amherst, MA 01002 United States
rss07@hampshire.edu

Francis St-Amour
Université Laval, Nordic Research chair on ecological disturbances, Centre Northern Studies
845 avenue Calixa-Lavallée app.2
Québec, QC G1S 3H1 Canada
francis.st-a.1@ulaval.ca

Alexandre Truchon-Savard
Université Laval - Center for Northern Studies
845 Calixa-Lavallée 2
Québec, QC G1S3H1 Canada
alexandre.truchon-savard.1@ulaval.ca

Ryan Vachon
University of Colorado
INSTAAR, Box 450
Boulder, CO 80309 United States
Ryan William Vachon
ryan.vachon@Colorado.edu

David Vaillencourt
Northern Arizona University
20 E Hunt Ave
Flagstaff, AZ 86001 United States
davev@nau.edu

Rachel Valletta
Syracuse University
36 DeWitt Rd
Sutton, MA 01590 United States
rdvallet@syr.edu

Cricket Wilbur
Antioch University
52 Clark Road
Ipswich, MA 01938 United States
cwilbur@antioch.edu

Laura Wilson
University of Colorado, Boulder
Department of Geological Sciences
UCB 399
Boulder, CO 80309 United States
Laura.Wilson@colorado.edu

Wentao Xia
University of Texas at San Antonio
One UTSA Circle
San Antonio, TX 78249 United States
kv85kv@hotmail.com

Nicolás Young
University at Buffalo
411 Cooke Hall
Dept. of Geology
Buffalo, NY 14260 United States
nyoung2@buffalo.edu

Paul Zander
Northern Arizona University
1404 Mark Lane
Flagstaff, AZ 86001 United States
padaza@gmail.com

Notes

Notes